CRISM 2011

Winds from Massive Stars

Bubble Nebula
(NGC 7635)
in Cassiopeia

wind-blown
bubble around
BD+602522
(O6.5IIIf)

a review by

Jo(achim) Puls
University Observatory Munich

with the help of

Achim Feldmeier, Peter Petrenz, Tamara Repolust, Jorge Rivero-Gonzalez,
Enrique (Quique) Santolaya-Rey, Uwe Springmann, Jon Sundqvist, Miguel Urbaneja,

Keith Butler, Rolf-Peter Kudritzki, Adi Pauldrach,

Artemio Herrero, Francisco (Paco) Najarro,

Stan Owocki

and the VLT-FLAMES massive star team

… in the upper HRD!

- decisively controls evolution/fate of massive stars

> “… a change of only a factor of two in the mass-loss rates of massive stars has a dramatic effect on their evolution”
> (G. Meynet et al. 1994)

→ energy/momentum release

→ stellar yields (→ chemical evolution of clusters and galaxies)

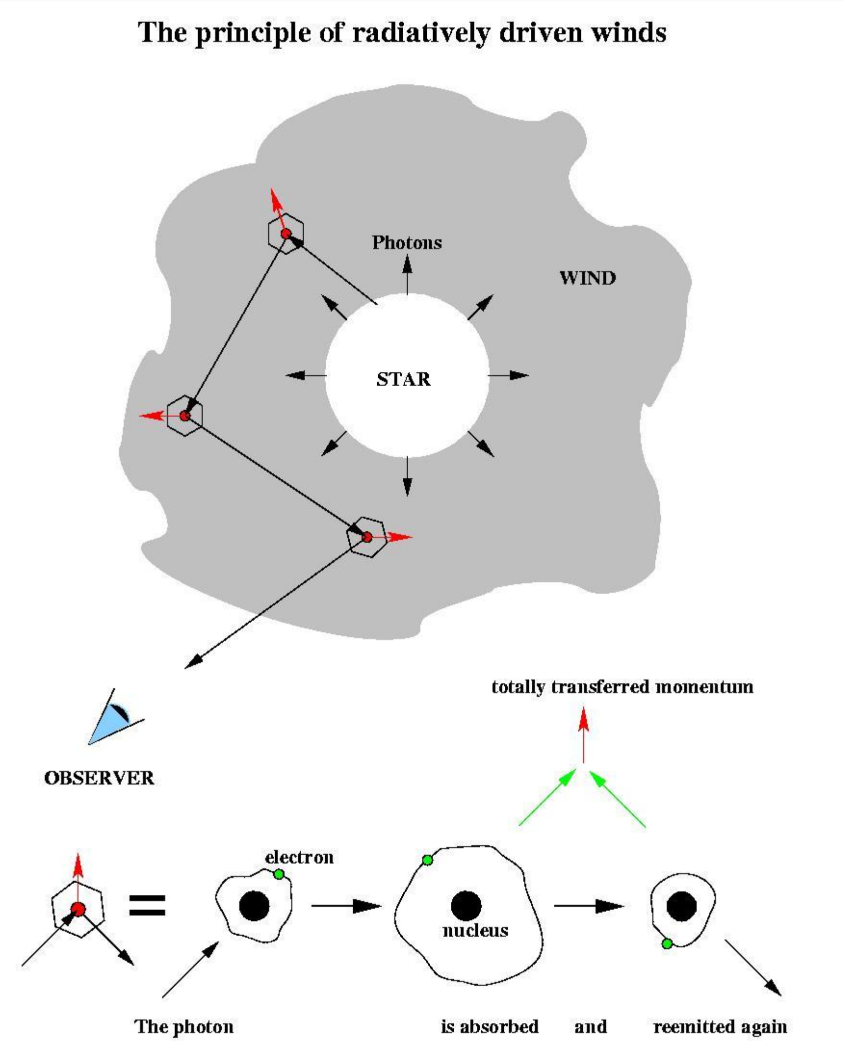

momentum transfer from metal ions (fraction 10^{-3}) to bulk plasma (H/He) via Coulomb collisions (e.g., Springmann & Pauldrach 1992, Krticka & Kubat 2000, Owocki & Puls 2002)

pioneering investigations by
Lucy & Solomon 1970, ApJ 159
Castor, Abbott & Klein 1975, ApJ 195

early improvements
(*quantitative* description/application**) by**
Friend & Abbott 1986, ApJ 311
Pauldrach, Puls & Kudritzki 1986, A&A 164

reviews
Kudritzki & Puls 2000, ARAA 38
Crowther 2007, ARAA 45 (Wolf-Rayets)
Puls, Vink & Najarro 2008, AARev 16/3

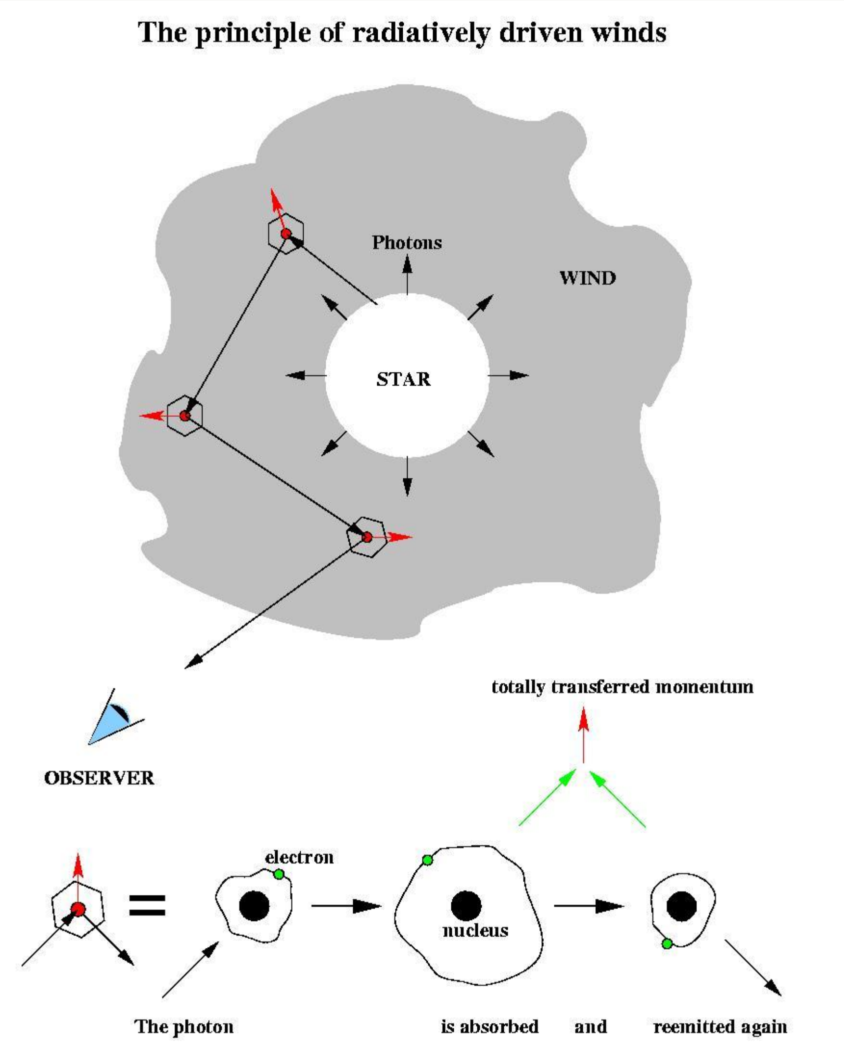

efficient line driving requires

- large number of photons → high luminosity → hot stars
- large number of interacting lines close to flux maximum
- mass-loss depends on metallicity!

$$\dot{M} \approx 10^{-7} \ldots 10^{-5}\ M_\odot / \mathrm{yr},\ v_\infty \approx 200 \ldots 2{,}000\ \mathrm{km/s}$$

for comparison: solar mass-loss $\approx 10^{-14} M_\odot / \mathrm{yr}$

pioneering investigations by
Lucy & Solomon 1970, ApJ 159
Castor, Abbott & Klein 1975, ApJ 195

early improvements
(*quantitative* description/application**) by**
Friend & Abbott 1986, ApJ 311
Pauldrach, Puls & Kudritzki 1986, A&A 164

reviews
Kudritzki & Puls 2000, ARAA 38
Crowther 2007, ARAA 45 (Wolf-Rayets)
Puls, Vink & Najarro 2008, AARev 16/3

Millions of lines ....

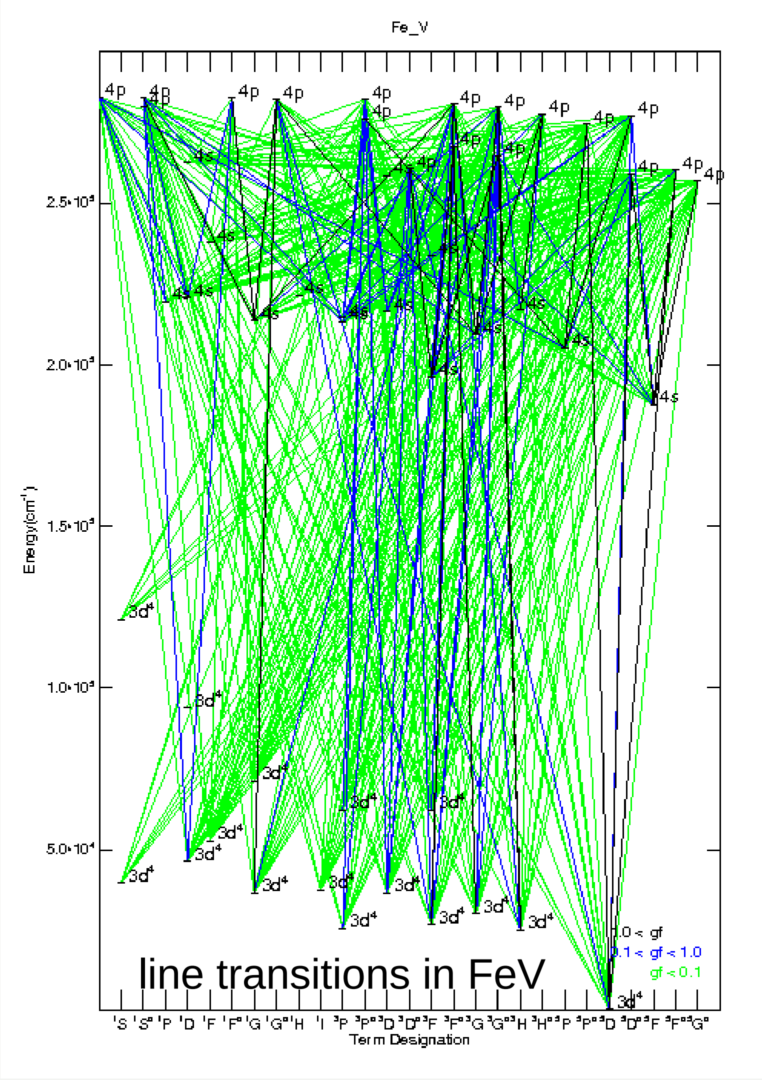

... are present
... and needed!

$$g_{rad}^{line} = \sum_{\text{all lines}} g_{rad}^{line,i}$$

The line-strength distribution function

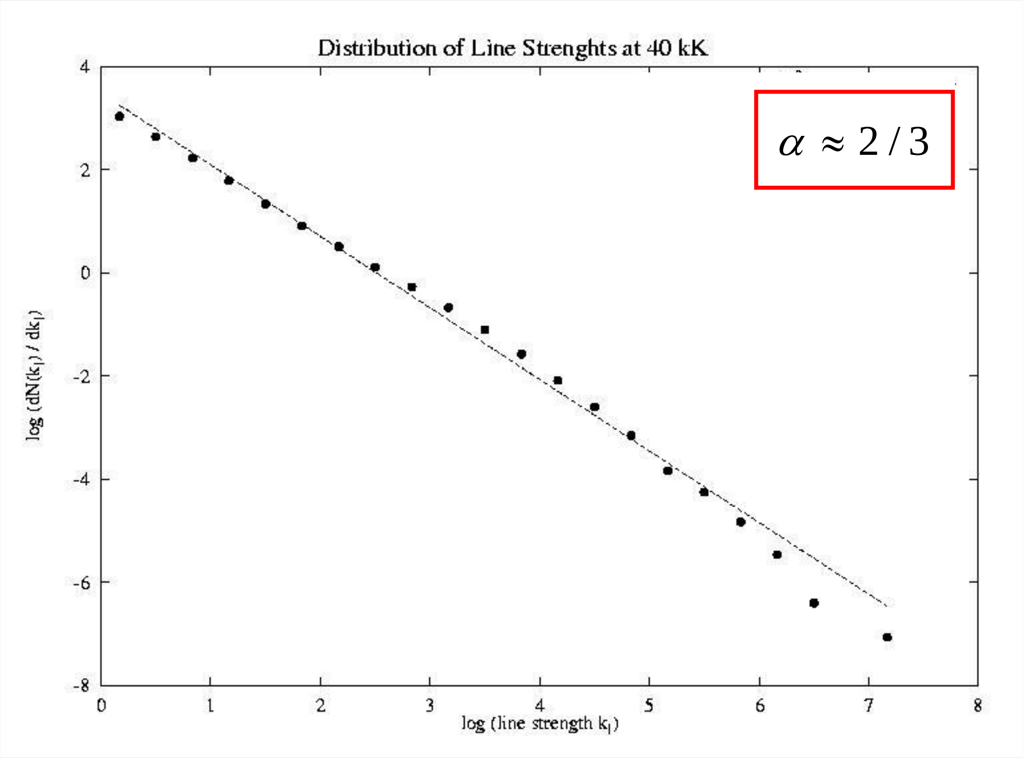

line-strength distribution function for an O-type wind at 40,000 K
4.2 Ml (Mega lines), 150 ionization stages (H – Zn), NLTE
(see Puls et al. 2000) .

line-strength $k^i = \dfrac{\bar{\chi}_i}{\Delta\nu_D\, \sigma_{Th}} =$

line opacity, measured in units of Thomson-scattering opacity

$$\frac{dN(k)}{dk} \propto N_{eff}\, k^{\alpha-2}, \quad \alpha \approx 0.5...0.7$$

N_{eff}: effective number of lines

α: slope of line-strength dist. function

dependent on metallicity and spectral type

Scaling relations (predicted)

- … calculate g_{rad}^{line} by integrating over line-strength distribution function (or explicit summation)
- solve equation of motion

=> scaling relations for line-driven winds (no rotation, non-Wolf-Rayets)

- $\dot{M} \propto N_{\mathrm{eff}}^{\frac{1}{\alpha'}} L^{\frac{1}{\alpha'}} \left(M(1-\Gamma)\right)^{1-\frac{1}{\alpha'}}$ scaling law for $\dot{M}$
- $v(r) = v_\infty \left(1 - \frac{R_*}{r}\right)^\beta$, β =0.8 (O-stars) ... 2 (BA-sg)
- $v_\infty \approx 2.25 \frac{\alpha}{1-\alpha} \underbrace{\left(\frac{2GM(1-\Gamma)}{R_*}\right)^{\frac{1}{2}}}_{\text{photospheric escape velocity}}$ scaling law for v_∞ $\begin{cases} \text{O-stars:} \approx 2{,}000 \text{ km/s} \\ \text{A-sg} \approx 200\text{-}400 \text{ km/s} \end{cases}$

Γ Eddington factor, accounting for acceleration by Thomson-scattering, diminishes effective gravity

$\alpha' = \alpha - \delta$, with δ ionization parameter, typical value for O-stars: $\alpha' \approx 0.6$

The wind-momentum luminosity relation (WLR)

- use scaling relations for $\dot{M}$ and v_∞, calculate modified wind-momentum rate

$$\dot{M} v_\infty \propto N_{\text{eff}}^{1/\alpha'} L^{1/\alpha'} \left(M(1-\Gamma)\right)^{1-1/\alpha'} \frac{\left(M(1-\Gamma)\right)^{1/2}}{R_*^{1/2}}$$

$$\dot{M} v_\infty R_*^{1/2} \propto N_{\text{eff}}^{1/\alpha'} L^{1/\alpha'} \cancel{\left(M(1-\Gamma)\right)^{3/2-1/\alpha'}}$$

$$\alpha' \approx \frac{2}{3} \rightarrow \frac{1}{\alpha'} \approx \frac{3}{2}$$

$$\log \dot{M} v_\infty \left(R_* / R_\odot\right)^{1/2} \approx \frac{1}{\alpha'} \log(L/L_\odot) + const(N_{\text{eff}})$$

- wind-momentum luminosity relation (WLR)
  (Kudritzki, Lennon & Puls 1995)

wind-momentum rate $\dot{M} v_\infty$, modified by $\left(R_* / R_\odot\right)^{1/2}$ depends almost exclusively on the stellar luminosity and on the distribution of the driving lines:

$$\boxed{\log\left(\dot{M} v_\infty \left(R_* / R_\odot\right)^{1/2}\right) \approx x \log\left(L_* / L_\odot\right) + const(z,\ \mathrm{sp.type})}$$

$x = \dfrac{1}{\alpha'}$, $\quad \alpha'$ related to slope of line-strength distribution function

$const \propto$ flux-weighted number of driving lines $\rightarrow f(z,\ \mathrm{sp.type})$

relation (almost) independent of M and Γ!!!!!

- Vink et al. (2000): “Mass-loss recipe” for solar abundance
  - validity of theoretical WLR concept!

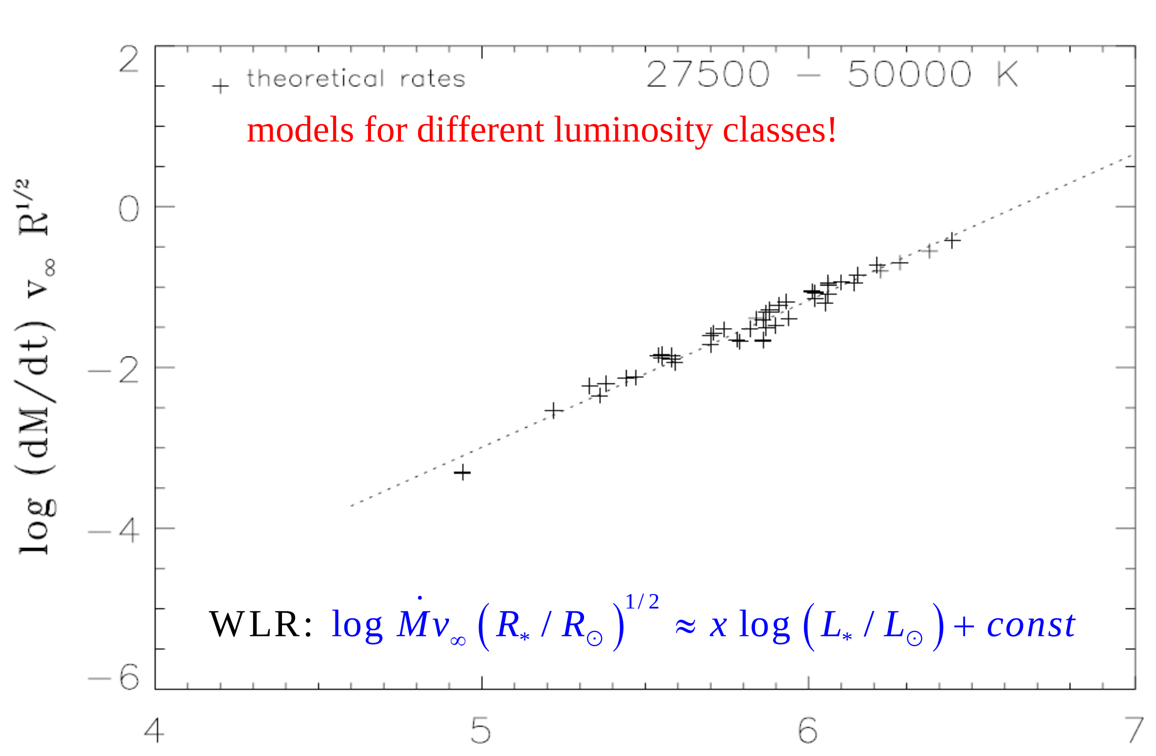

From Vink et al. (2000)

alternative 1-D models by

- Pauldrach (1987) and Pauldrach et al. (1994/2001), “WM-basic”
- Krticka & Kubat (2000/01/04/09), Krticka (2006)
- Kudritzki (2002, based on Kudritzki et al. 1989)
- Gräfener & Hamann (2005, 2008)
- Lucy (2007a, 2007b)
- Müller & Vink (2008)

Observational tests

- vast literature in the recent decade
- spectroscopic analyses performed by (spherical) NLTE atmosphere/spectrum synthesis codes, e.g.,
  - CMFGEN (Hillier & Miller),
  - WM-Basic (Pauldrach & co-worker),
  - Fastwind (Puls & co-worker)
- most important diagnostic tool to infer mass-loss rates:
  - H_α (Hydrogen – Balmer$_{alpha}$)

Essential results

- O-stars and BA-sg (also extragalactic) follow specific WLRs

Observational tests

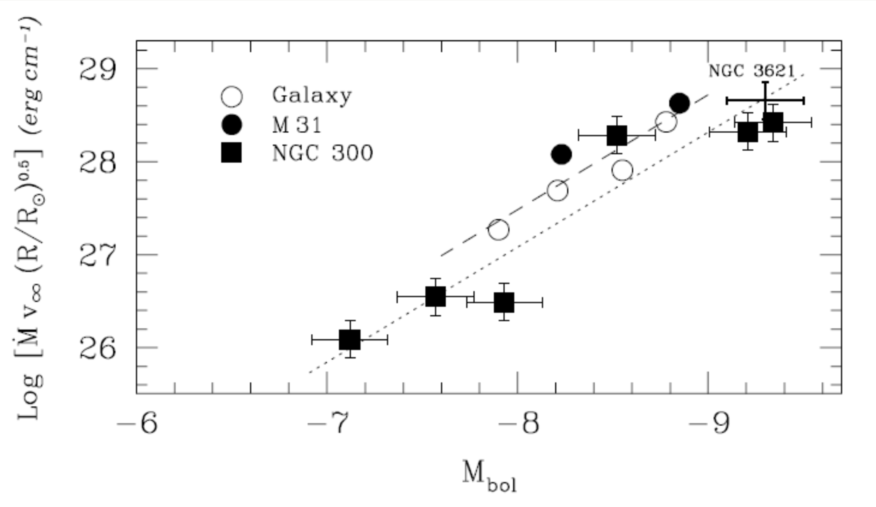

WLR for Galactic and extragalactic A-sg

- Dashed: Linear regression for Galactic and M31 (0.75 Mpc) objects.
- Dotted: Galactic relation scaled to the mean abundance of NGC 300 (2 Mpc) and NGC 3621 (6.7 Mpc), $z/z_\odot = 0.4$.

From Bresolin & Kudritzki 2004

Essential results

- O-stars and BA-sg (also extragalactic) follow specific WLRs

Observational tests

- vast literature in the recent decade
- spectroscopic analyses performed by (spherical) NLTE atmosphere/spectrum synthesis codes, e.g.,
  - CMFGEN (Hillier & Miller),
  - WM-Basic (Pauldrach & co-worker),
  - Fastwind (Puls & co-worker)
- most important diagnostic tool to infer mass-loss rates:
  - H_α (Hydrogen – Balmer$_{alpha}$)

Essential results

- O-stars and BA-sg (also extragalactic) follow specific WLRs
- scaling $v_{inf} \sim v_{esc}$ confirmed
- theoretical WLR from Vink et al. (2000) met, except for
  - some (all?) low luminosity O-dwarfs (both Galactic and SMC): derived wind-momenta much “too low” → ‘weak winds’

Observational tests

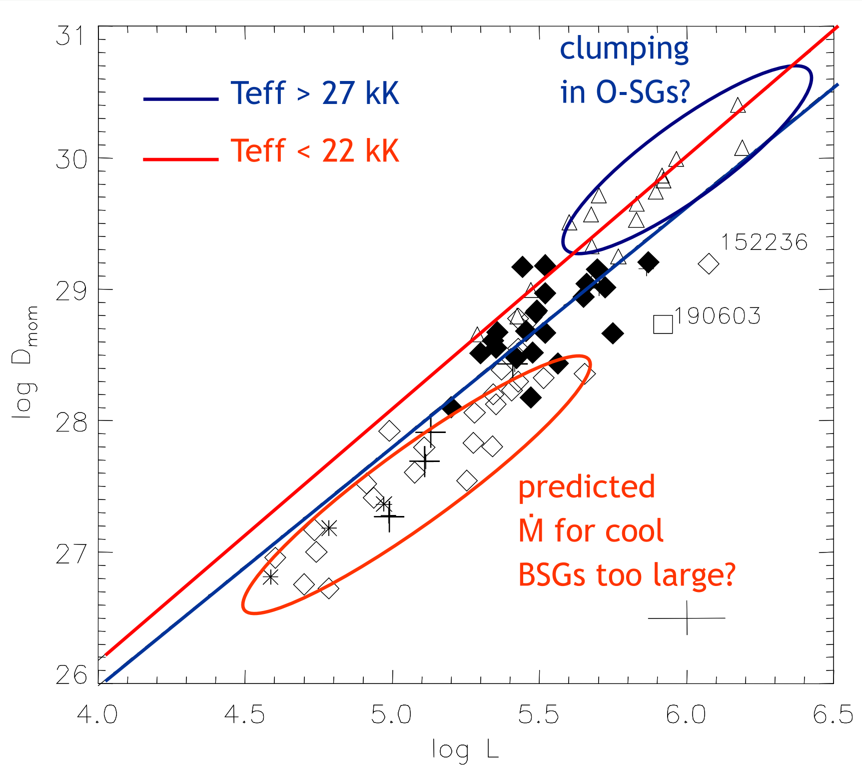

D_{mom} = modified wind momentum rate

Observed WLR for Galactic OB-supergiants
(from Markova & Puls 2008, including results by Crowther et al. 2006)

Essential results

- O-stars and BA-sg (also extragalactic) follow specific WLRs
- scaling $v_{inf} \sim v_{esc}$ confirmed
- theoretical WLR from Vink et al. (2000) met, except for
  - some (all?) low luminosity O-dwarfs (both Galactic and SMC): derived wind-momenta much “too low” → ‘weak winds’
  - O-sg with rather dense winds: derived wind-momenta “too large” → clumping (later)
  - B-sg display lower wind-momenta than predicted
    (for aficionados: lower than predicted from ‘bi-stability jump’)

Metallicity dependence

- line driving due to metal lines → less metals, less driving
- theoretical predictions from hydro-models
  - Kudritzki (2002), Krticka (2006): $v_\infty \propto z^{0.06...0.12}$
  - Vink et al. (2001), Krticka (2006): $\dot{M} \propto z^{0.64...0.69}$

- roughly 60 SMC/LMC O-/early B-stars from the **VLT FLAMES survey of massive stars**
  - S. Smartt (PI), Evans et al. (2005/2006/2008) and many more
- data analysis by Mokiem et al. (2006, 2007)

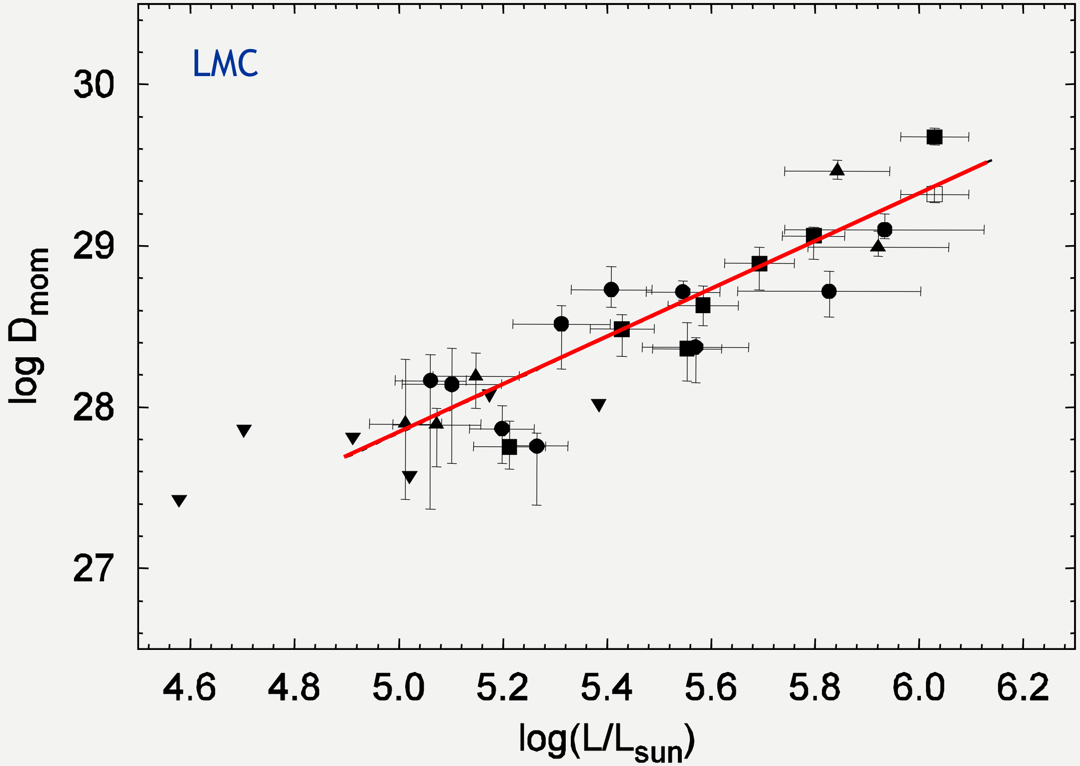

circles: lc I
squares: lc III
triangles: lc V
inverted triangles: upper limits

Metallicity dependence of wind-momenta: observations vs. theory

- roughly 60 SMC/LMC O-/early B-stars from the **VLT FLAMES survey of massive stars**
  - S. Smartt (PI), Evans et al. (2005/2006/2008) and many more
- data analysis by Mokiem et al. (2006, 2007)
- combination with data from previous investigations

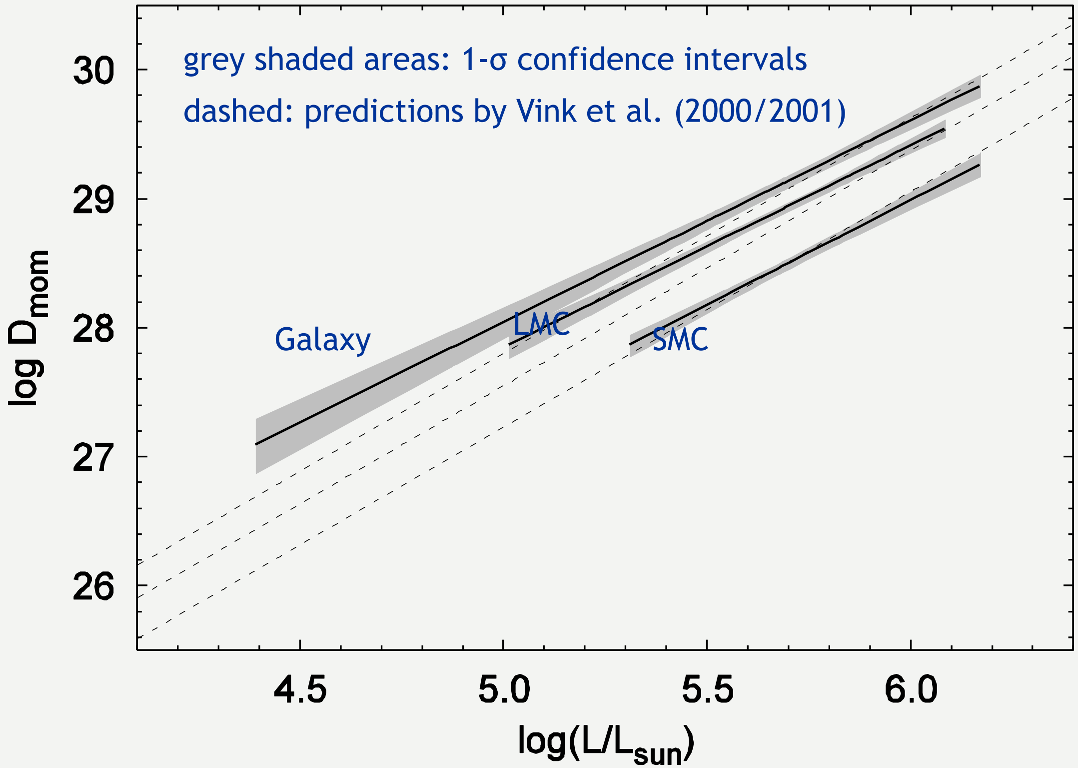

Final results

- wind-momenta increase with z as

$$\boxed{\dot{M} \propto z^{0.62\pm0.15}}$$

✓ consistent with the predictions from hydrodynamical models (and line statistics)

Mass-loss from Wolf-Rayet stars

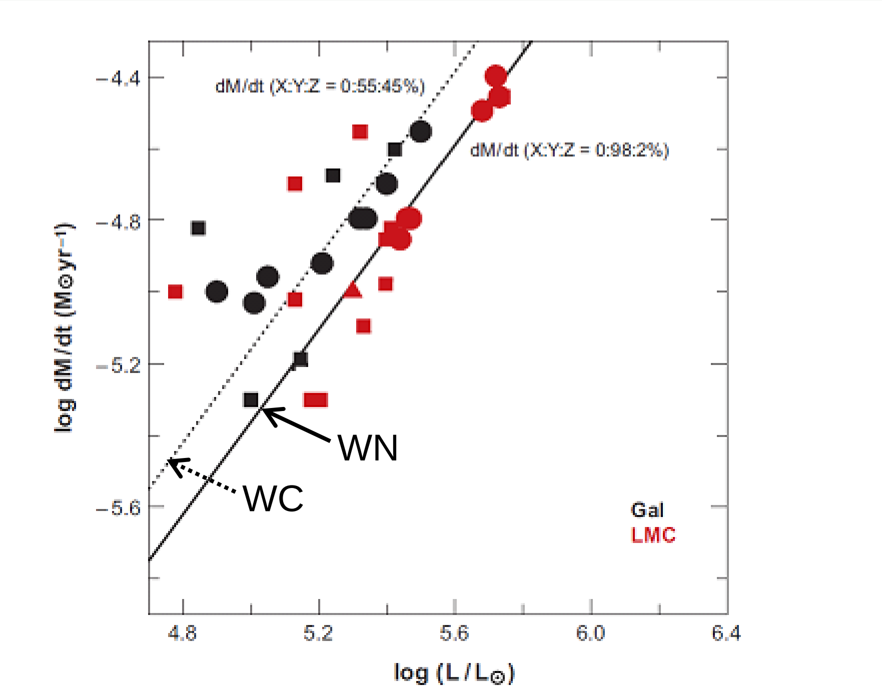

squares: WN (no surface hydrogen)
circles: WC

solid/dotted line**: empirical** 'Mass-loss recipe' from Nugis & Lamers (2000) for WN and WC stars

From Crowther (2007)

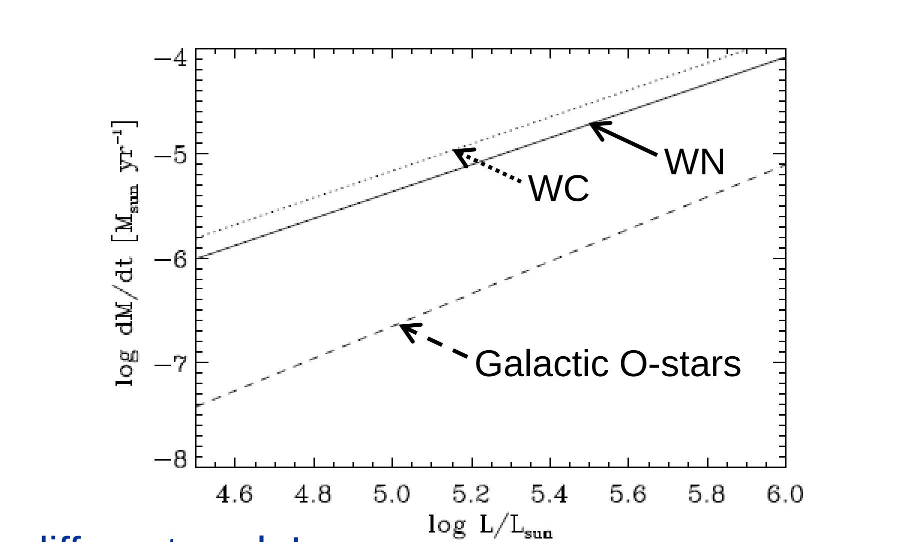

different scale!

difference in mass-loss rate more than a factor of 10!

'standard theory' fails!

Hydrodynamical models of WR winds

Gräfener & Hamann (2005/2006/2007):

→ two ingredients required to produce large mass-loss rate + large v_{inf} (≈2,000 km/s)

- large Eddington factor
  → low effective gravity
  → deep lying sonic point at high temperature
- mass-loss initiated at opacity ‘bump’ due to Fe (until XVII) at >160,000 K
  (idea by Nugis & Lamers 2002)

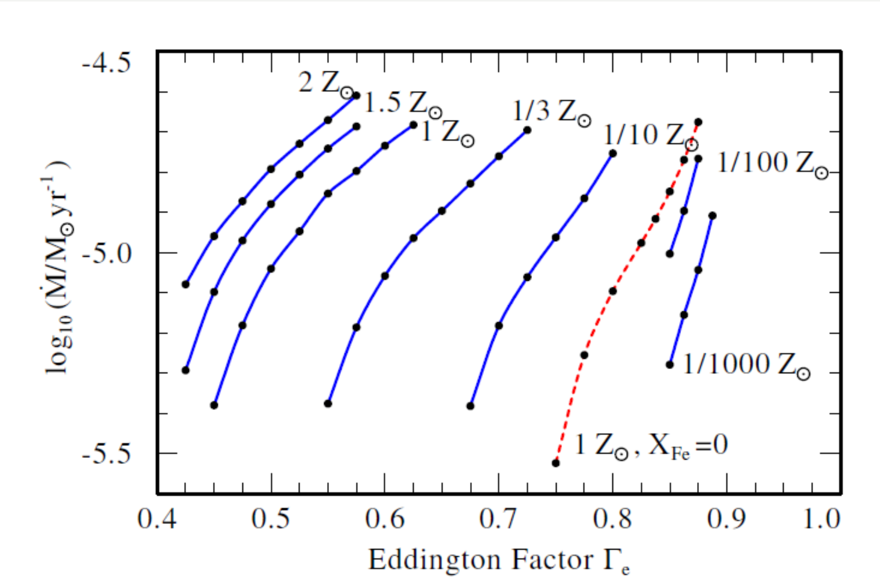

From Gräfener & Hamann (2008)

Alternative wind models from Vink et al.(2011)

- for Γ_e >0.7, winds become optically thick, ‘more’ mass-loss created
- certain differences to models by Gräfener

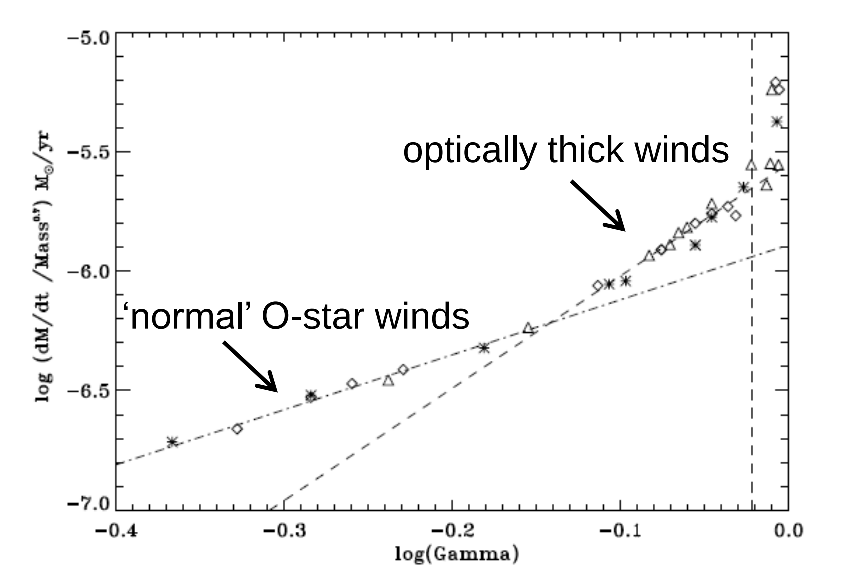

From Vink et al. (2011)

NOTE: WR mass-loss still not completely understood!

- Clumping hypothesis
  - various direct and indirect indications that winds not smooth
  - instead, small scale density inhomogeneities present:

    matter concentrated in overdense clumps, inter-clump medium almost void

- Theory …

The line driven instability

- Winds from hot stars driven by radiative line acceleration

g_{rad}^{line} highly unstable (Lucy & Solomon 1970, Owocki & Rybicky 1984, 1985, Owocki & Puls 1999)

$\rightarrow$ density/velocity inhomogeneities

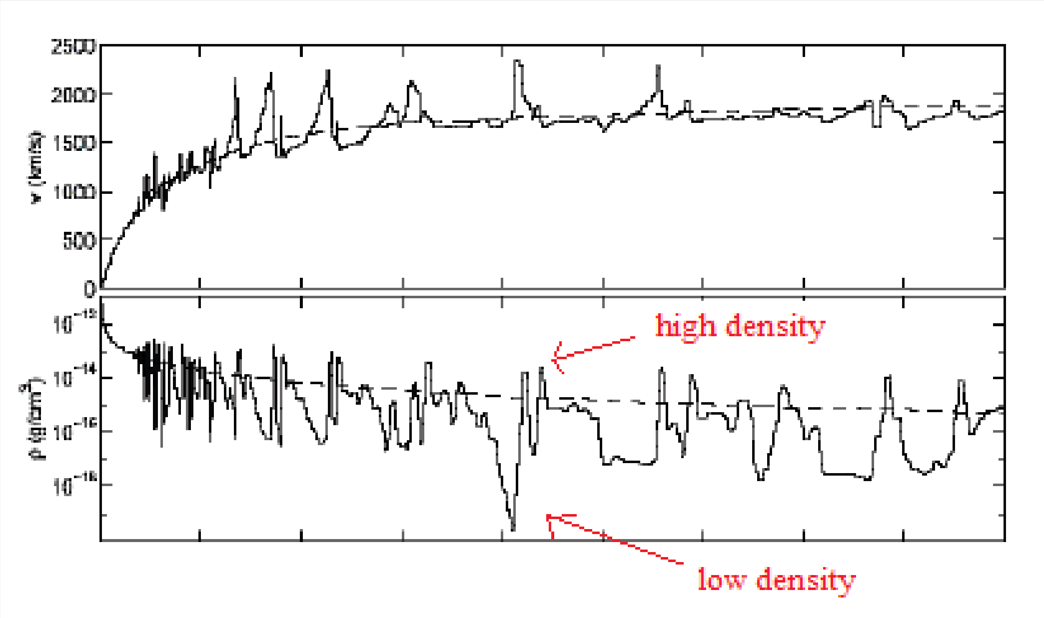

- Snapshot from a 1-D radiation hydrodynamic, time-dependent model from Runacres & Owocki (2002).
- Spatial/time-averaged structure/mass-loss rate very similar to *stationary* theoretical wind models.

… however, the resulting structure seriously affects the radiative transfer, and hence the mass-loss rates *inferred from observations,*

… diagnostic tools (stationary atmospheres) need to account for inhomogeneities

Reduction of mass-loss rates

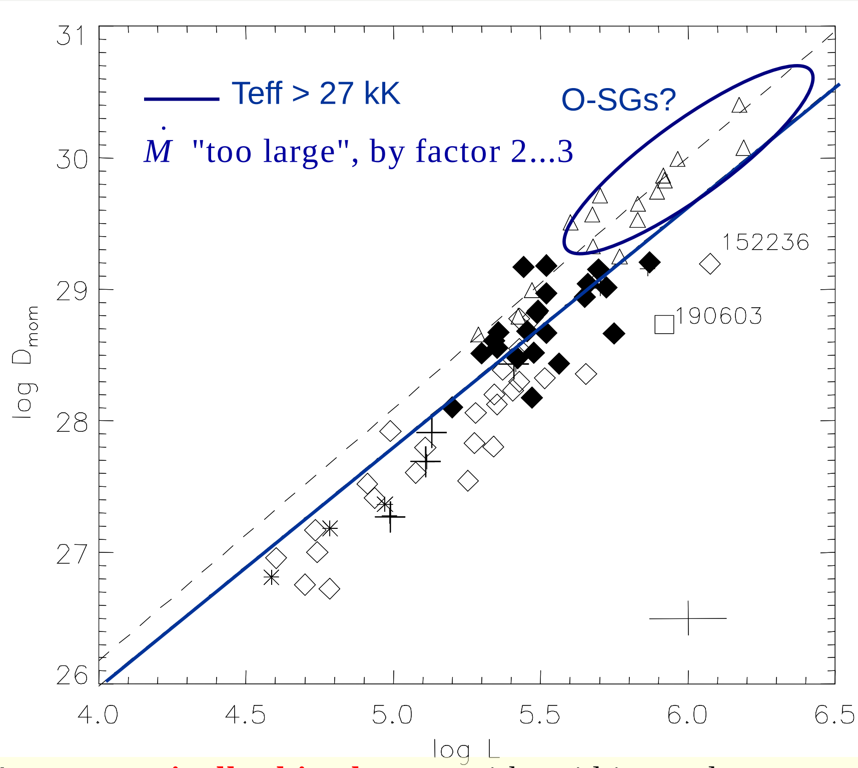

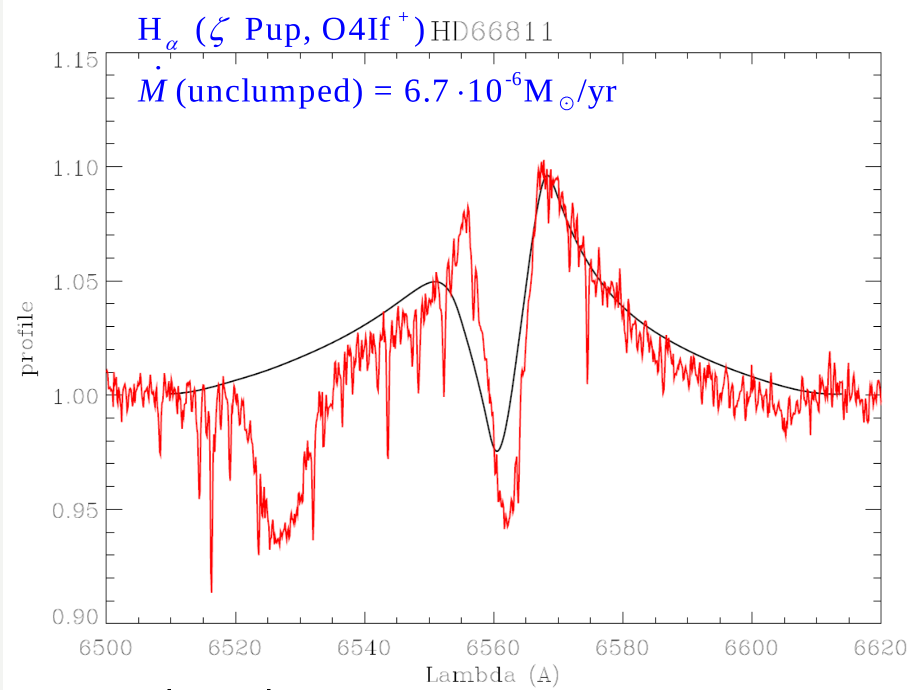

From Puls et al. 2006

Assume **optically thin clumps** with void inter-clump matter

$\rho_{cl} = f_{cl} \langle \rho \rangle$, with $\langle \rho \rangle$ average (= smooth, stationary) density

is overdensity inside clumps, f_{cl} is 'clumping factor'

$\Rightarrow$ All recombination based diagnostics (H_α, radio free-free)

require lower $\dot{M}$ than derived from homogeneous models,

by factor $\sqrt{f_{cl}}$

Reduction of mass-loss rates

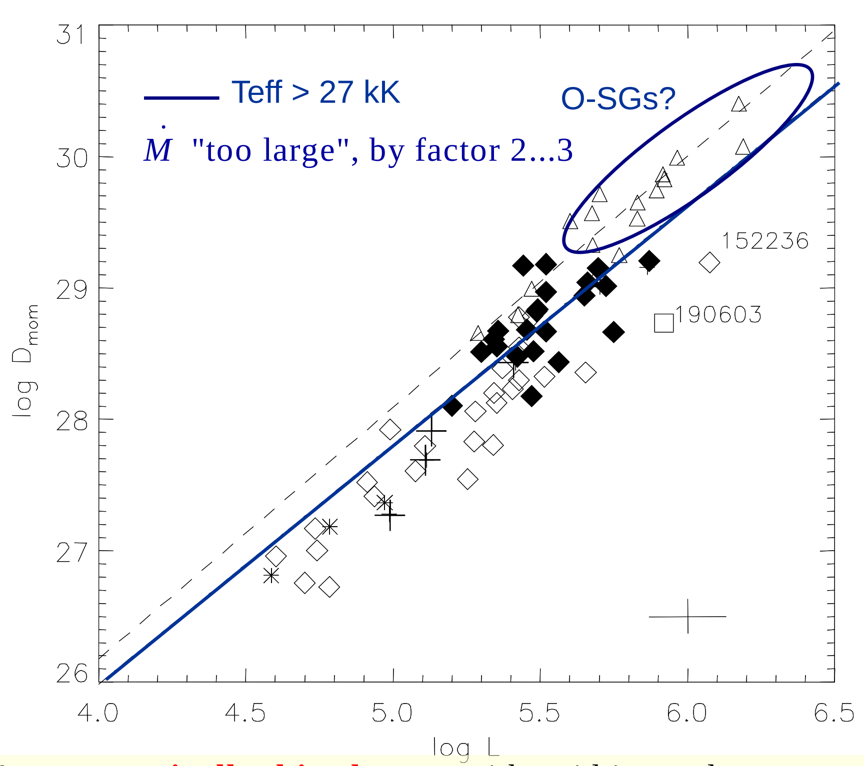

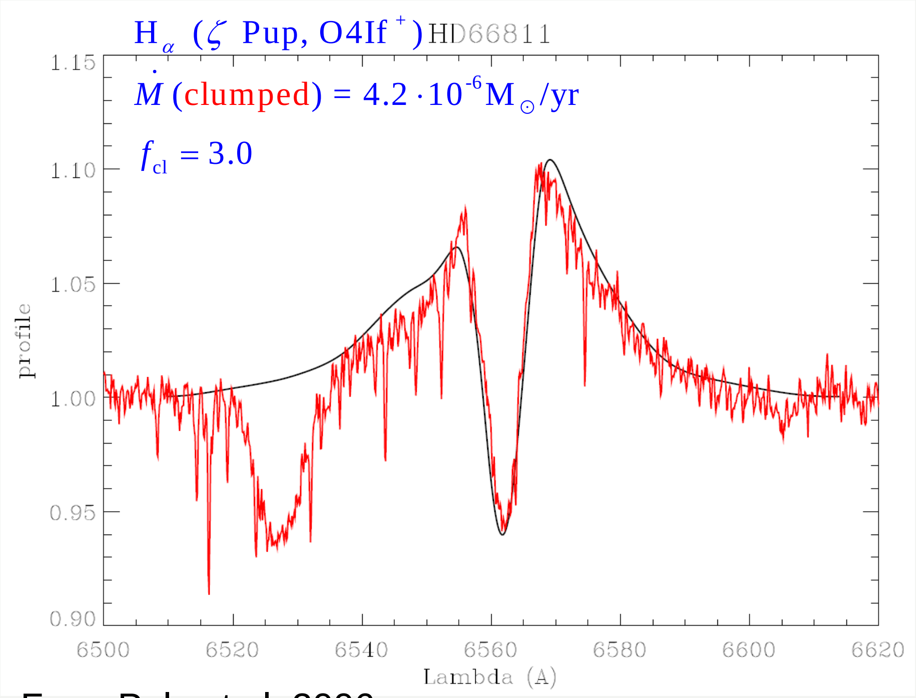

From Puls et al. 2006

Assume **optically thin clumps** with void inter-clump matter

$\rho_{cl} = f_{cl} \langle \rho \rangle$, with $\langle \rho \rangle$ average (= smooth, stationary) density

is overdensity inside clumps, f_{cl} is 'clumping factor'

$\Rightarrow$ All recombination based diagnostics (H_α, radio free-free)

require lower $\dot{M}$ than derived from homogeneous models,

by factor $\sqrt{f_{cl}}$

- (F)UV line-diagnostics (FUSE)
  - Massa et al. (2003) and Fullerton et al. (2006)
    PV (Phosphorus^{4+}) line at 1120 Å indicates factor of 10 (or more) lower mass-loss rates than derived from unclumped Hα and/or radio diagnostics (i.e., $f_{\mathrm{cl}} \gtrsim 100$!!!!)
  - Prinja et al (2005) : similar effect in FUV wind lines from lower luminosity B supergiants
  - If such large reductions in mass-loss rate were true, enormous consequences for stellar evolution and feed-back
  - "allowed" reduction from evolutionary constraints: at most by a factor of 2-4 (Hirschi 2006)
  - Where is the mass then lost?
  - LBV phase? (Smith & Owocki 2006)

Porosity?

- **possible resolution:** “Porosity”
  (Oskinova et al. 2007, based on an idea by
  Owocki et al. 2004)
  - idea: clumps optically thick in resonance lines
    → *geometrical distribution, size and shape* become important
  - effective opacity is reduced (i.e., wind becomes more transparent),
    - because radiation can propagate through “holes” in between clumps, and
    - because of saturation effects
      (e.g., clumps “hidden” behind others become ineffective
      (since first clump already optically thick)

- **speculation:** less mass-loss reduction than suggested by PV-diagnostics?

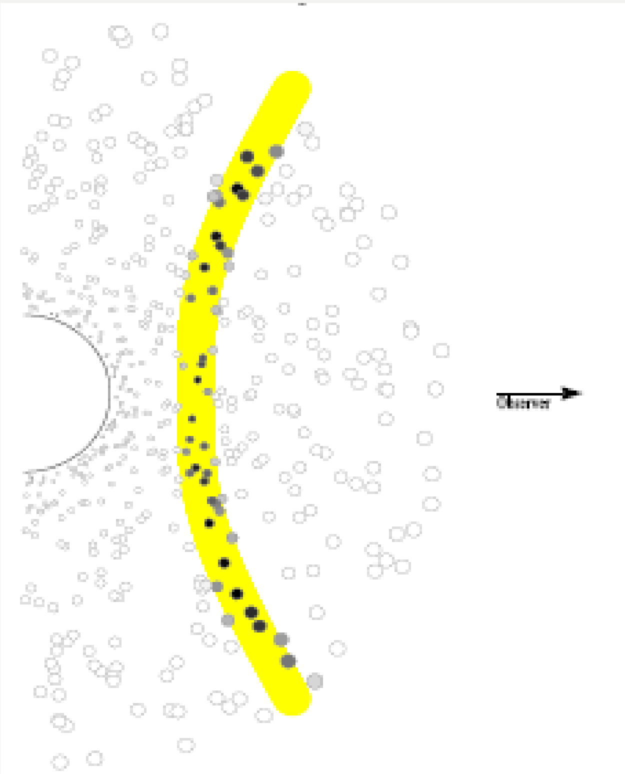

From Oskinova et al. (2007)

Optically thick clumps

Sundqvist et al. (2011):
clumps indeed optically thick in resonance lines!

→need to improve clumping model

- 2D/3D winds constructed either from **hydrodynamic** or **stochastic models** involving a parameterized description of clump structure and distribution

\+ detailed radiative transfer directly on structured medium to compute synthetic spectra

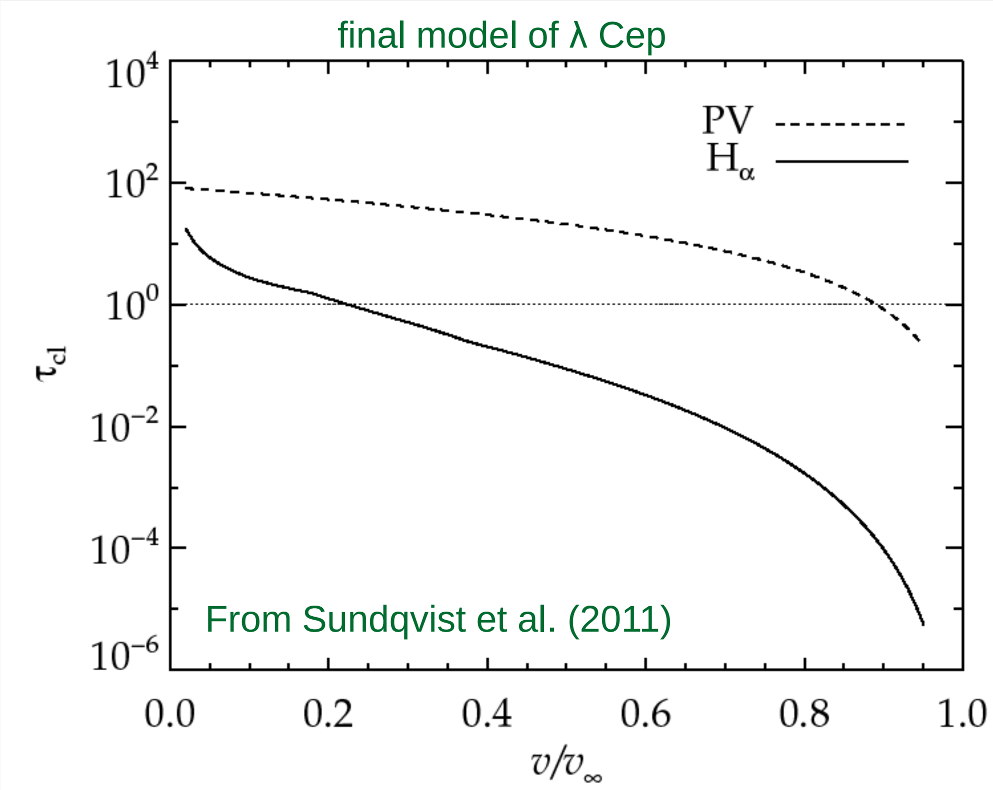

End of clumping crisis?

Test bed λ Cep

H_α and PV consistent with $dM/dt=1.5\cdot10^{-6}\ M_\odot/yr$

for comparison
$dM/dt=3.20\cdot10^{-6}\ M_\odot/yr$ (theoretical)
$dM/dt=0.25\cdot10^{-6}\ M_\odot/yr$ (optically thin clumps)

‘only’ factor of two discrepancy between theory and inferred mass-loss rate

promising, but not the last word
Multi-wavelength studies of many stars required!

Thus remember:

- Mass-loss rates from OBA-stars insecure
- situation for WR-winds seems to be clearer

From Sundqvist et al. 2011

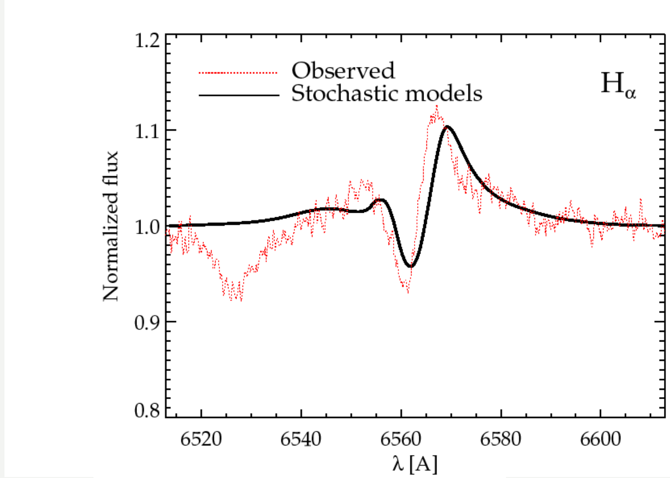

$dM/dt = 1.5\cdot10^{-6}\ M_\odot/yr$

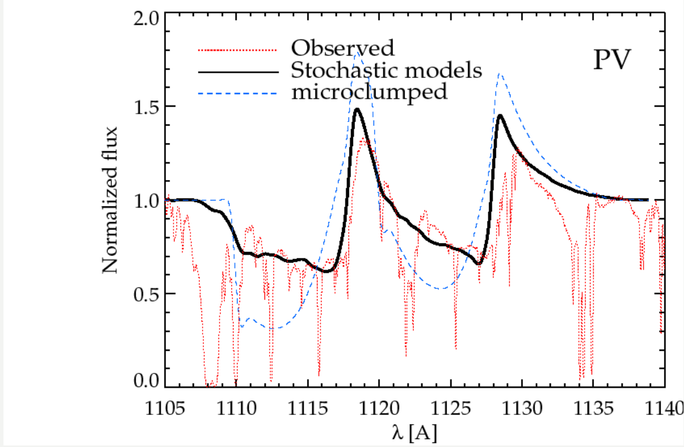

Non-thermal radio emitters

- most massive stars with winds of significant strength are thermal radio emitters: f-f emission in the wind
- but, decent number of known non-thermal radio emitters
  - different spectral slope, much higher brightness temperature, variability in radio-flux
  - 17 WR-, 16 O-stars, see review by de Becker (2007, AARev)
- early suggestion: *synchrotron radiation* (White 1985)
- needs B-field and
  shocks + B-field for acceleration of electrons (DSA)

- B-fields:
  - 'strong' fields (> 100 Gauss at surface) **not** common in OB-stars
    occurrence in less than 10%; see recent work by J.-F. Donati et al., C. Neiner et al., S. Hubrig et al. + MiMeS collaboration (G. Wade et al., 'Magnetism in massive stars')
  - but required field-strength – O(1-10 Gauss) below present detection limit
- three different sites of shocks …

Non-thermal emission/cosmic rays from wind-embedded shocks?

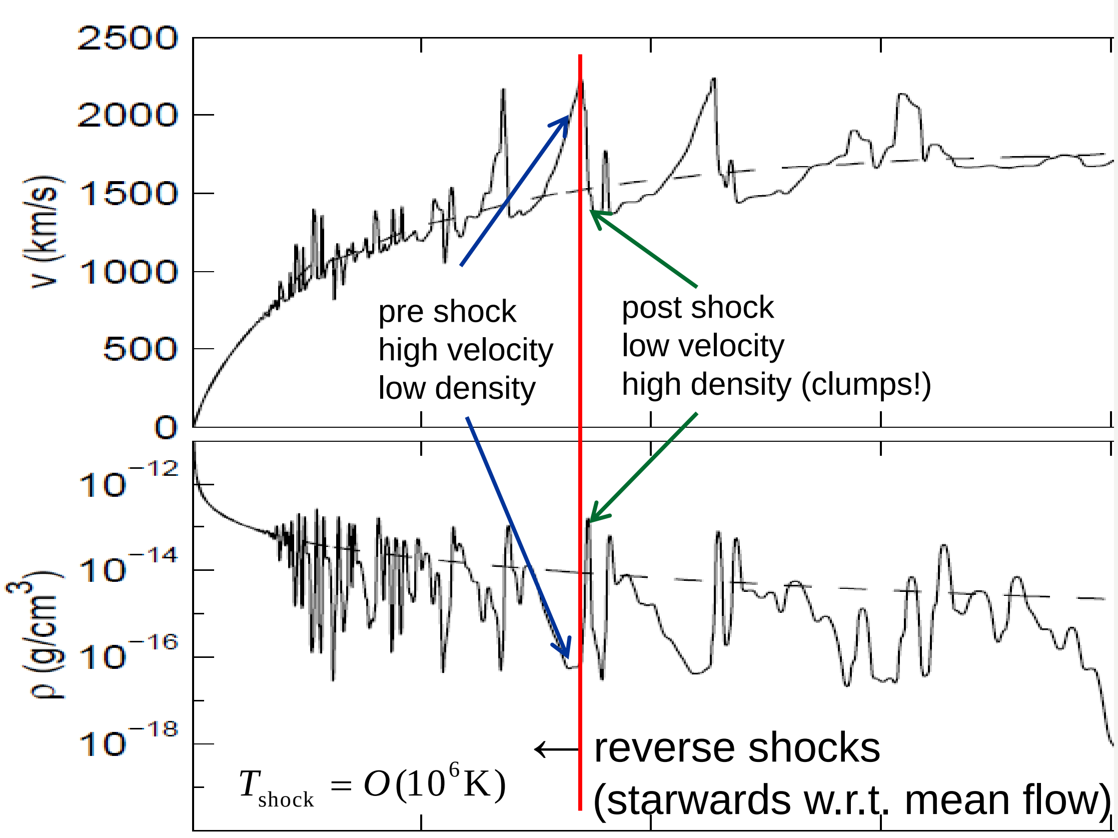

Note: very high compression ratio in intermediate wind, since isothermal shock (effective radiative cooling)

White, R.L. (1985)
- wind-embedded (forward!) shocks accelerate electrons to relativistic energies
- acceleration by multiple shocks
- hot stars potentially strong emitters of γ- and cosmic rays

White & Chen (1992)
- similar model; relativistic ions (protons) collide with thermal ions (protons)
- e.g., $p+p \rightarrow p+p+\pi^0$; $\pi^0 \rightarrow 2\gamma$

van Loo et al. (2006)
- 'intermediate' wind cannot contribute to observed non-thermal emission, since f-f absorption
- synchrotron flux needs to be created around radio-photosphere (> 50-100 R_*)
- in the outer wind, velocity jumps and compression ratios too low to produce enough synchrotron flux

P. Edmon (2010, thesis)
- 2-D MHD-DSA simulations
- wind-embedded shocks capable of accelerating electrons up to 100 MeV and protons up to 1 GeV with $f(p) \sim p^{-4}$
- presumably no radio emission, due to f-f absorption

Situation still unclear!

Pressure of relativistic particles on shocks needs to be accounted for!

Wind-wind collisions (O+O or O+WR)

seminal papers (not complete)

- Prilutskii & Usov (1976)
- Kallrath (1991)
- Pittard (2009)
- Luo et al. (1990)
- Stevens et al. (1992)

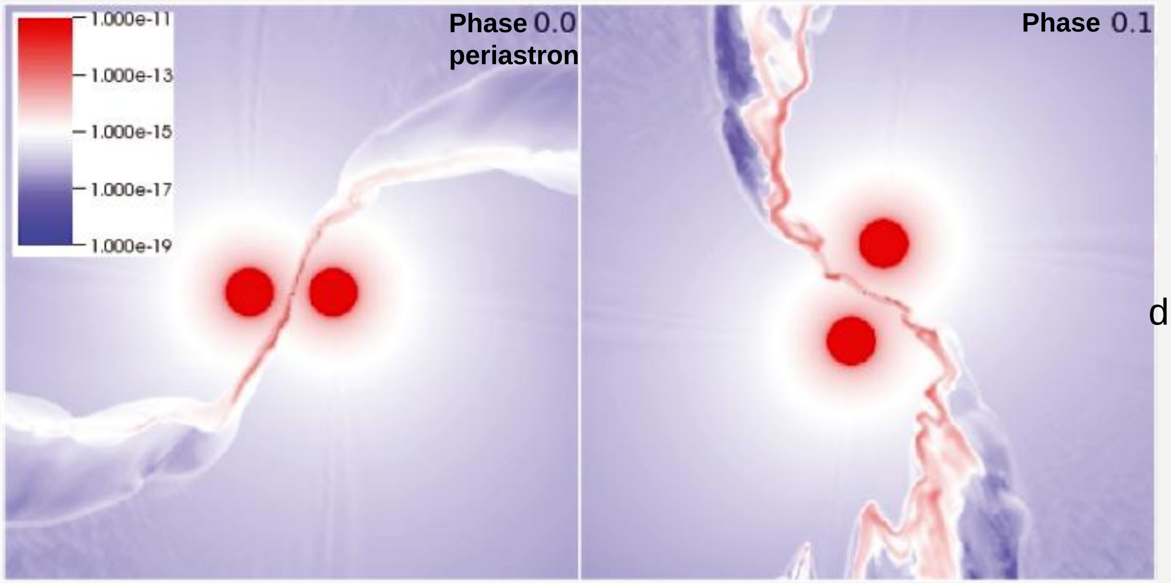

3-D hydro simulations of an O6V+O6V binary with eccentric orbit and colliding winds (from Pittard 2009)

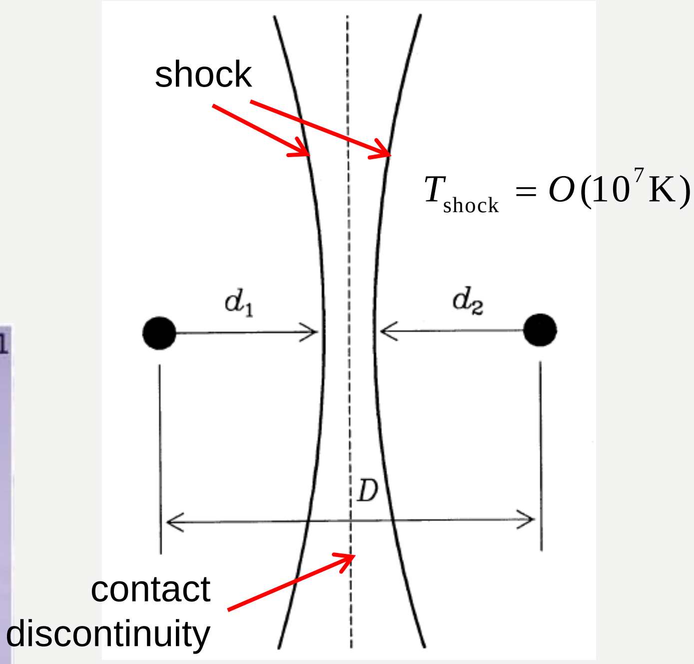

wind-wind collision from two identical stars/winds, rotational effects neglected (from Stevens et al. 1992)

Wind-wind collisions (O+O or O+WR)

seminal papers (not complete)

- Prilutskii & Usov (1976)
- Kallrath (1991)
- Pittard (2009)
- Luo et al. (1990)
- Stevens et al. (1992)

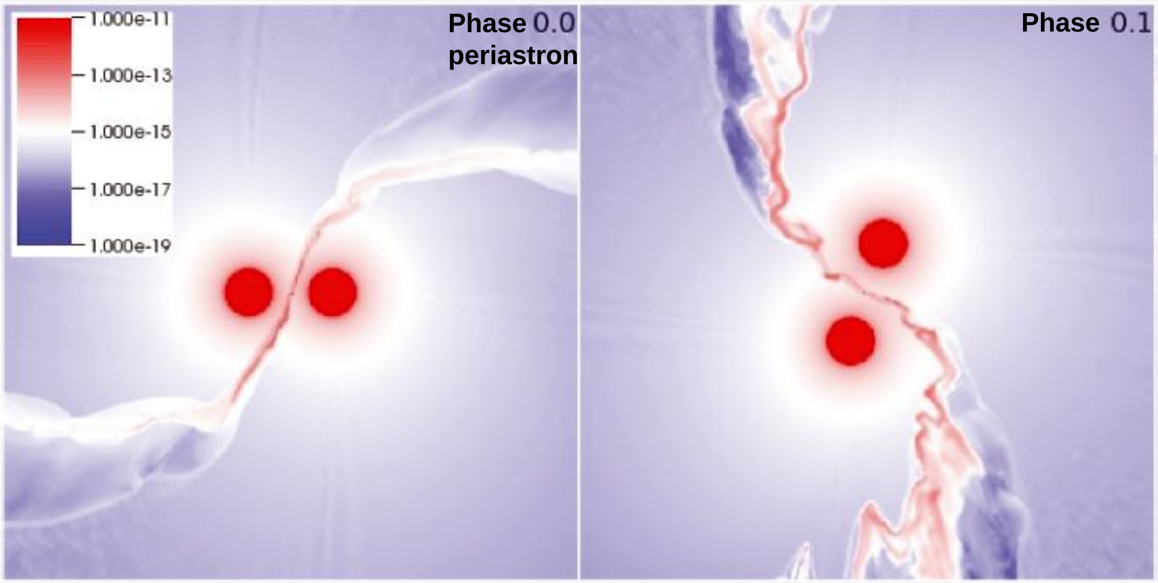

3-D hydro simulations of an O6V+O6V binary with eccentric orbit and colliding winds (from Pittard 2009)

Review by de Becker (2007)

- wind-wind collision most likely scenario for non-thermal emission from WRs and O-stars

Many results/models inspired by observations of **WR 140** (WC7+O5)

- long period (7.9yr), highly eccentric (e=0.88)
- e.g., Dougherty et al. (2005)
- multi-wavelength studies during periastron passage in 2009 (reviewed by Williams 2009)

Lots of recent developments, e.g.

Pittard & Dougherty (2006)

- influence of relativistic electrons on shock structure, stepwise acceleration of electrons (at first in wind, then in collision zone)

Reimer et al (2006)

- self-consistent particle acceleration, high energy electron and proton spectra with emission from IC (Thomson + Klein Nishima) and π^0 - decay

P. Edmon (2010, thesis)

- 2-D MHD-DSA simulations, including feedback by cosmic rays
- strong shocks capable of accelerating electrons up to 1 GeV and protons up to 1 TeV with $f(p) \sim p^{-4}$

Cosmic rays from wind terminal shock?

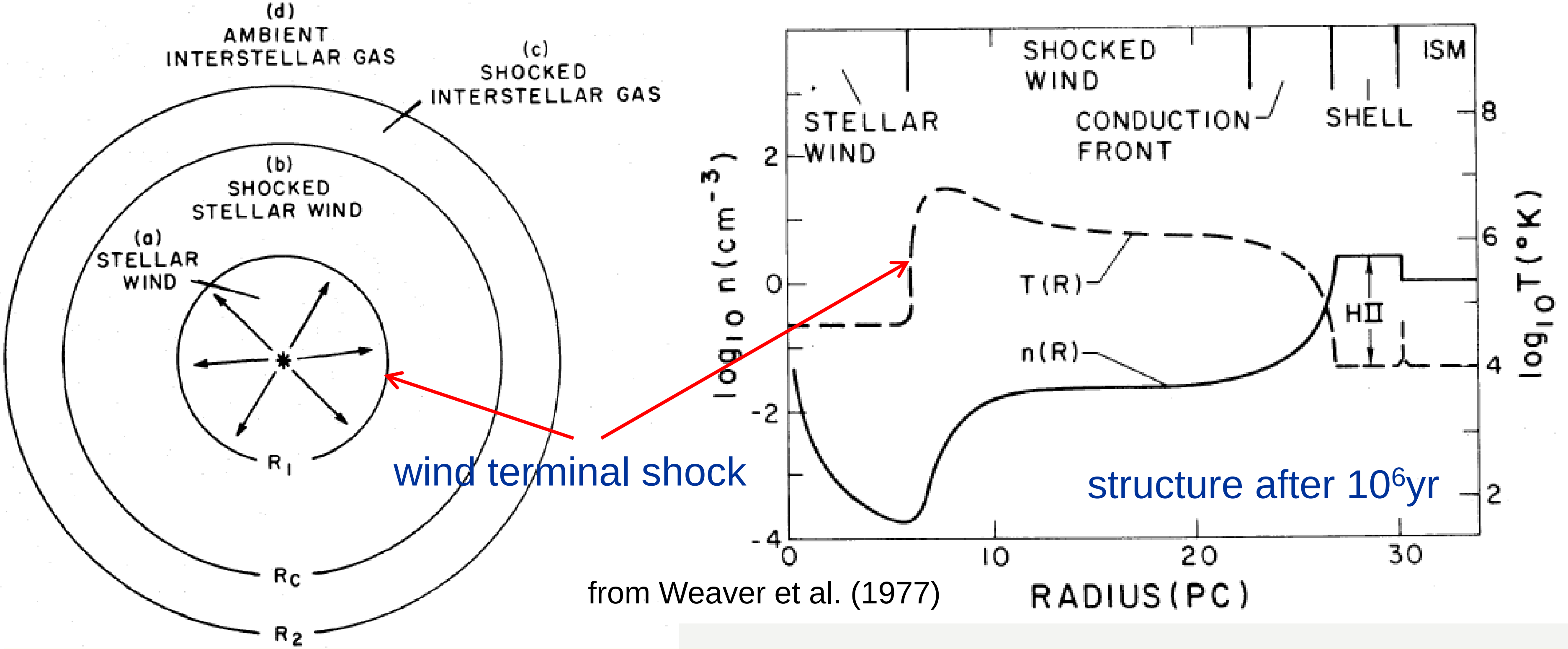

from Weaver et al. (1977)

structure and evolution of 'wind bubble' : first description by Castor et al. (1975), Weaver et al. (1977)

- early studies on acceleration of CRs: Casse' & Paul 1980, Völk & Forman (1982) …
- evolution of massive star: bubble shaped by winds of different strengths
  O-star (fast wind of intermediate strength) → BA supergiant (intermediate velocity and strength) → RSG (slow, dense) → WR (fast, dense) → SN
- SN shock wave interacts with bubble, e.g., Dwarkadas (2005), **and next talk …**

No summary …

… but remember

- winds from hot stars fairly well understood (incl. rotational effects, not covered here…)
- however, mass-loss rates (both theoretical and observationally inferred) still affected by uncertainties, due to wind-clumping
- massive star evolution strongly depends on mass-loss rates, thus also insecure …

… leads to *deformation of photosphere* and *gravity darkening*

(following effects important only for $v_{rot} \geq 0.7 v_{crit}$)

- deformation of photosphere due to centrifugal forces (Collins 1963, Collins & Harrington 1966, see also Cranmer & Owocki 1995).
- theory (using a Roche model with point mass): maximum value of R(equator)/R(pole) = 1.5 at critical rotation

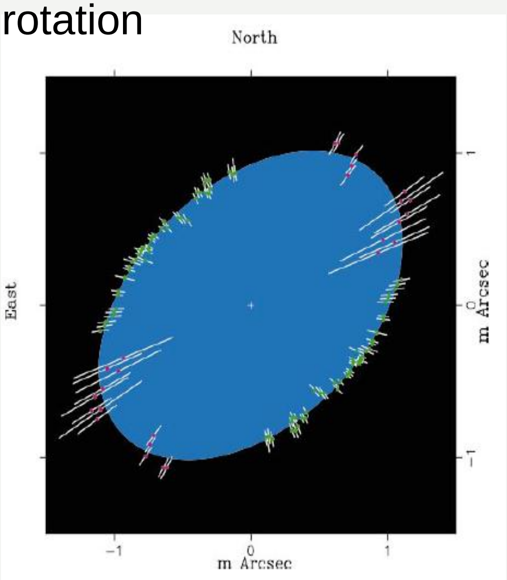

- first observational test bed:
  Achernar (α Eridani, HD10144, B3Vpe),
  brightest Be star known;
  Domiciano de Souza et al. 2003) with VLTI:
  R(equator)/R(pole) = 1.56 ± 0.05
- to date, 6 rapid rotators observed/analyzed
  (-> reviewed by van Belle 2010)

- Gravity darkening (von Zeipel, 1923, + Maeder, 1998)

$$\mathbf{F} \propto \mathbf{g}_{\rm eff}\,(1+\zeta(\vartheta)), \qquad |\zeta(\vartheta)| < 0.1 \text{ in most cases, with co-latitude } \vartheta$$

$$\mathbf{g}_{\rm eff} = \mathbf{g}_{\rm grav} + \mathbf{g}_{\rm cent} \begin{cases} = \ \mathbf{g}_{\rm grav} & \text{at pol} \\ < \ \mathbf{g}_{\rm grav} & \text{at equator} \end{cases}$$

$$\Rightarrow T_{\rm eff}(\vartheta) \propto g_{\rm eff}(\vartheta)^{1/4} \text{ for radiative envelopes, decreases towards equator, 'gravity darkening'}$$

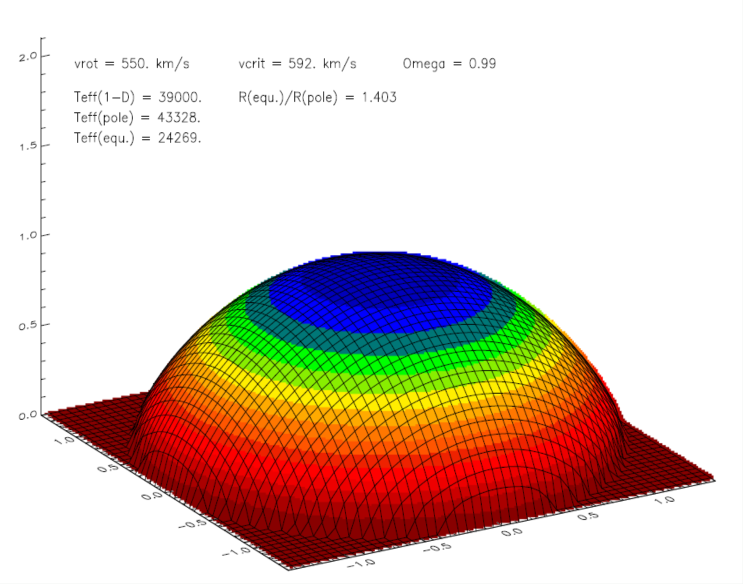

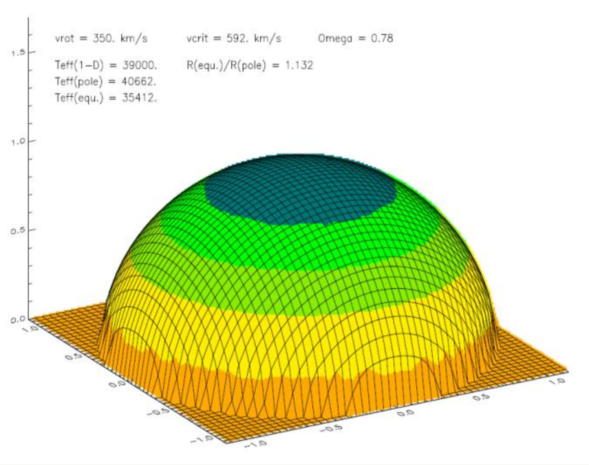

Rapid rotation and winds

- including gravity darkening into radiative line-driving/hydro-simulations

two possibilities:

a) ionisation equilibrium rather constant as a function polar angle, θ (O-stars)

$\Rightarrow \dot{M}(\theta) \propto g_{\rm eff}(\theta)$, prolate wind (less loss of angular momentum!),

since $g_{\rm eff}(\theta) \rightarrow F(\theta)$ largest at pole

[$g_{\rm eff}$ – effect, Owocki et al. 1998, Maeder 1999, Maeder & Meynet 2000]

b) *if* ionisation equilibrium (strongly) dependent on polar angle θ (since $T_{\rm eff}$ decreases towards equator)

$\Rightarrow \dot{M}(\theta) \propto \left(N_{\rm eff}(\theta)\right)^{1/\alpha'(\theta)} g_{\rm eff}(\theta)$,

might induce oblate wind in B-supergiants (no thin disk!)

[κ – effect, Maeder 1999, Maeder & Meynet 2000]

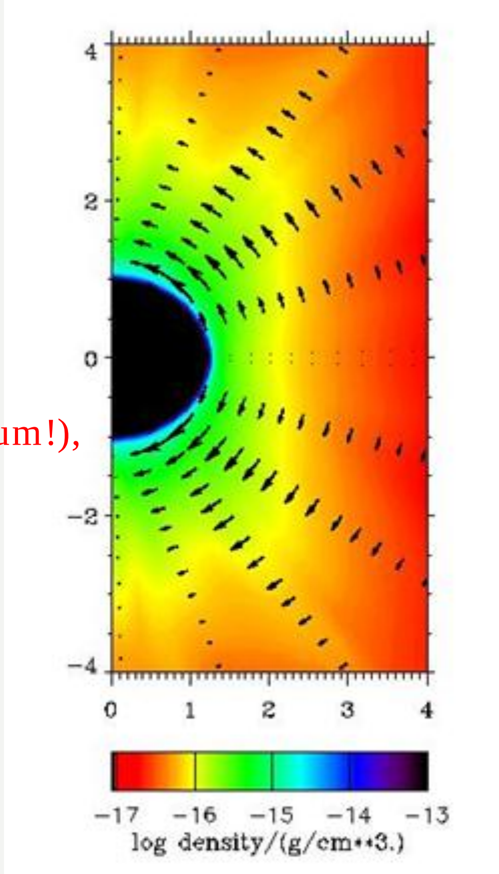

from Petrenz & Puls (2000)

No clear-cut observational evidence so far!
(neither for a) nor for b))

η Carinae? … aspherical ejecta

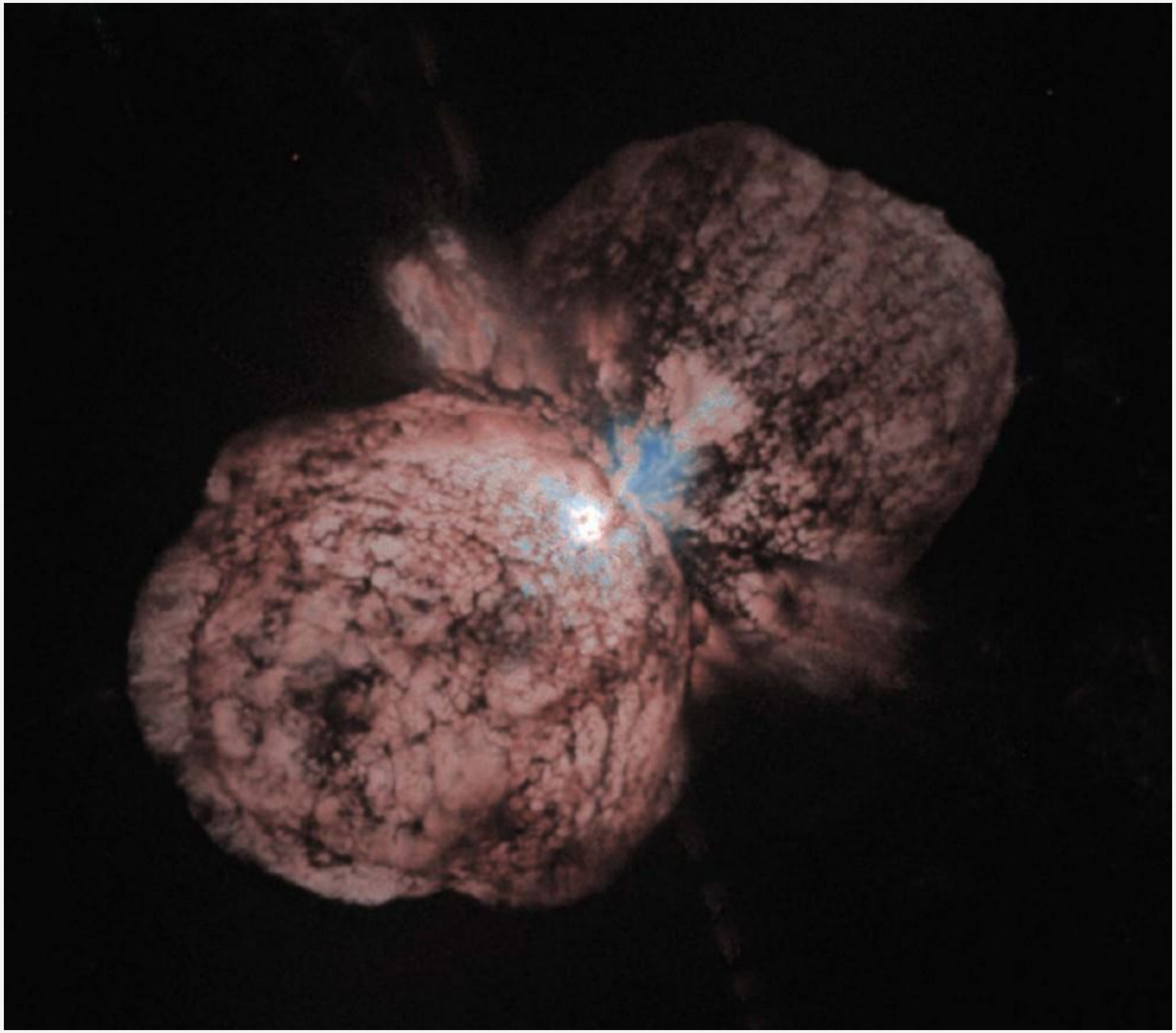

image credit
NASA, STScI

Magnetic fields in massive stars

- many investigations to derive/analyze surface B-fields
  - working groups by J.-F. Donati; C. Neiner; S. Hubrig
  - MiMeS collaboration (G. Wade et al.) ‘Magnetism in massive stars’
- so far, only few (10% or less) massive stars found with significant B (100 Gauss or more)
- origin still not clear (dynamo difficult, fossil?)

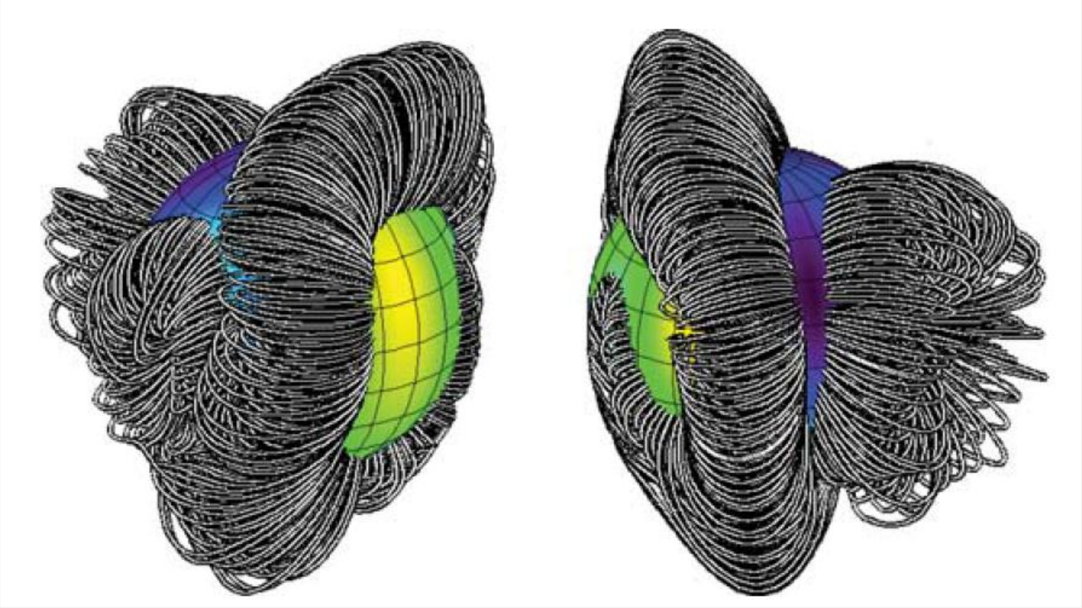

Closed magnetic field lines of the extended magnetic configuration of τ Sco, extrapolated from a photo-spheric map. $B_{polar} \approx 500$ G.

The star is shown at phases 0.25 (left) and 0.83 (right).

Note the warp of the magnetic equator.

(From Donati et al. 2006)

The confinement parameter

pioneering investigations by ud-Doula & Owocki (2002); see also Owocki & ud-Doula (2004) for a comprehensive analytical investigation

Most important quantity: confinement parameter

$$\eta_* = \frac{E_B}{E_{wind}}(R_*) = \frac{B^2(\theta = 90^\circ)R_*^2}{\dot{M}v_\infty} = \frac{(B_p/2)^2 R_*^2}{\dot{M}v_\infty} \approx 0.19\,\frac{B_{100}^2 R_{10}^2}{\dot{M}_{-6} v_8},$$

confinement parameter also related to Alven radius $\rightarrow$ closed loops for $\eta_*>1$

for typical O-supergiants, $B_p \approx 320$ G needed to obtain $\eta_* = 1$

BUT

Sun: $\dot{M}_{-6} \approx 10^{-8}, v_8 = 0.5, B_p \approx 1\mathrm{G} \;\Rightarrow\; \eta_* \approx 40!$

and

$B_p \approx 32$(!!!) G for $\eta_* = 1$ and $\dot{M} = 10^{-8} M_\odot/\mathrm{yr}$, v_∞=2000 km/s

($\rightarrow$ weak winds?)

Winds with magnetic fields

initial condition:
dipole field superposed upon a spherically symmetric outflow

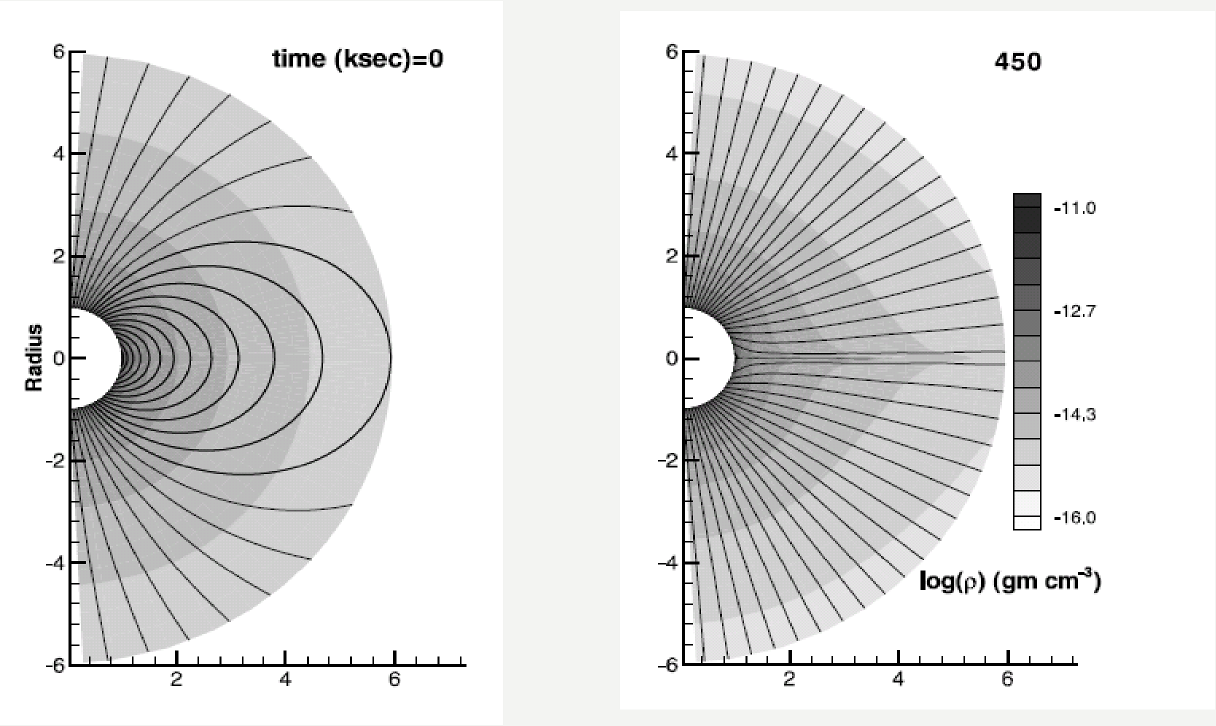

final configuration:
stretched field lines, development of a thin equatorial disk.

For larger field strength (η_*=10):

- closed loops near equatorial surface
- strong wind collisions near the loop tops
- shock velocity jumps of up to 1,000 km/s

→ hard X-ray emission

Density (logarithmic gray scale) and magnetic field (lines), for the case of moderate magnetic confinement, $\eta_*=\sqrt{10}$.
From ud-Doula & Owocki 2002.

G. Meynet et al.: Evolution of stars with high mass loss

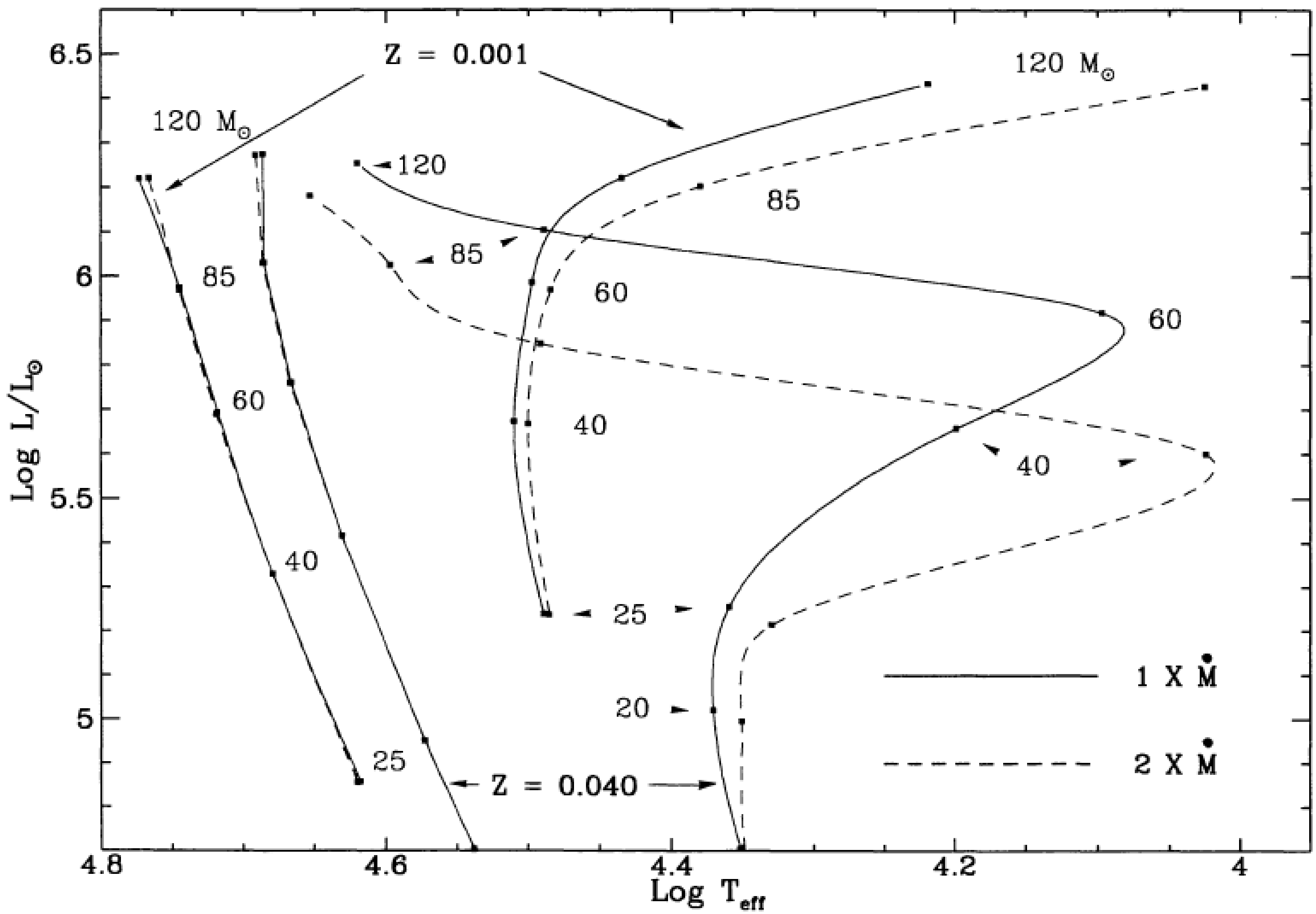

Fig. 7. The ZAMS and the envelopes of the MS for the models at $Z = 0.001$ and $Z = 0.040$, with a normal and a doubled loss rate, are represented in the theoretical HR diagram. The positions of the different initial stellar masses are indicated the stars which become WR star during the MS (see Figs. 5 and 6), the point on the envelope corresponds to the stage the star enters the WR phase

Why α ≈ 2/3?

Simple (but maybe interesting) argument

(cf. Puls et al. 2000)

Remember

$$\frac{dN(k)}{dk} \propto -k^{\alpha-2}, \qquad k \propto \frac{n_{abs}}{\rho} \underbrace{\frac{\pi e^2}{m_e c} f}_{\text{cross section}}$$

for resonance lines $k \sim f$

(lower level = ground state of ion)

The most simple case: the hydrogen atom

"Kramersformula" for resonance lines

$$f(1,n) = \frac{32}{3\sqrt{3}\pi}\left(1-\frac{1}{n^2}\right)^{-3}\frac{1}{n^3} \approx \frac{C}{n^3}$$

summed over all contributing angular momenta

[from Q.M.]

Why α ≈ 2/3?

Simple (but maybe interesting) argument

(cf. Puls et al. 2000)

Remember

$$\frac{dN(k)}{dk} \propto -k^{\alpha-2}, \qquad k \propto \frac{n_{abs}}{\rho} \underbrace{\frac{\pi e^2}{m_e c} f}_{\text{cross section}}$$

for resonance lines $k \sim f$

(lower level = ground state of ion)

The most simple case: the hydrogen atom

"Kramersformula" for resonance lines

$$f(1,n) = \frac{32}{3\sqrt{3}\pi}\left(1-\frac{1}{n^2}\right)^{-3}\frac{1}{n^3} \approx \frac{C}{n^3}$$

summed over all contributing angular momenta

[from Q.M.]

Number of lines until a certain principal q.n. n

$$N(n) = n - 1$$

$$f(n) = \frac{C}{n^3}$$

$$n = \left(\frac{C}{f(n)}\right)^{\frac{1}{3}}$$

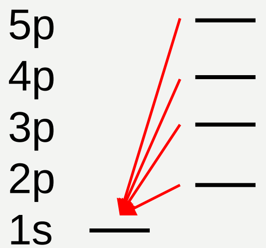

example: 4 resonance lines until n=5

$$N\left(f \geq f(n)\right) = n - 1 = C^{\frac{1}{3}}\left[f(n)\right]^{-\frac{1}{3}} - 1$$

⇒ distribution function

$$\boxed{\frac{dN}{df} \propto -f^{-\frac{4}{3}}} \qquad \text{compare with} \quad \frac{dN}{dk} \propto -k^{\alpha-2}$$

$$\Rightarrow \alpha = \frac{2}{3}!!!$$

- inclusion of other (non hydrogenic) ions (particularly from iron group elements) complicates situation
- general trend: α decreases !

Predictions from line statistics

Let z be the (global) abundance relative to its solar value, i.e., solar comp. is z =1

- number of effective lines scales (roughly) with $z^{1-\alpha}$
  - more metallicity => more lines

- **consequence**

  both mass-loss and wind-momentum should scale with

$$z^{\frac{1-\alpha}{\alpha'}} \approx \sqrt{z} \quad \text{for } \alpha, \alpha' \approx 2/3 \text{ (O-type winds)}$$

$$\ldots z^{1.5} \quad \text{for } \alpha, \alpha' \approx 0.4 \text{ (A-type winds)}$$

- example for z=0.2 (≈ SMC abundance)
  - $\dot{M}$ (40kK) factor of 0.45 decrease
  - $\dot{M}$ (10kK) factor of 0.09 decrease

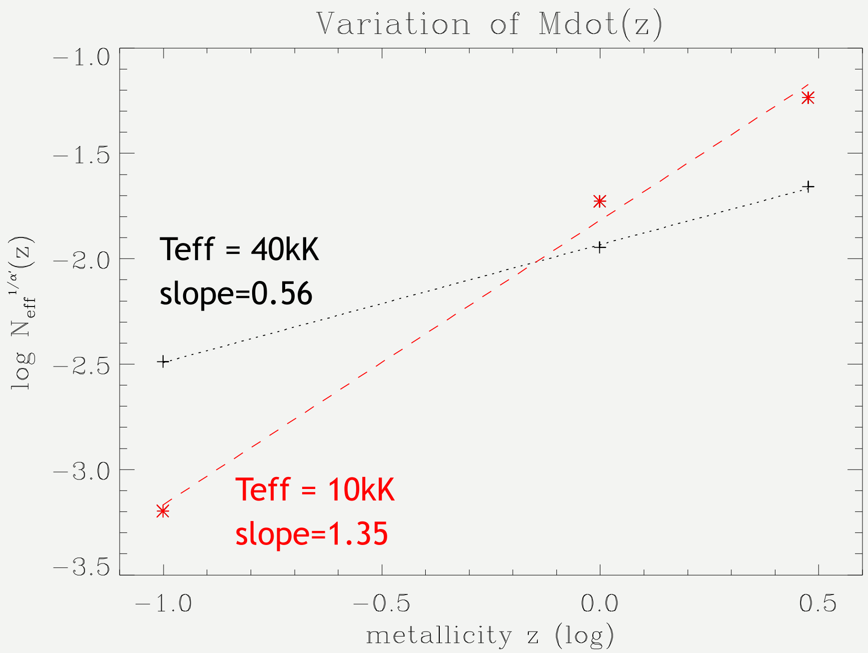

adapted from Puls et al. (2000)

Predictions from line statistics

- Differential importance of Fe-group and lighter elements (CNO)
  - cf. Pauldrach 1987; Vink et al. 1999, 2001; Puls et al 2000; Kriticka 2005
  - lines from Fe group elements dominate acceleration of lower wind
    $\rightarrow$ determine mass-loss rate $\dot{M}$
  - lines from light elements (few dozens!) dominate acceleration of outer wind
    $\rightarrow$ determine terminal velocity v_∞

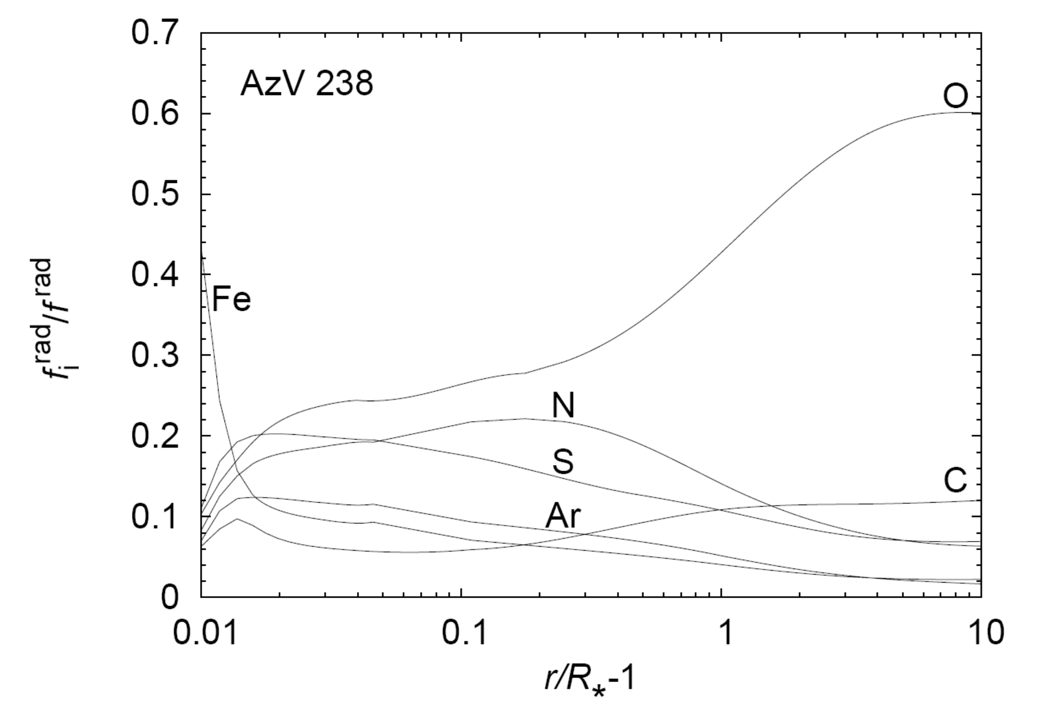

From Kritcka (2005)

Theoretical 1-D wind-models

- most cited models: Vink et al. (2000/2001)
  - Monte-Carlo approach following Abbott & Lucy (1985):
  - derive (iterate) $\dot{M}$ from **global** energy conservation
  - pre-described velocity field

- Pauldrach (1987) and Pauldrach et al. (1994/2001): "WM-basic"
  - consistent hydrodynamic solution (stationary)
  - NLTE line-force with Sobolev line transfer

- Krticka & Kubat (2000/01/04/09), Krticka 2006
  - solution of equation of motion with NLTE, Sobolev-line force
  - more-component description (metal ions + H/He)

Theoretical 1-D wind-models

- Kudritzki (2002, based on Kudritzki et al. 1989)
  - analytic “cooking recipe” coupled with approx. NLTE, very fast

- Gräfener & Hamann (2005, 2008)
  - self-consistent hydrodynamic solution
  - NLTE line force, comoving frame solution

    – see **Mihalas**, Kunasz & Hummer, 1975-1977 –

    for all lines/continua

- Lucy (2007a, 2007b); Müller & Vink (2008)
  - NLTE line force, mass-flux from regularity condition at **sonic** point

Wind properties of OB stars at different metallicities

- vast literature in the recent decade
- right-hand table for OB-stars
  - without Galactic center objects
  - without FLAMES
  - without IR/radio analyses

- spectroscopic analyses performed by NLTE atmosphere/ spectrum synthesis codes (spherical, allowing for smooth winds):
  CMFGEN (Hillier & Miller)
  WM-Basic (Pauldrach & co-worker)
  Fastwind (Puls & co-worker)

Halpha	Lamers & Leitherer (1993) Puls et al. (1996) Kudritzki et al. (1999) Markova et al. (2004)	Gal. O-stars Gal./LMC/SMC O-stars Gal. BA-supergiants Gal. O-stars
UV	Bianchi & Garcia (2002) Garcia & Bianchi (2004) Martins et al. (2004) Fullerton et al. (2006)	Gal. O-stars Gal. O-stars SMC O-dwarfs Gal. O-stars – PV
UV + optical	Crowther et al. (2002) Hillier et al. (2003) Bouret et al. (2003) Evans et al. (2004) Martins et al. (2005) Bouret et al. (2005) Marcolino et al. (2009)	LMC/SMC O-supergiants SMC O-supergiants SMC O-dwarfs LMC/SMC OB-supergiants Gal. O-dwarfs Gal. Ostars Gal. O-dwarfs
optical	Herrero et al. (2002) Repolust et al. (2004) Trundle et al. (2004) Trundle & Lennon (2005) Massey et al.(2004/05/09)	Cyg-OB2 OB-stars Gal. O-stars SMC B-supergiants SMC B-supergiants LMC/SMC O-stars
	Urbaneja(2004) Crowther et al. (2006) Lefever et al. (2007) Markova & Puls (2008)	Gal. B-supergiants Gal. B-supergiants Gal. B-supergiants Gal. B-supergiants

state of the art, NLTE, line-blanketed model atmospheres used to analyze OB-stars with winds

	PoWR (Hamann)	Phoenix (Hauschildt)	CMFGEN (Hillier)	WM-basic (Pauldrach)	Fastwind (Puls)
major drawback(s)		no clumping?	(photosphere from Tlusty)	Sobolev line-transfer, approx. photo-sphere, no clumping	approximate line-blanket., no X-rays
major application	WRs	stars below 10kK, SNe	OB(A)-stars, WRs, SNe	hot stars with dense winds, ion. fluxes, SNe UV-spectroscopy	OB-stars, early A-sgs, optical to IR
execution time	hours	hours	hours	1 to 2 h	few minutes to 0.5 h

- The VLT-FLAMES survey of massive stars (PI: S. Smartt)
  - high resolution multi-object spectroscopy of 8 young and old clusters in the Galaxy, SMC and LMC;
  - 86 O-stars, 615 B-stars
  - overview/summary papers: Evans et al. (2005, A&A 437; 2006, A&A 456; 2008, ESO Messenger 131)

- major objectives
  - rotation and abundances (test rotational mixing)
  - stellar mass-loss as a function of metallicity
    Mokiem et al. (2006, A&A 456: SMC); (2007, A&A 465: LMC);
    2007, A&A 473: empirical metallicity dependence)
  - binarity (fraction, impact)

LMU

USM

The VLT-FLAMES survey of massive stars
(Fibre Large Array Multi-Element Spectrograph)

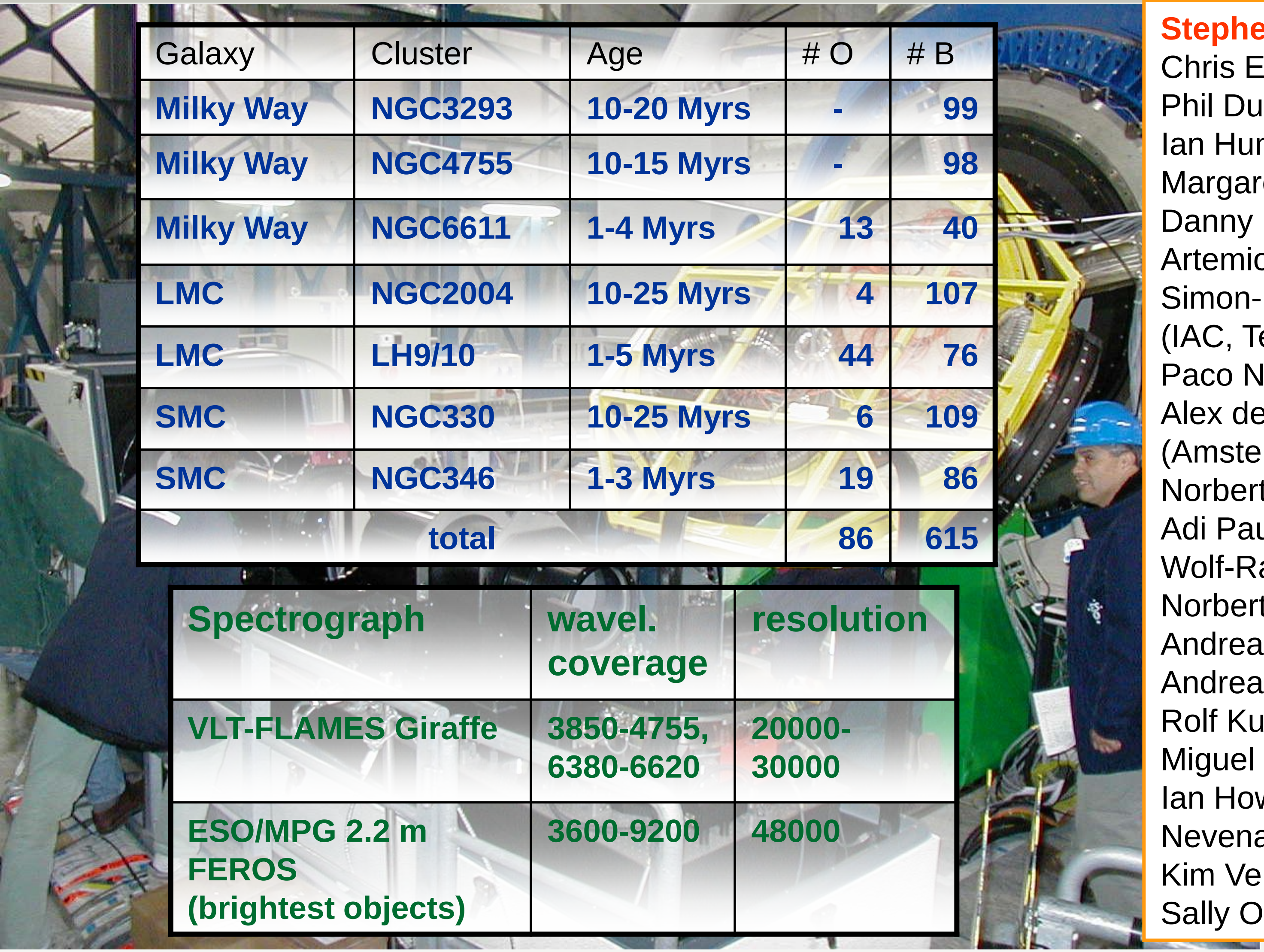

Galaxy	Cluster	Age	# O	# B
Milky Way	**NGC3293**	**10-20 Myrs**	**-**	**99**
Milky Way	**NGC4755**	**10-15 Myrs**	**-**	**98**
Milky Way	**NGC6611**	**1-4 Myrs**	**13**	**40**
LMC	**NGC2004**	**10-25 Myrs**	**4**	**107**
LMC	**LH9/10**	**1-5 Myrs**	**44**	**76**
SMC	**NGC330**	**10-25 Myrs**	**6**	**109**
SMC	**NGC346**	**1-3 Myrs**	**19**	**86**
	total		**86**	**615**

Spectrograph	**wavel. coverage**	**resolution**
VLT-FLAMES Giraffe	**3850-4755, 6380-6620**	**20000-30000**
ESO/MPG 2.2 m FEROS (brightest objects)	**3600-9200**	**48000**

Stephen Smartt (PI, Belfast)
Chris Evans (Edinburgh)
Phil Dufton, Carrie Trundle,
Ian Hunter, J.K. Lee (Belfast)
Margaret Hendry (Cambridge)
Danny Lennon (Baltimore)
Artemio Herrero, Sergio
Simon-Diaz, Charo Villamariz,
(IAC, Teneriffa)
Paco Najarro (CSIC, Madrid)
Alex de Koter, Rohied Mokiem
(Amsterdam)
Norbert Langer (Bonn)
Adi Pauldrach, Jo Puls (Munich)
Wolf-Rainer Hamann (Potsdam)
Norbert Przybilla (Bamberg)
Andreas Korn (Uppsala)
Andreas Kaufer (ESO)
Rolf Kudritzki, Fabio Bresolin,
Miguel Urbaneja (IfA, Hawaii)
Ian Howarth (UCL, London)
Nevena Markova (Sofia)
Kim Venn (Victoria)
Sally Oey (Ann Arbor)

The bi-stability jump : predictions

- prediction by Vink et al. (2000, 2001):
- below 23000 K, ionization of Fe switches abruptly from FeIV to Fe III (more driving lines !!!)
  - → $\dot{M}$ increases by factor 5, vinf decreases by factor 2
  - → wind-momentum rates for B stars predicted to be larger than for O-stars

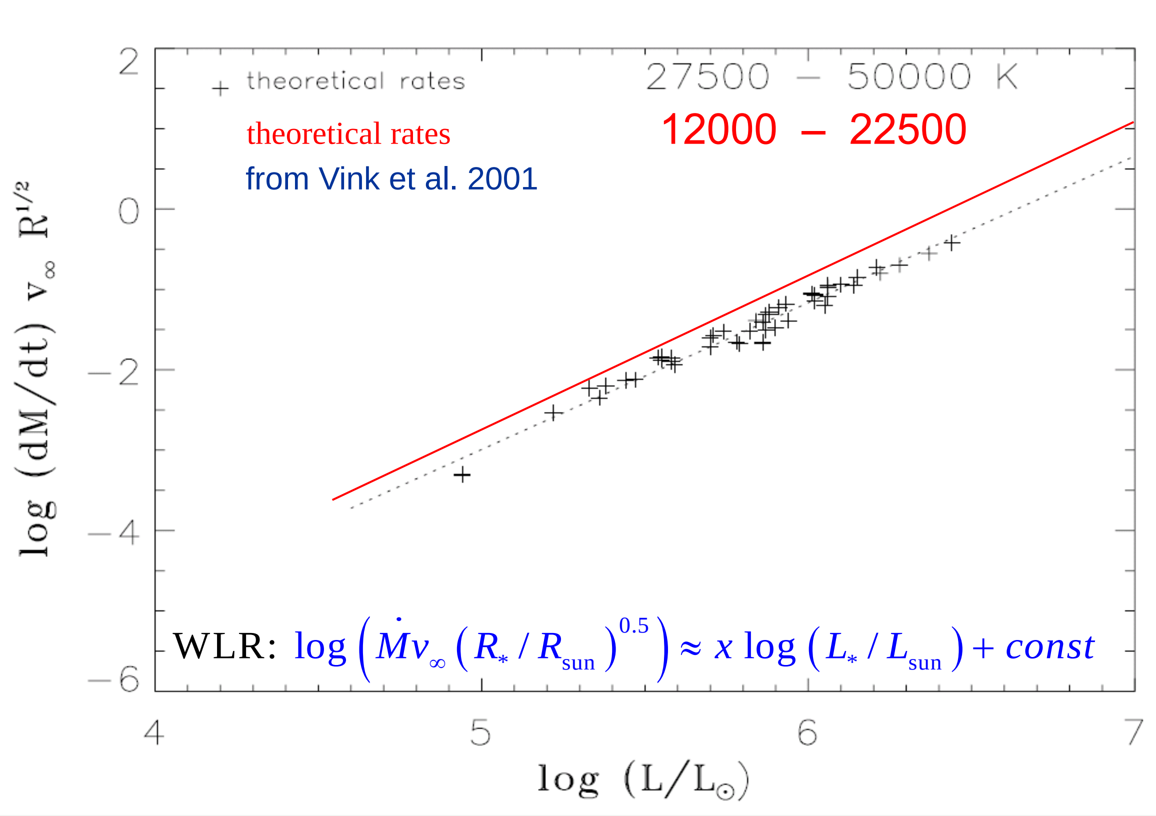

Note:
mass-loss rate primarily controlled by number/ distribution of *Fe-lines* (e.g., Vink et al. 2000, Puls et al. 2000, Krticka 2005)

The bi-stability jump: observations vs. theory

- prediction by Vink et al. (2000, 2001):
- below 23000 K, ionization of Fe switches abruptly from FeIV to Fe III (more driving lines !!!)
  - → $\dot{M}$ increases by factor 5, vinf decreases by factor 2
  - → wind-momentum rates for B stars predicted to be larger than for O-stars

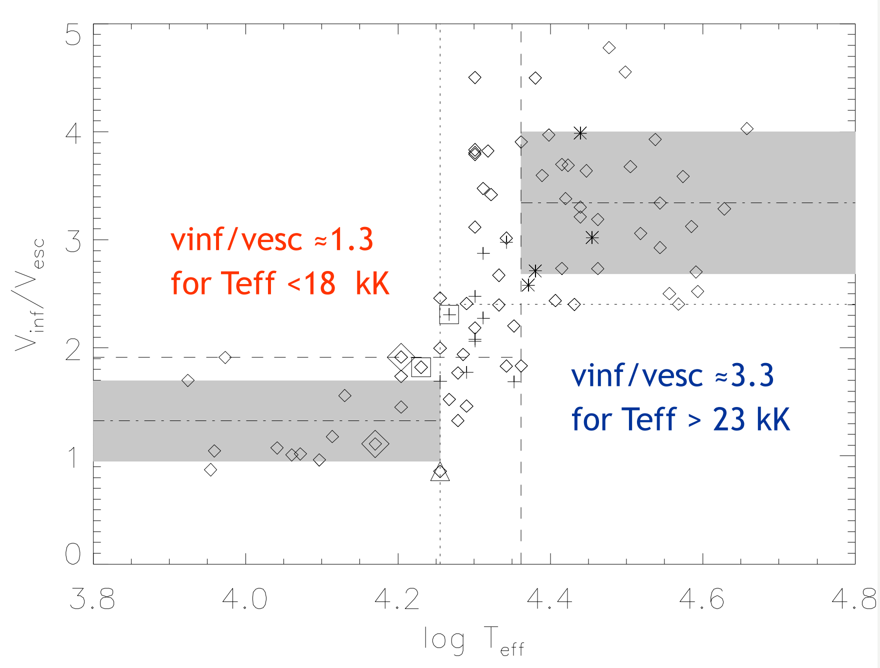

Observations: Evans et al. (2004), Crowther et al. (2005)
gradual decrease of vinf/vesc betweem 23 < Teff < 18 kK

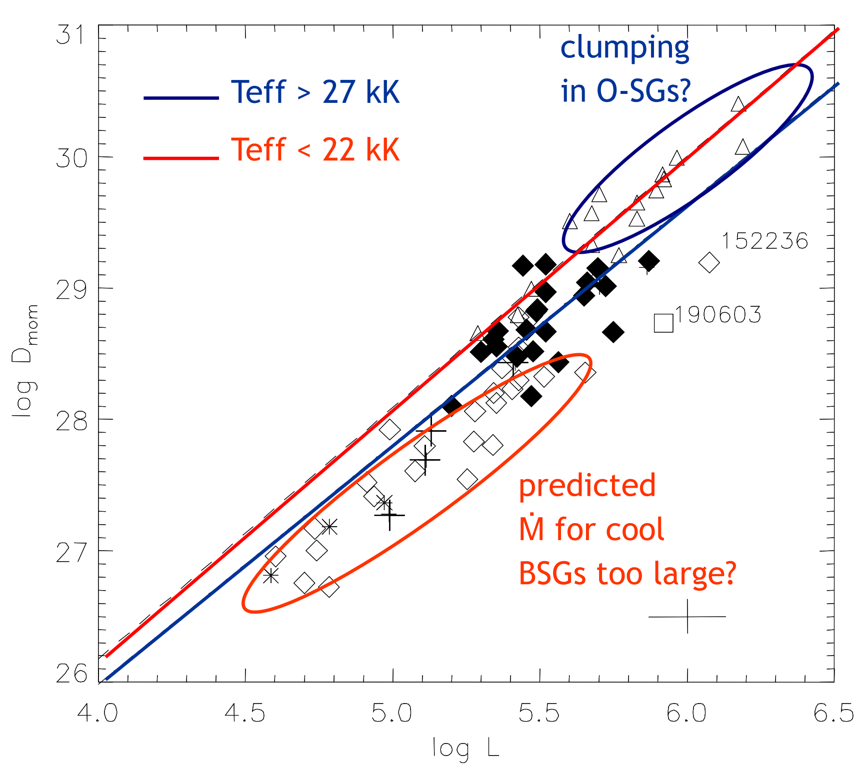

From Markova & Puls 2008, similar results by Crowther et al. 2006)

Snapshot of density, velocity and temperature structure

- dashed line: smooth model
- red arrows overdense clumps
- blue arrows “void” inter-clump medium
- **NOTE:** average density and v-field remains unaffected
- shock heating, cooling by X-ray emission (observed by all X-ray observato-ries)

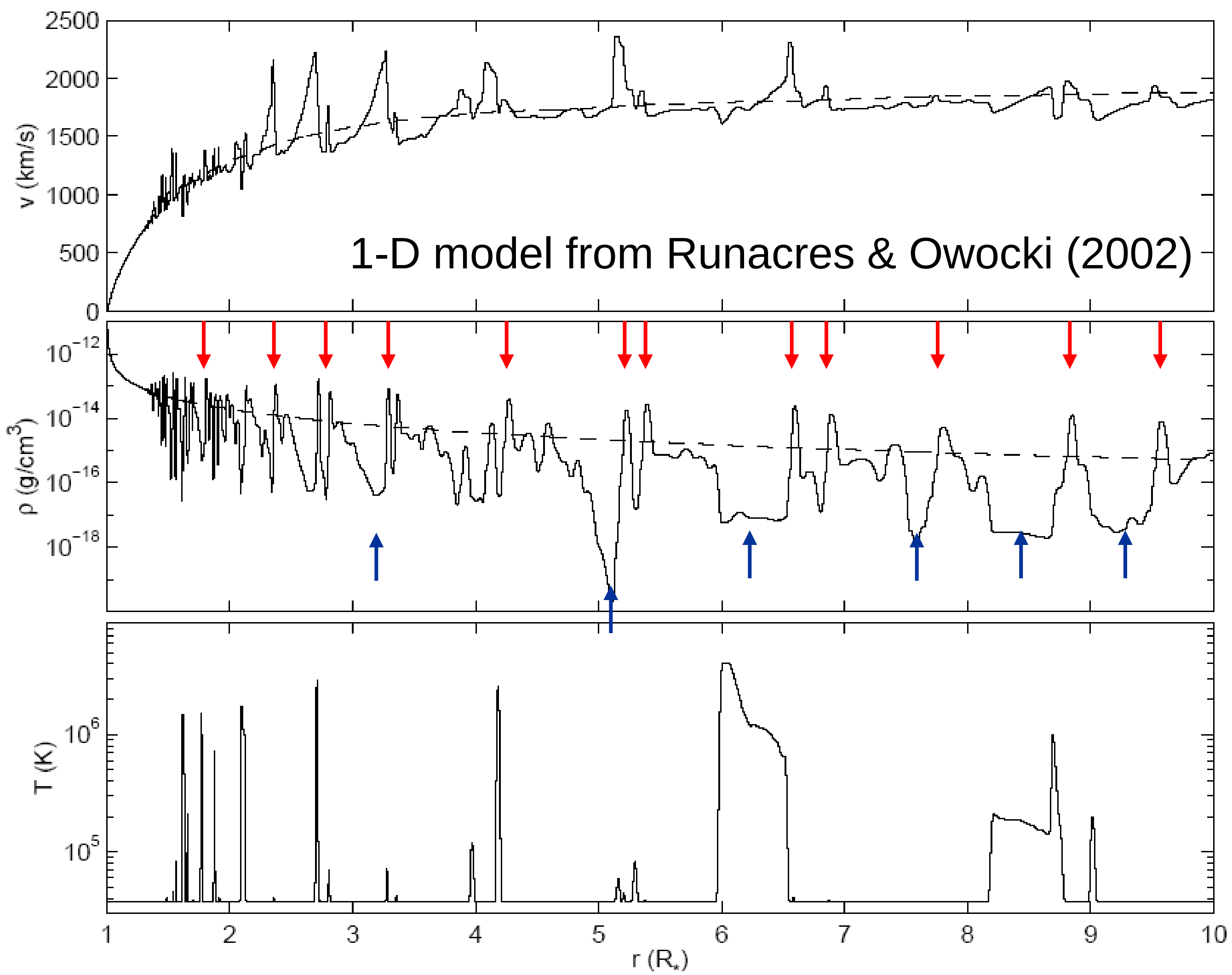

A word of warning …

- *almost* all clumping diagnostics in OB-stars only indirect
- relies strongly in our belief in theoretical modeling
  - NLTE atmospheres (lines in different bands do not fit simultaneously)
  - hydrodynamic simulations (line-driven instability)
  - predictions from (stationary) models (observed Mdot deviate)
- and to analogy arguments with respect to WR-winds
  (moving bumps on top of emission lines, inconsistency between strengths of recombination lines and their electron scattering wings)
- and the presence of X-ray emission in single stars (shocks!) +
  extended troughs in saturated P Cygni lines (non-mono v-field)

- Note: individual diagnostics usually do not require clumping to reproduce observations
- only if different diagnostics are combined (e.g., UV + optical + IR), problems become apparent

Direct evidence for clumping

“pure” observational evidence:

- from a temporal analysis of HeII 4686, Eversberg et al. (1998) found “outward moving inhomogeneities” in the wind of ζ Pup, *from regions near the photosphere out to 2* R_{star}

Other evidence “only” indirect …

…in the following, “clumping factor”
= inverse of “volume filling factor”

$$f_{\rm cl} = \frac{1}{f_V} = \frac{\langle \rho^2 \rangle}{\langle \rho \rangle^2} > 1$$

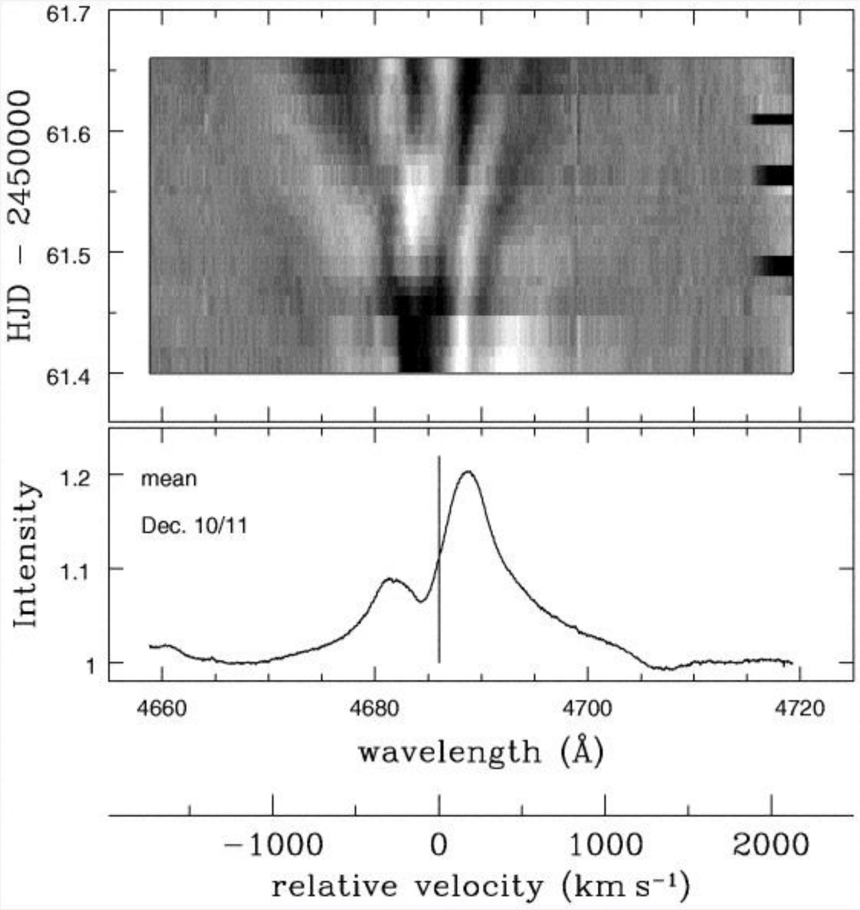

Gray-scale plot of nightly residuals from the mean rectified spectrum (lower plot). From Eversberg et al. (1998)

Effects of clumping

Assume optically thin clumps with void inter-clump matter

$\rho_{\mathrm{cl}} = f_{cl} \langle \rho \rangle$, with $\langle \rho \rangle$ average (= smooth, stationary) density

is overdensity inside clumps

a) $\chi(\mathrm{r}) \propto \rho(r)$, e.g., UV resonance lines of dominant ions

inhomogeneities "cancel" after spatial integration, no effect;

b) $\chi(\mathrm{r}) \propto \rho^2(r)$, all recombination induced processes (H_α, radio free-free)

inhomogeneities do not cancel, optical depth larger than for smooth flow,
by factor f_{cl}

- consequence: if Mdot derived from ρ^2-diagnostics for an unclumped model, same fit quality for a clumped model with Mdot lower by factor $\sqrt{f_{cl}}$

Effects of clumping

- standard assumption (used in most diagnostic methods)
  - optically thin clumps, void inter-clump medium
  - undisturbed velocity field
  - clumping factor f_{cl}, measures over-density inside clumps w.r.t. average density
  - in atmosphere codes: multiply density by over-density, multiply opacities and emissivities by volume filling factor (inverse of clumping factor)

- most important consequence:
  - $\dot{M}$ derived from ρ^2-diagnostics (Hα, radio) using homogeneous models need to be scaled down by factor $\sqrt{f_{cl}}$
    - square of over-density “wins” against smaller emitting/absorbing volume, lower $\dot{M}$ required to obtain similar optical depths/emission measures as in smooth models
  - *in this scenario*, $\dot{M}$ derived from ρ-diagnostics (e.g., UV resonance lines) remains uncontaminated
    - over-density cancels against smaller absorbing/emitting volume
  - ionization equilibrium modified, due to enhanced recombination

Indirect indications of *significant* clumping in OB-star winds

- Presence of X-rays / spectroscopy → talk by D. Cohen
- NLTE-model atmosphere analysis of UV + optical spectra
  - Crowther et al. (2002), Hillier et al. (2003), Bouret et al. (2003), Bouret et al. (2005): $f_{cl} \approx 10...50$, clumping starts at wind base
- Wind-momentum rates
  - Puls et al. (2003), Markova et al (2004) and Repolust et al. (2004): from comparison with "theoretical" WLR, dense winds from supergiants were suggested to be clumped, with $f_{cl} \approx 5$ (Mdot reduced by factors 2…3)
- Radial stratification of clumping factor
  - Puls et al. (2006) derive constraints on the radial stratification of the clumping factor by simultaneous modeling of Ha (lower/intermediate wind), IR and mm/radio (outer wind)
  - **Result:** different clumping stratification in high and lower density winds
    - for lower density winds, clumping properties similar in inner and outer part
    - for strong winds, clumping stronger in lower wind
  - corresponding Halpha mass-loss rates need to be reduced at least by factors 2…3

$$f_{cl}(\text{inner wind}) \approx 4...6 \text{ times } f_{cl}(\text{outer wind})$$

Results (very brief summary)

- Crowther et al. (2002), Hillier et al. (2003), Bouret et al. (2003/2005):
  $f_{cl} \approx 10\ldots50$, clumping starts at/close to wind base,
  reduction of $\dot{M}$ by factors 3…7

- radial stratification of clumping factor
  (from simultaneous modeling of Hα, IR and mm/radio, Puls et al. 2006)
  - for strong winds, clumping stronger in lower wind, by factors 4…6, compared to the outer wind
  - corresponding Hα mass-loss rates need to be reduced at least by factors 2…3

L-Band spectroscopy

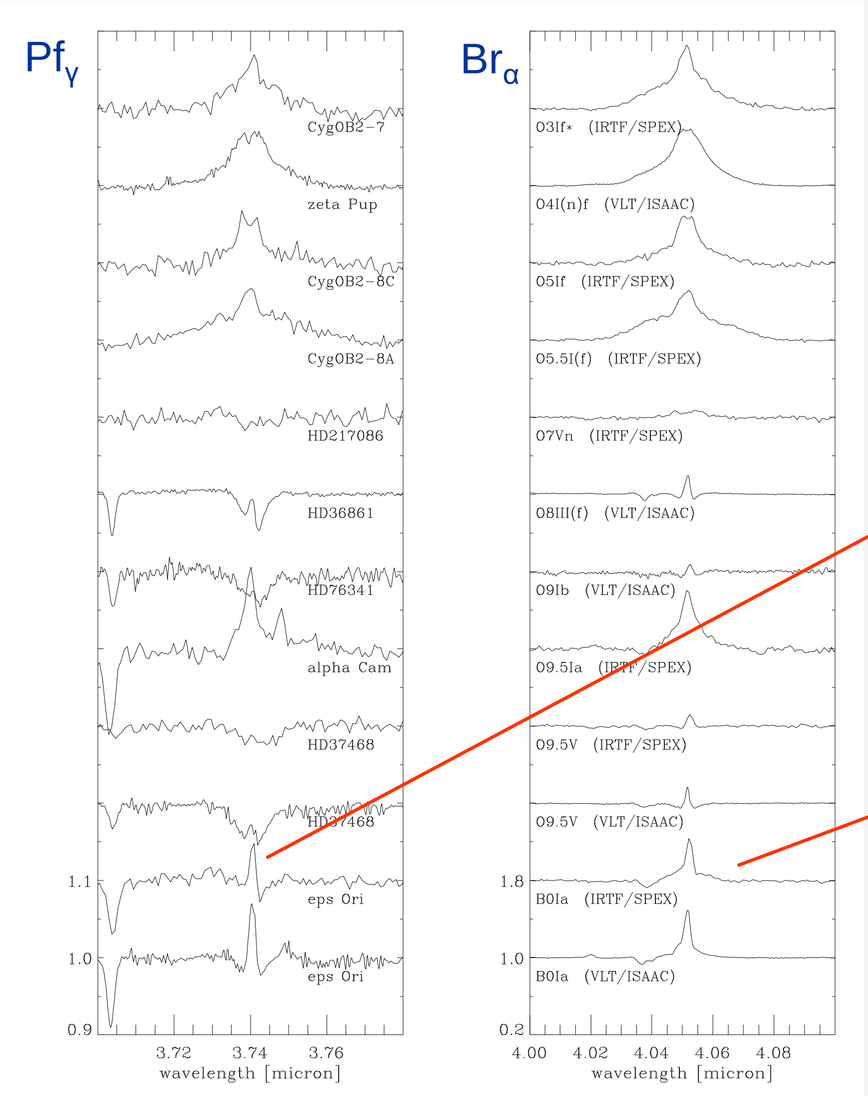

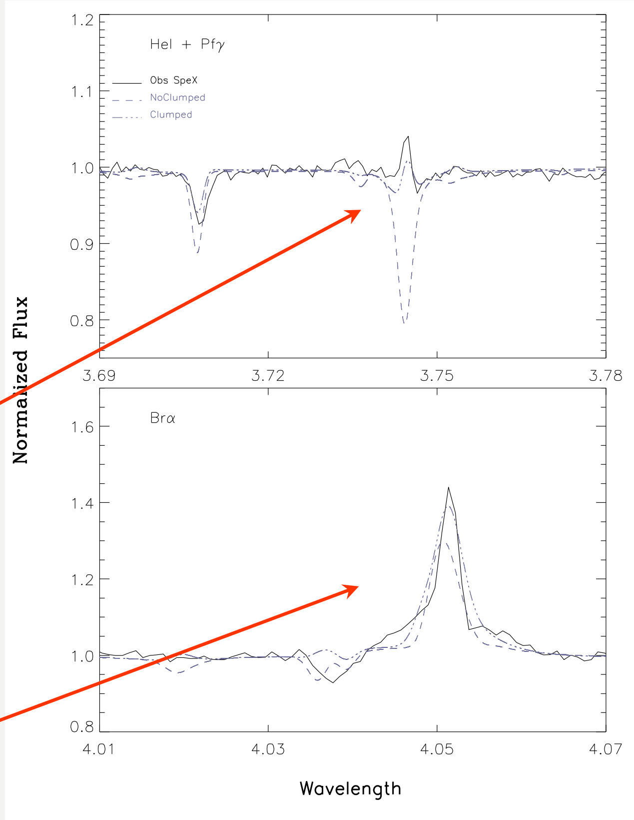

- clumping required, Mdot reduced by ≈ factor 3
- Observations: ISAAC@VLT, SPeX@IRTF (From Najarro, Hanson & Puls, in prep. for A&A)

The PV problem

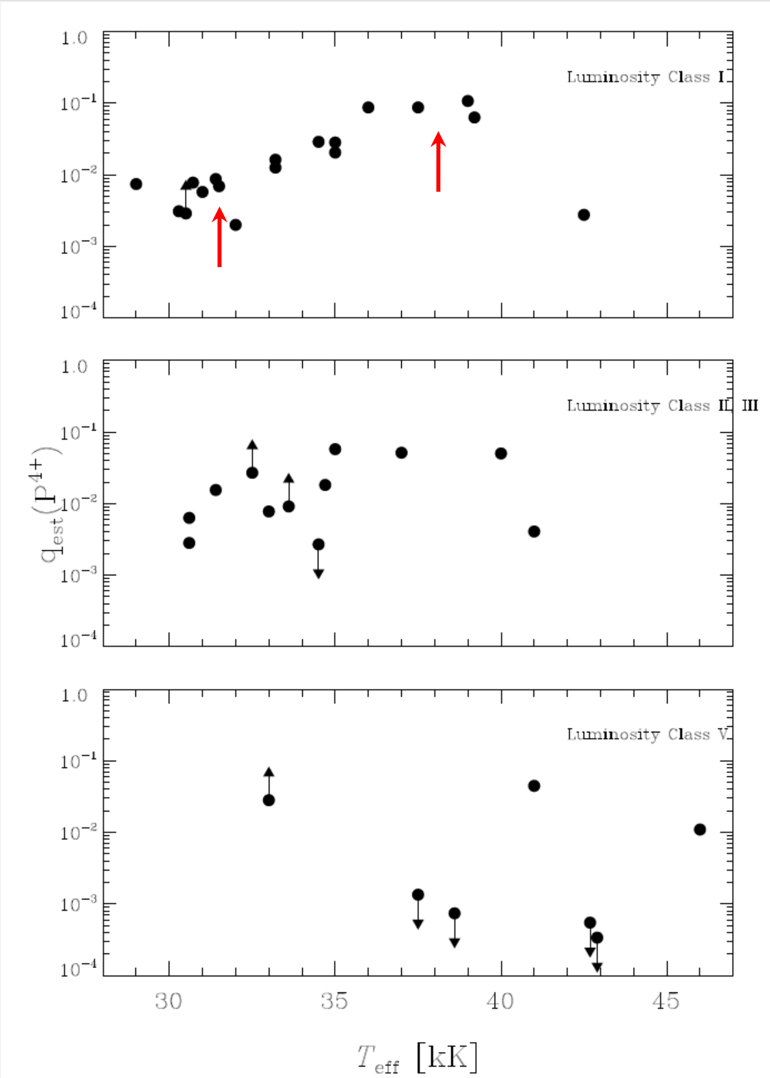

- major result from investigation by Fullerton et al. (2006)

$$q_{est}(P^{4+}) = \frac{\langle q\dot{M}\rangle_{obs}}{\dot{M}_{Halpha}} \xrightarrow{\text{in terms of "standard" interpretation}} \frac{\langle q\dot{M}\rangle_{obs}}{\dot{M}\sqrt{f_{cl}}} \rightarrow \frac{\langle q\rangle}{\sqrt{f_{cl}}}$$

with $\langle q\rangle$ spatial average of Phosphorus ionization fraction

(assuming that resonance lines remain unaffected from clumping)

- if PV dominant ion at Teff ≈ 40000 K, then f_{cl} = O(100)

- BUT: test calculations
  → PV dominant ion below O7

- would imply f_{cl} = O(10000)!!!

Test bed λ Cep – modeling

- 2D/3D winds constructed by assembling snapshots in wind slices (patch method of Dessart and Owocki 2002)
- either from **hydrodynamic** or **stochastic models** involving a parameterized description of clump structure and distribution

+ detailed radiative transfer directly on structured medium to compute synthetic spectra

3D geometry

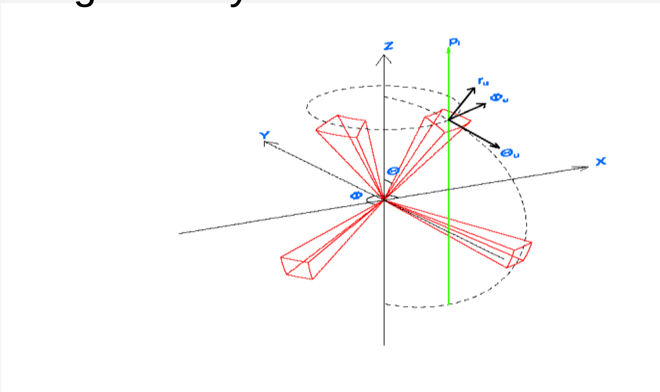

2D density contours

Smooth | Stochastic | Hydrodynamic

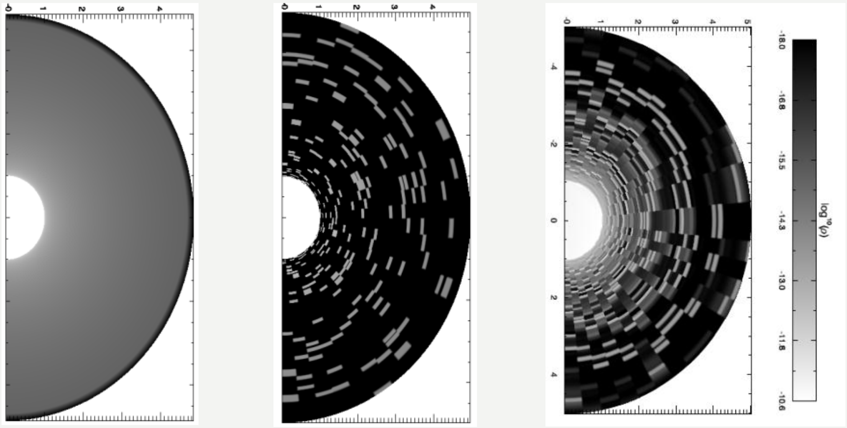

Test bed λ Cep –
Radiation hydrodynamic models

Same mass-loss rate cannot fit PV and H_α simultaneously!

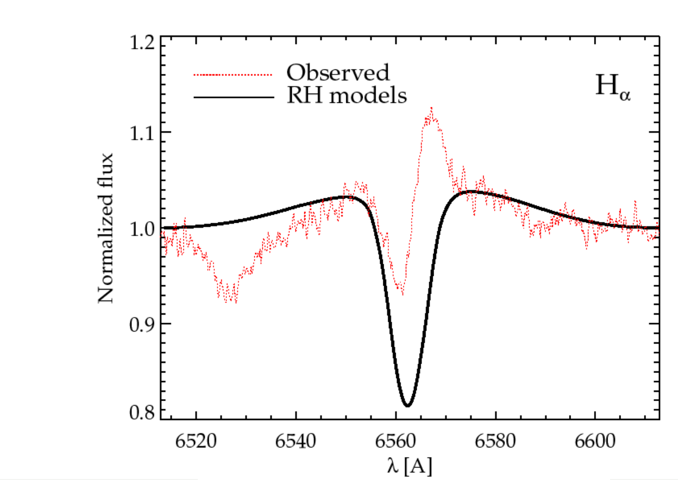

dM/dt = 1.5 $\cdot 10^{-6}$ $M_\odot$/yr

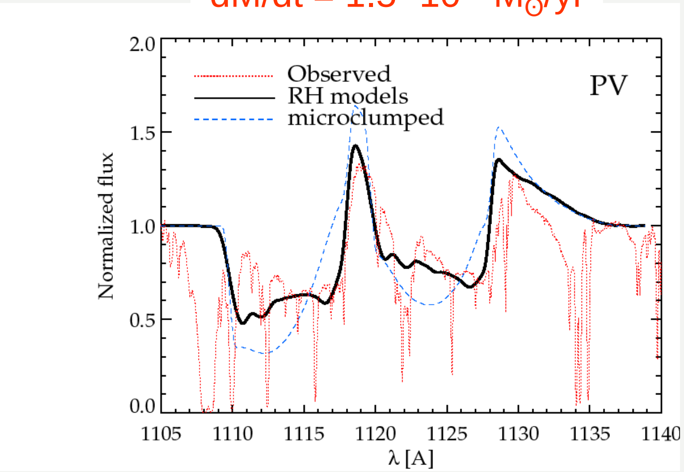

Basic (structure) problems:

H_α → need ‘more clumping’ in lower wind
(also Bouret et al. 2005, Puls et al. 2006)

PV → Δv inside clumps too large
→ velocity ‘holes’ too small
(also Owocki 2008, Sundqvist et al. 2010)

Test bed λ Cep – Clumping factors

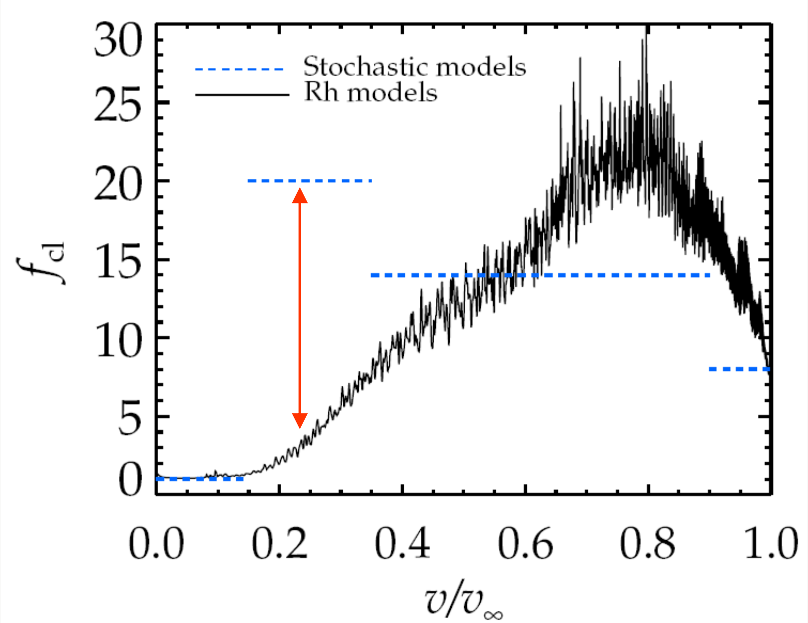

How could predicted and observed clumping factors be reconciled?

Suggestions:

Sub-surface convection? *[→ Cantiello]*

Pulsations?

- Gravity darkening – observations – test beds

SUMMARY OF OBSERVATIONAL RESULTS TO DATE ON RAPID ROTATORS

Star	Spectral Type	Velocity v (km s^{-1})	Inclination i (deg)	$v/v_{\rm crit}$	Orientation α (deg)	Gravity darkening β	$T_{\rm pole}$ (K)	$T_{\rm eq}$ (K)	$R_{\rm pole}$ ($R_\odot$)	$R_{\rm eq}$ ($R_\odot$)	Ref.
Altair (α Aql)	A7IV-V	$v \sin i = 210 \pm 13$, $i > 30$			-21.6 ± 6.2[b]	none applied	$< 7680 \pm 90 >$			1.8868 ± 0.0066	(1)
		273 ± 13	64	0.73 ± 0.037	123.2 ± 2.8	0.25 (fixed)	8740 ± 140	6890 ± 60	1.636 ± 0.022	1.988 ± 0.009	(2)
		285 ± 10	57.2 ± 1.9	0.923 ± 0.006	-61.8 ± 0.8	0.19 ± 0.012[c]	8450 ± 140	6860 ± 150	1.634 ± 0.011	2.029 ± 0.007	(3)
Achernar (α Eri)	B3Vpe	225[a]	>50	0.79–0.96	39 ± 1	0.25 (fixed)	20000 (fixed)	9500–14800	8.3–9.5	12.0 ± 0.4	(4)
Vega (α Lyr)	A0V	270 ± 15	4.7 ± 0.3	0.91 ± 0.03	not cited	0.25 (fixed)	10500 ± 100	8250^{+415}_{-315}	2.26 ± 0.07	2.78 ± 0.02	(5)
		274 ± 14	4.54 ± 0.33	0.926 ± 0.021	8.6 ± 2.7	0.25 (?, fixed)	9988 ± 61	7557 ± 261	2.306 ± 0.031	2.873 ± 0.026	(6)
Regulus (α Leo)	B8IVn	317 ± 3	90^{+0}_{-15}	0.86 ± 0.03	85.5 ± 2.8	0.25 ± 0.11	15400 ± 1000	10300 ± 1000	3.14 ± 0.06	4.16 ± 0.08	(7)
Rasalhague (α Oph)	A5IV	237	87.70 ± 0.43	0.885 ± 0.011	-53.88 ± 1.23	0.25 (fixed)	9300 ± 150	7460 ± 100	2.390 ± 0.014	2.871 ± 0.020	(8)
Alderamin (α Cep)	A7IV-V	283 ± 19	$88.2^{+1.8}_{-13.3}$	$0.8287^{+0.0482}_{-0.0232}$	3 ± 10	$0.084^{+0.026}_{-0.049}$	8440^{+430}_{-700}	"~ 7600"	2.175 ± 0.046	2.82 ± 0.10	(9)
		225	55.70 ± 6.23	0.941 ± 0.020	-178.84 ± 4.28	0.216 ± 0.021[c]	8588 ± 300	6574 ± 200	2.162 ± 0.036	2.74 ± 0.044	(8)

[a]Fixed from Slettebak (1982).
[b]In error, reflecting $\{u, v\}$ coordinates swap.
[c]Second solution with $\beta = 0.25$ (fixed) also presented in manuscript.

References: (1) van Belle et al. (2001); (2) Peterson et al. (2006a); (3) Monnier et al. (2007); (4) Domiciano de Souza et al. (2003); (5) Aufdenberg et al. (2006); (6) Peterson et al. (2006b); (7) McAlister et al. (2005); (8) Zhao et al. (2009); (9) van Belle et al. (2006).

Rapid rotation

- Gravity darkening
  - von Zeipel (1923, assuming rotational laws which can be derived from a potential, e.g., uniform or cylindrical) +
  - Maeder (1999), considering shellular rotation: ω = ω(r) (more precisely: const on horizontal surfaces, Zahn 1992)

$$\mathbf{F} \propto \mathbf{g}_{\text{eff}}(1+\zeta(\vartheta)), \quad |\zeta(\vartheta)| < 0.1 \text{ in most cases, with co-latitude } \vartheta$$

$$\mathbf{g}_{\text{eff}} = \mathbf{g}_{\text{grav}} + \mathbf{g}_{\text{cent}} \begin{cases} = \mathbf{g}_{\text{grav}} \text{ at pol} \\ < \mathbf{g}_{\text{grav}} \text{ at equator} \end{cases} \qquad \mathbf{g}_{\text{eff}} \text{ independent of radiative acceleration!}$$

$$\Rightarrow T_{\text{eff}}(\vartheta) \propto g_{\text{eff}}(\vartheta)^{1/4} \text{ for radiative envelopes, decreases towards equator, 'gravity darkening'}$$

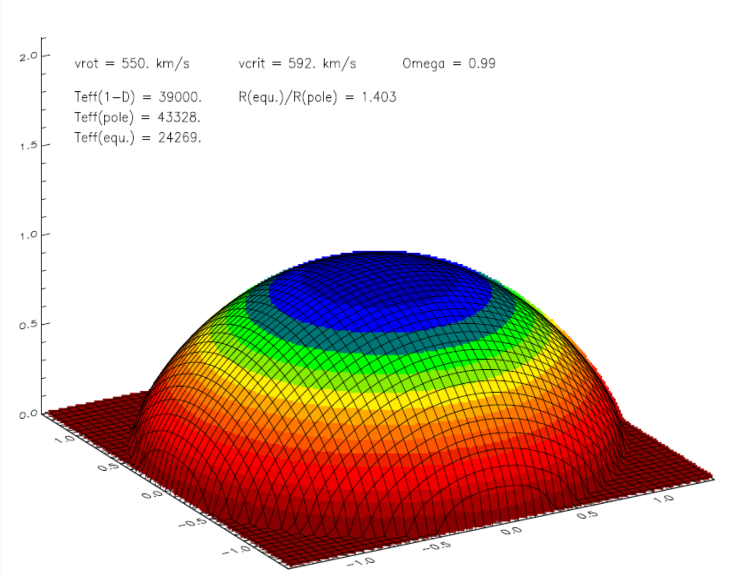

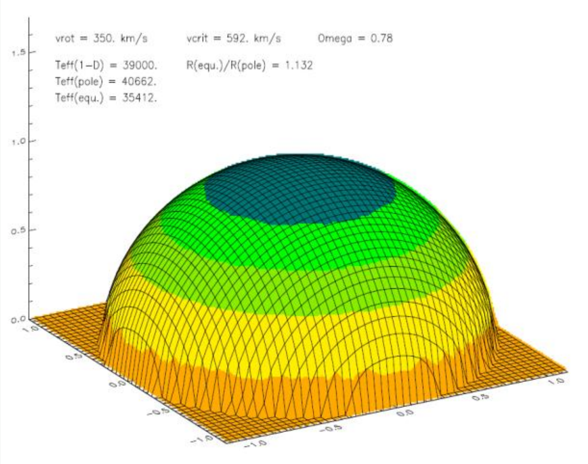

USM

Influence of magnetic fields

- no strong convection zones in hot stars (no HII hydrogen recombination)
  → difficult to obtain strong, *dynamo-generated* magnetic fields
- but: most hot stars rapidly rotating
  → dynamo generation might still be possible within thin, near-surface convection zones due to HeII recombination
- cores of massive stars strongly convective
  - Cassinelli & MacGregor (2000; see also Charbonneau & MacGregor 2001): dynamo-generated magnetic flux tubes from this interior can diffuse to surface over a timescale of a few million years.
  - would imply surface magnetic fields in slightly evolved hot stars
- other possibilities
  - magnetic fields from early, convective phase during stellar formation
  - through compression of interstellar magnetic flux during initial collapse.
    - would imply strongest magnetic fields in youngest stars, then gradually decaying or
    - dynamical stable configuration of fossil fields on long time-scales possible (Moss 2001, Braithwaite & Spruit 2004, Braithwaite & Nordlund 2006)

Magnetic fields in OB-stars

Properties of the known magnetic massive stars, excluding chemically peculiar Ap/Bp stars. The magnetic field strength B_p is the strength at the magnetic pole of the (approximately) dipolar field.

Star	Spec. type	Mass ($M_\odot$)	B_p (Gauss)	rotation period (days)	reference
θ^1 Ori C	O4-6V	45	1100±100	15.4	Donati et al. (2002)
HD 191612	O6-8	~40	~1500	538[a]	Donati et al. (2006a)
τ Sco	B0.2V	~15	~500	41	Donati et al. (2006b)
ξ^1 CMa	B1III	14	~500	<37	Hubrig et al. (2006a)
β Cep	B1IV	12	360±40	12.00089	Henrichs et al. (2000)
V2052 Oph	B1V	10	250±190	3.63883	Neiner et al. (2003b)
ζ Cas	B2IV	9	340±90	5.37045	Neiner et al. (2003a)
ω Ori	B2IVe	8	530±200	1.29	Neiner et al. (2003c)

[a] To be confirmed

nitrogen enriched βCep stars from Morel et al

Spectropolarimetry with MuSICoS polarimeter (Donati et al. 1999) @Telescope Bernard Lyot, Pic du Midi and @AAT, ESPaDOnS@CFHT, FORS1@VLT

Magnetic fields in OB-stars

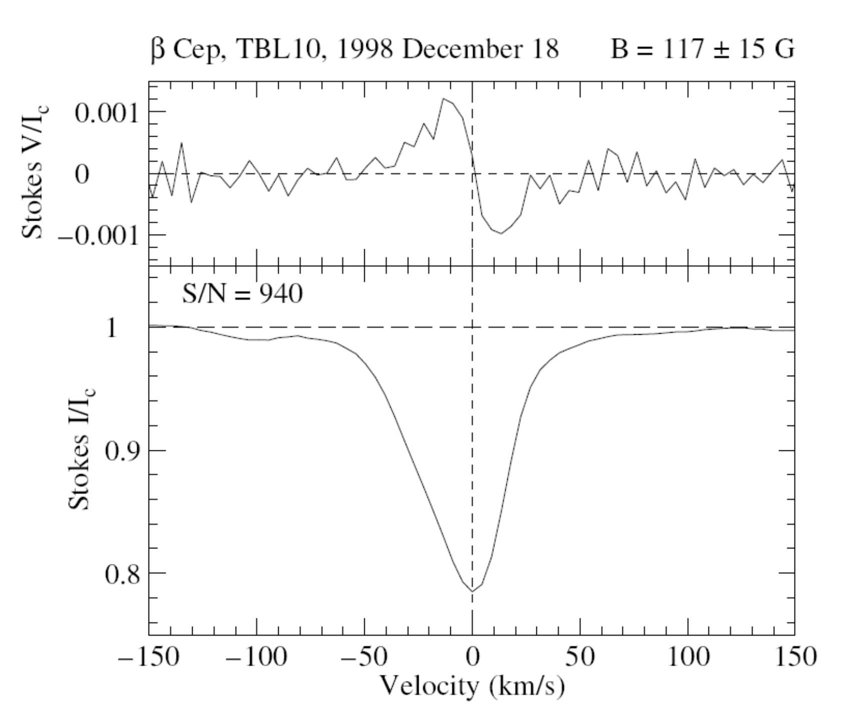

from Henrichs et al. 2005

Zeeman triplet

distance of σ-components (circular polarized) to line center

$\Delta v[\mathrm{m/s}] = 1.4 \cdot \lambda g_{\mathrm{eff}} B$

λ in μm, B in G, g_{eff} Lande´ factor

λ = 5500 Å, B = 100 G $\Rightarrow$ Δv = 77 m/s !!!

Stokes V: difference of $I^{\pm}$ corresponding to $\sigma_{\pm}$:

$V(\mathrm{v}) \propto B_{long} \dfrac{dI_o}{d\mathrm{v}}$ (oblique rotator: angle between rotational and magnetic axis!)

for a nice explanation, see Ignace & Gayley 2003

B_{eff} (long., averaged over disk) $\propto \int \mathrm{v} V(\mathrm{v})\, d\mathrm{v}$

Representative LSD Stokes unpolarized I (lower panel) and circularly polarized V (upper panel) profiles of βCep. The effective magnetic field is proportional to the first moment of the Stokes V profile
LSD - here: least square deconvolution, cf. Semel 1989 & Donati et al. 1997

The surprising magnetic topology of τ Sco

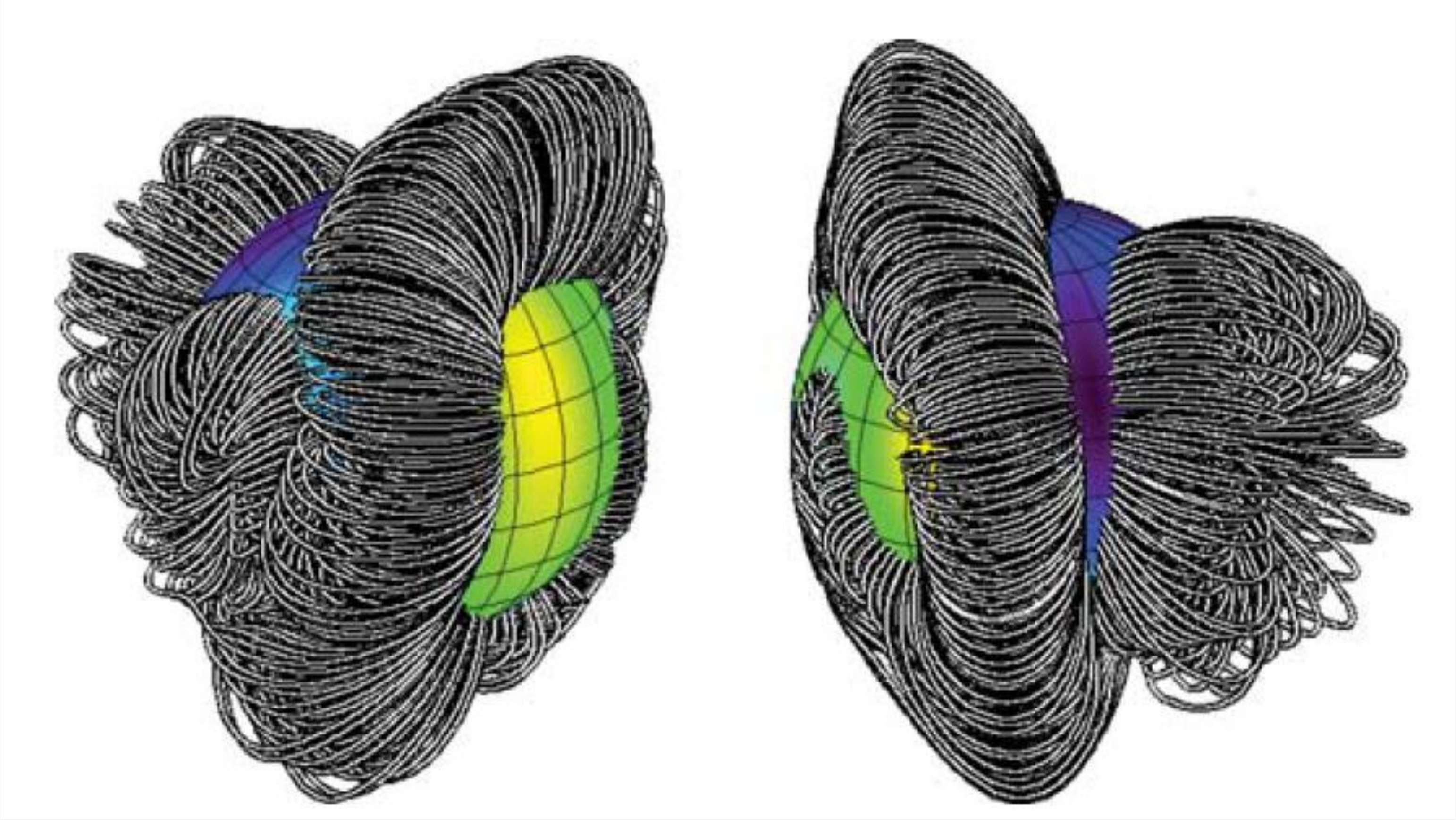

Closed magnetic field lines of the extended magnetic configuration of *τ* Sco, extrapolated from a photospheric map. The star is shown at phases 0.25 (left) and 0.83 (right). Note the warp of the magnetic equator. (From Donati et al. 2006)

Fossil fields?

- Donati and co-workers: magnetic fields in hot stars fossil and *not* due to dynamo processes
- dynamical stable configuration of fossil fields on long time-scales possible (Moss 2001, Braithwaite & Spruit 2004, Braithwaite & Nordlund 2006).
- “An additional argument against dynamo processes is that they should essentially succeed (…) at producing magnetic fields in most hot stars and not only in a small fraction of them. The fact that magnetic fields are detected in a star like τ Sco, known for its peculiar spectroscopic morphology (…), after having been detected in other peculiar hot stars (like θ^1 Ori C, HD 191612 and β Cep), represents further evidence **that magnetic fields** (at least those of moderate to high intensity) **are not a common feature of most hot stars, but rather a rare occurrence**.” (Donati et al. 2006)

for details, see

ud-Doula & Owocki (2002), and

Owocki & ud-Doula (2004) for a comprehensive analytical investigation

Simultaneous solutions of MHD equations including line-force

$$\frac{\mathrm{D}\rho}{\mathrm{D}t} + \rho \underline{\nabla} \cdot \underline{v} = 0$$

$$\frac{\mathrm{D}\underline{v}}{\mathrm{D}t} = -\frac{1}{\rho}\underline{\nabla} p + \frac{GM(1-\Gamma)}{r^2} + \underline{g}_{rad}^{lines} + \underbrace{\frac{1}{\rho}\frac{1}{4\pi}(\underline{\nabla} \times \underline{B}) \times \underline{B}}_{\propto\, \underline{j} \times \underline{B}}$$

Lorentz force

$$\underline{\nabla} \cdot \underline{B} = 0$$

$$\frac{\partial \underline{B}}{\partial t} = \underline{\nabla} \times (\underline{v} \times \underline{B}), \quad \text{for infinite conductivity (MHD approx.)}$$

The confinement parameter

$$\eta(r,\theta) =: \frac{E_B}{E_{wind}} \approx \frac{B^2/8\pi}{\rho v^2/2} = \frac{B^2(\theta)R_*^2}{\dot{M}v_\infty}\frac{(r/R_*)^{2-2q}}{(1-R_*/r)^\beta}$$, assuming

a β-velocity field for the wind and $B(r) \propto (R_*/r)^q$, q=3 for dipole field.

Define confinement parameter $[B_{\rm dipol}(R_*,\theta) = B_p\sqrt{(\cos^2\theta + 1/4\sin^2\theta)}]$

$$\eta_* = \frac{B^2(\theta=90^\circ)R_*^2}{\dot{M}v_\infty} = \frac{(B_p/2)^2R_*^2}{\dot{M}v_\infty} \approx 0.19\frac{B_{100}^2R_{10}^2}{\dot{M}_{-6}v_8},$$

example

ζ Pup: $R_{10} \approx 2, \dot{M}_{-6} \approx 4, v_8 = 2 \Rightarrow B_p \approx 320$ G for $\eta_* = 1$

BUT

Sun: $\dot{M}_{-6} \approx 10^{-8}, v_8 = 0.5, B_p \approx 1$G $\Rightarrow \eta_* \approx 40!$

and

$B_p \approx 32$(!!!) G for $\eta_* = 1$ and $\dot{M} = 10^{-8} M_\odot/\mathrm{yr}$, v_∞=2000 km/s

($\rightarrow$ weak winds?)

Alfven radius

- Why confinement parameter?
- MHD waves propagate with Alfven speed,

$$v_A = \frac{B}{(4\pi\rho)^{1/2}} \Rightarrow M_A = \frac{v}{v_A} = \frac{1}{\sqrt{\eta}}$$

$$\Rightarrow \text{Alfven radius from } M_A(R_A) = 1 \quad \equiv \quad \eta(r,\theta) = 1$$

Alfven radius corresponds roughly to

maximum radius of closed loop ($\Rightarrow$ wind confined)

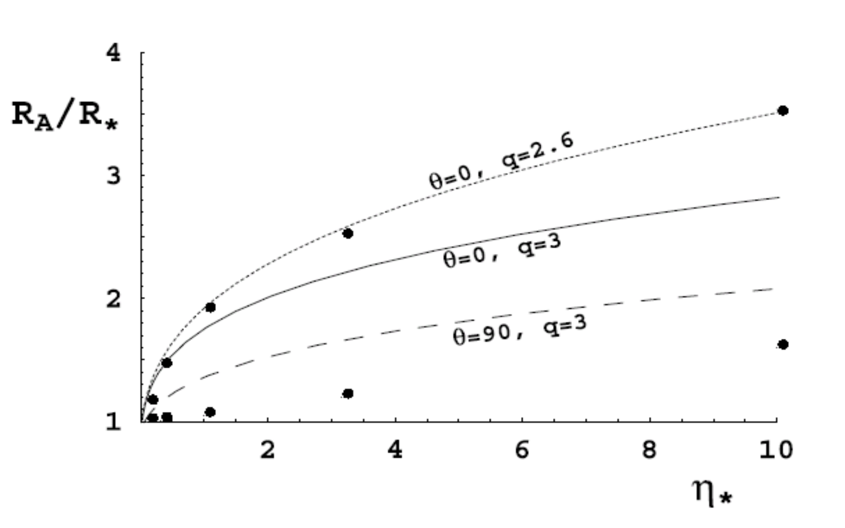

Alfven radius as a function of confinement parameter, for the pole and the equator, from an analytic approximation (curves) and results from consistent MHD simulations. The effective radial dependence of the B-field is reduced due to stretching by the stellar wind, to q ≈-2.6
(from ud-Doula & Owocki 2002)

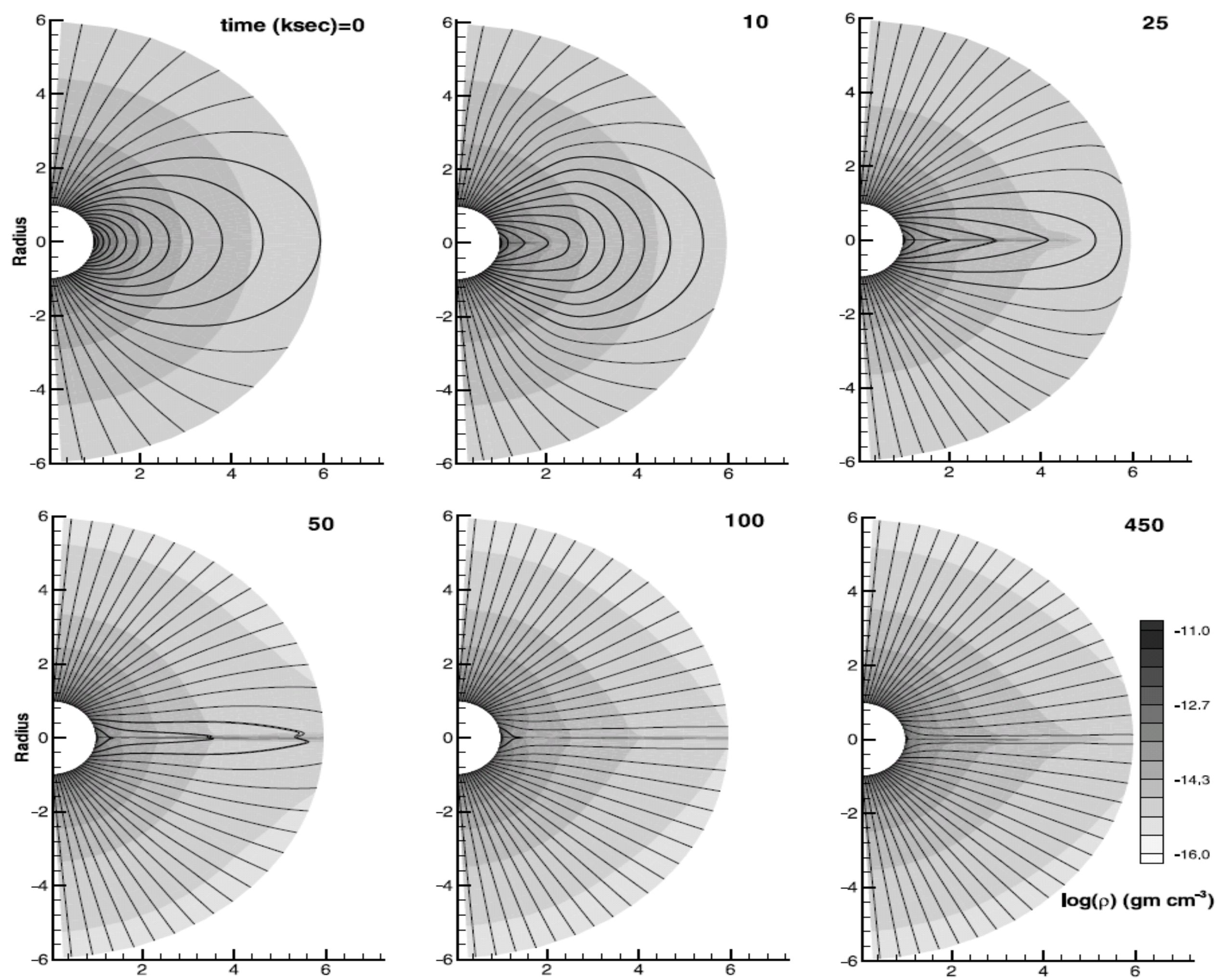

Snapshots of density (logarithmic gray scale) and magnetic field (lines) at the labeled time intervals, starting from the initial condition of a dipole field superposed upon a spherically symmetric outflow, for a case of moderate magnetic confinement $\eta_* = \sqrt{10}$.

Note the stretching of the field lines and the development of a thin equatorial disk.

(from ud-Doula & Owocki 2002)

(from ud-Doula & Owocki 2002)

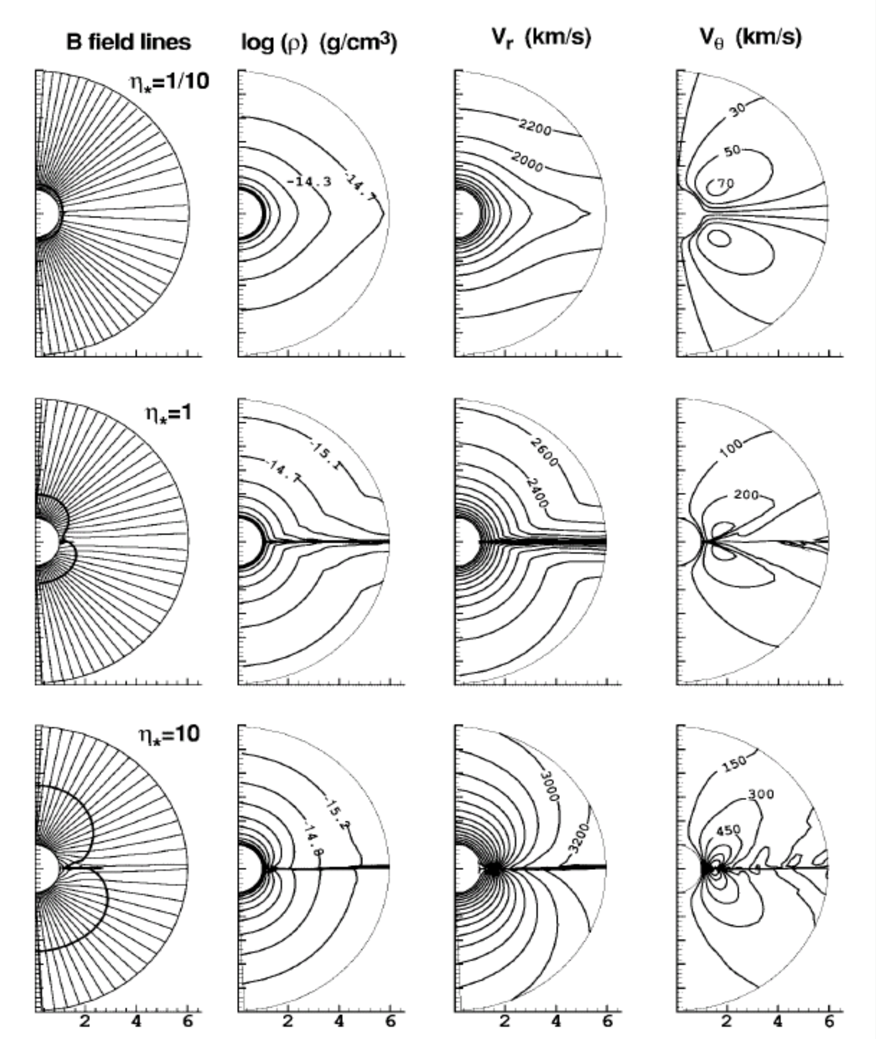

thick contour overplotted on field lines is Alfven-radius

moderately small confinement, $\eta_* = 1/10$:

- surface magnetic field extended by the wind into an open, nearly radial configuration.
- still noticeable global influence of B on the wind, enhancing density and decreasing flow speed near magnetic equator.

intermediate confinement, $\eta_* = 1$:

- field lines still opened by the wind outflow, but near the surface they retain a significant non-radial tilt channeling the flow toward the magnetic equator. (latitudinal v-component as high as 300 km/s).

strong confinement, $\eta_* = 10$:

- field remains closed in loops near the equatorial surface.
- wind outflows accelerated and channeled upward from opposite polarity footpoints
- strong collision near the loop tops, with shock velocity jumps of up to 1000 km/s $\rightarrow$ hard X-ray emission (> 1 keV).
- even for large η_*, the more rapid radial decline of magnetic versus wind kinetic energy density means that the field eventually becomes dominated by the flow, and extended into an open configuration.

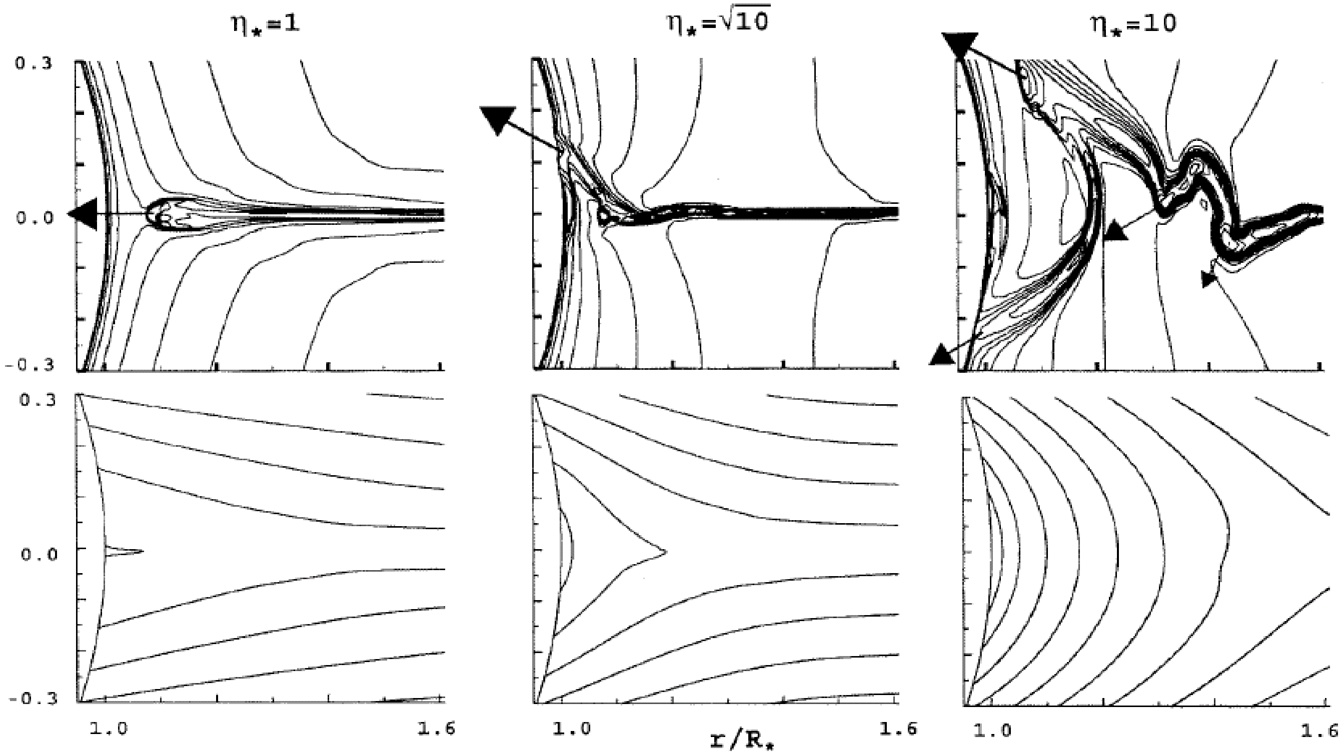

FIG. 4.—Contours of log of density (*top*) and magnetic field lines (*bottom*) for the inner, magnetic equator regions of MHD models with moderate ($\eta_* = 1$; *left*), strong ($\eta_* = \sqrt{10}$; *middle*), and strongest ($\eta_* = 10$; *right*) magnetic confinement, shown at a fixed, arbitrary time snapshot well after ($t \geq 400$ ks) the initial condition. The arrows represent the direction and magnitude of the mass flux and show clearly that the densest structures are undergoing an infall back onto the stellar surface. For the moderate magnetic confinement, $\eta_* = 1$, this infall is directly along the equator, but for the higher confinements, $\eta_* = \sqrt{10}$ and 10, the equatorial compressions that form at larger radii are deflected randomly toward the north or south as they fall in toward the closed field near the surface. The intent here is to illustrate how increasing magnetic confinement leads to an increasing complexity of flow and density structure within closed magnetic loops. This complexity is most vividly illustrated in the time animations available at http://www.bartol.udel.edu/~owocki/MHD_animations.

(from ud-Doula & Owocki 2002)

Impact on hydro-structure

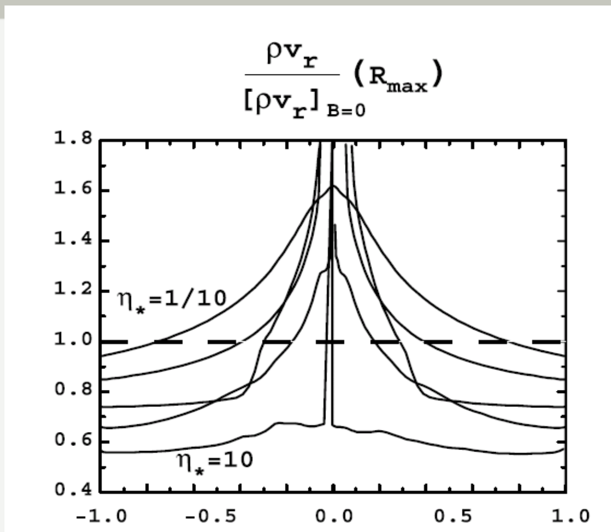

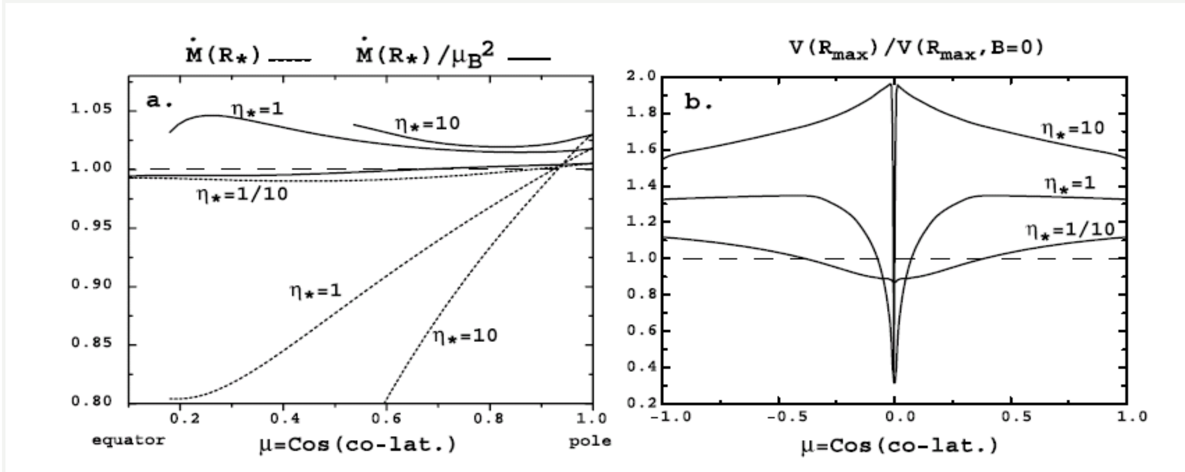

left and right: mass-flux in the outer wind and terminal velocity, as a function of confinement parameter and co-latitude, scaled to standard wind without B. Mass flux in outer wind increases towards magnetic equator due to the tendency of the field to divert the flow toward this direction.
middle: as left, but for the base mass flux. Note that the quantity $\dot{M}(R_*)/\mu_B^2$ with $\mu_B = \underline{\hat{B}} \cdot \underline{\hat{r}}$ the radial projection of a unit vector along the base magnetic field remains almost constant. The base Mdot becomes reduced because of the tilted B-field leading to a tilted flow (projection effect regarding the flow, and lower dv/dr (grad!) due to projection. For a detailed explanation, see Owocki & ud-Doula 2004).

LMU

USM

no B

	MODEL							
							$\eta_* = \sqrt{10}$	
QUANTITY	$\eta_* = 0$	$\eta_* = 1/10$	$\eta_* = 1/\sqrt{10}$	$\eta_* = 1$	$\eta_* = \sqrt{10}$	$\eta_* = 10$	low $\dot{M}$	θ^1 Ori C
α	0.6	0.6	0.6	0.6	0.6	0.6	0.6	0.5
$\bar{Q}$	500	500	500	500	500	500	20	700
δ	0.0	0.0	0.0	0.0	0.0	0.0	0.0	0.1
$R_*(10^{12}$ cm)	1.3	1.3	1.3	1.3	1.3	1.3	1.3	0.5
$B_{\rm pole}$(G)	0	93	165	295	520	930	165	480
ρ_0 (10^{-11}g cm^{-3})	4.3	4.3	4.3	4.3	4.3	4.3	0.54	2.8
max(v_r) (km s^{-1})	2300	2350	2470	2690	2830	3650	2950	2620
max(v_θ) (km s^{-1})	0	70	150	300	400	1200	400	450
$\dot{M}_{\rm net}$ (10^{-6} $M_\odot$ yr^{-1})	2.6	3.0	2.8	2.5	2.2	1.8	0.22	0.3

- global Mdot only weakly affected, but factor 1.5 faster polar wind
- in contrast to rapidly rotating models, slow, dense "disk" and thin, fast polar wind
- non-radial line-forces (almost) irrelevant, since polar velocities much larger
- oblique rotator (magnetic axis tilted w.r.t. to rotational axis) might explain part of UV-variability and induce CIRs, due to large density/velocity contrast w.r.t. the magnetic equator
- X-rays to be expected from channeled flows colliding at loop tops and from shocks neighboring the compressed "disk"

Weak winds – early indications

- Chlebowski & Garmany (1991):
  $\dot{M}$ from late O-dwarfs significantly lower (factor 10) than expected
- Kudritzki et al. (1991), Drew et al. (1994):
  $\dot{M}$ from two BII stars lower (factor 5) than expected (UV-line diagnostics)
- Puls et al. (1996):
  low luminosity dwarfs/giants (log L/Lsun < 5.3) show lower wind-momenta than expected (upper limits, $\dot{M}$ from Hα)

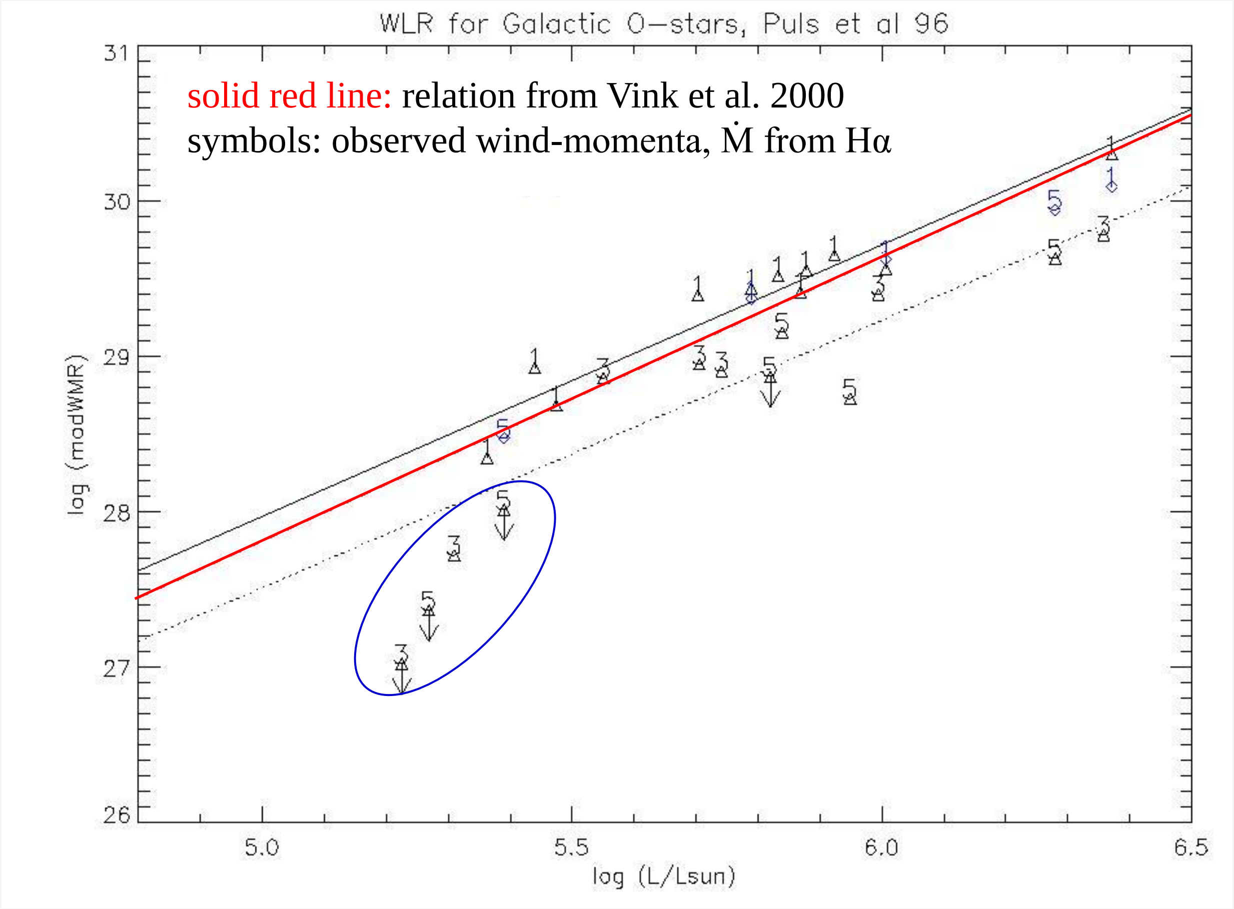

Weak winds → more details in talk by J. Hillier

Weak winds – $\dot{M}$-diagnostics

- for $\dot{M} < 5.0\cdot10^{-8}$ …10^{-8} Msun/yr,
  Hα becomes insensitive!

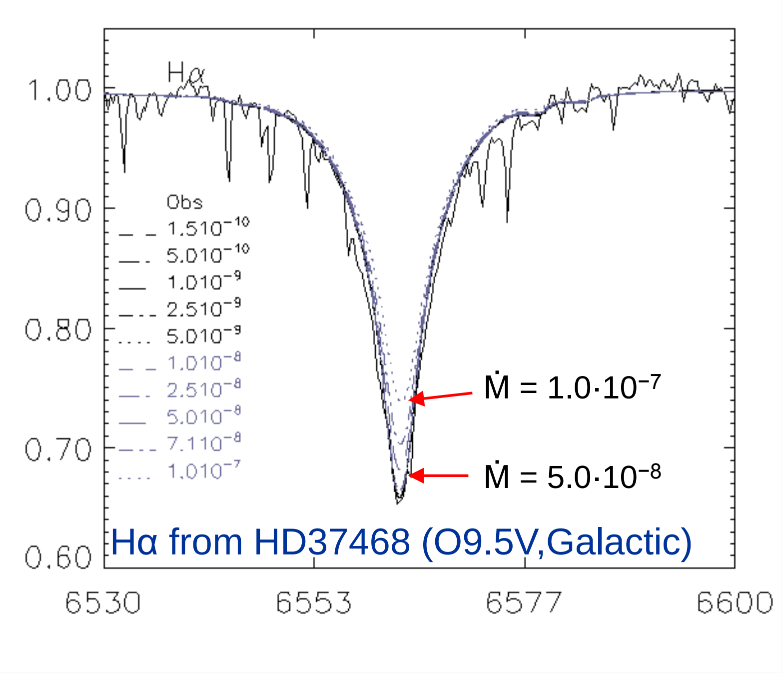

From Najarro, Hanson & Puls, in prep. for A&A

see also Marcolino et al. 2009

Weak winds – $\dot{M}$-diagnostics

- for $\dot{M} < 5.0 \cdot 10^{-8} \ldots 10^{-8}$ Msun/yr, Hα becomes insensitive!

- “conventional” diagnostics for weak winds: UV-resonance lines (CIV, SIV, CIII, …)
- see Martins et al 2004, Marcolino et al 2009

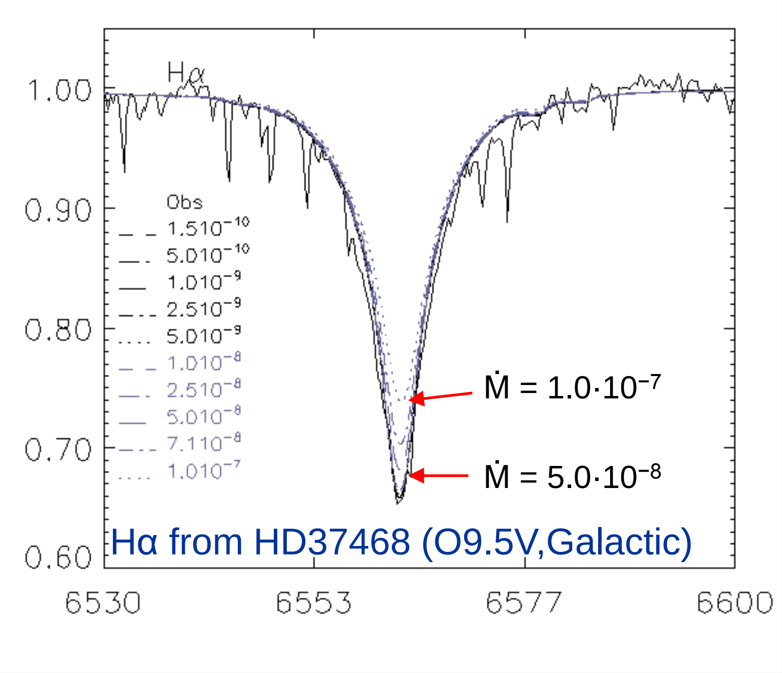

From Najarro, Hanson & Puls, in prep. for A&A
see also Marcolino et al. 2009

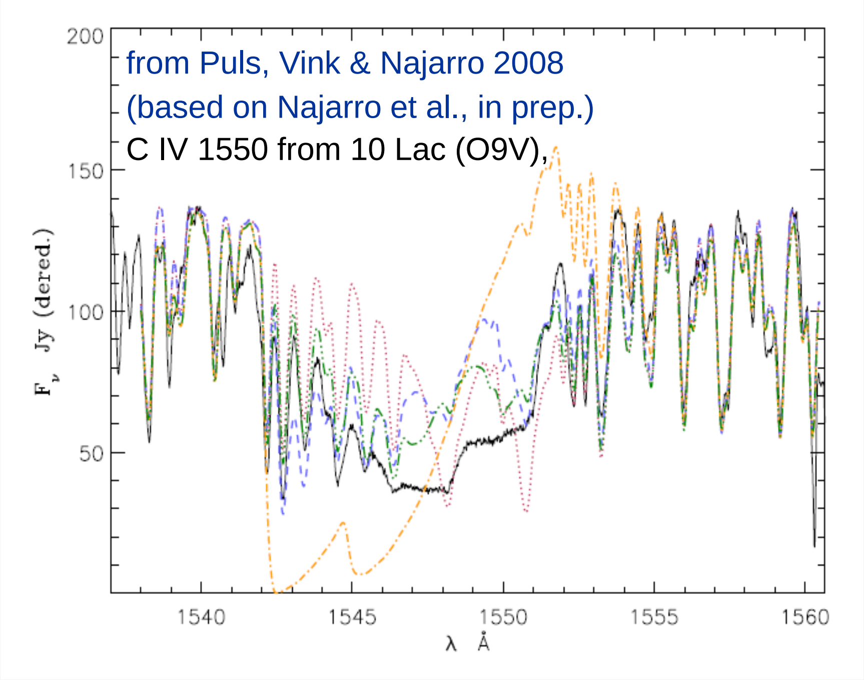

orange: $\dot{M} = 1.0 \cdot 10^{-9}$ Msun/yr: too strong
red: $\dot{M} = 1.0 \cdot 10^{-10}$ Msun/yr: too weak
blue: $\dot{M} = 2.5 \cdot 10^{-10}$ Msun/yr: roughly OK

Weak winds – recent evidence

weak winds in the Magellanic Clouds

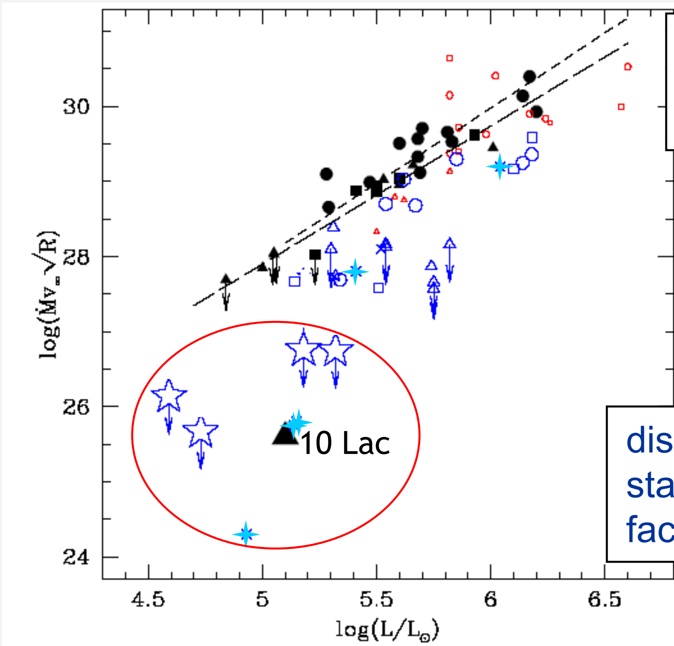

$\dot{M}$ (weak winds) from UV

discrepancy with “normal stars” and predictions: factor ≥10

- open star symbols: extremely young SMC O-dwarfs in N81 (Martins et al. 2004)
- ✦: O-dwarfs in NGC 346 (LMC) (Bouret et al. 2003)
- additionally: 10 Lac (O9V, Galactic)

weak winds in the Galaxy

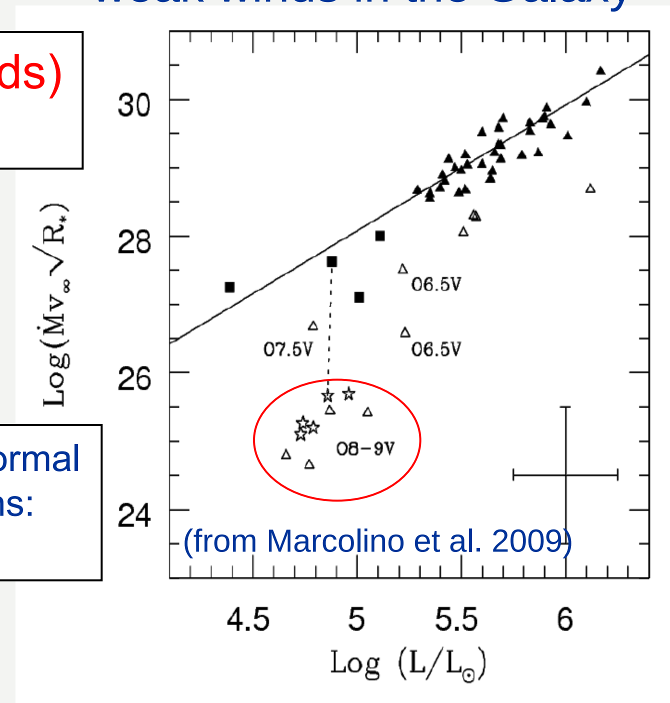

- opens star symbols: late Galactic dwarfs (Marcolino et al. 2009)
- open triangles: Galactic dwarfs/giants (Martins et al. 2005).

… challenge radiation driven wind theory

- Explanations?
  - X-rays (embedded in wind, later) contaminate UV-profiles; but “normal” mass-loss rates only for unrealistically high L_x values (Marcolino et al. 2009)
  - Martins et al. (2004) investigated a variety of candidate processes …
    (e.g., ionic decoupling, shadowing be photospheric lines, curvature effects of velocity fields), …
    … but none turned out to be strong enough.
- … to be continued

Weak winds …continued

Brief summary:

- Much lower mass-loss rates from UV line-profile analyses than from Hα/radio (Fullerton et al. 2006, O-stars; Prinja et al. 2005, B-supergiants)
- might be explained by porosity/vorosity (*macro*-clumping) effects
- remember: weak winds as discussed so far rely on the same UV diagnostics
- Question: Similar problem?
  - under-estimation of the „true“ mass-loss rates due to insufficient physics?
- additional, independent diagnostics required!

Weak winds – $\dot{M}$ from Brα

THE ASTROPHYSICAL JOURNAL, Vol. 156, June 1969

BRACKETT-ALPHA EMISSION IN NON-LTE MODEL STELLAR ATMOSPHERES

L. H. AUER
Yale University Observatory
AND
DIMITRI MIHALAS
Yerkes Observatory, Department of Astronomy and Astrophysics, University of Chicago

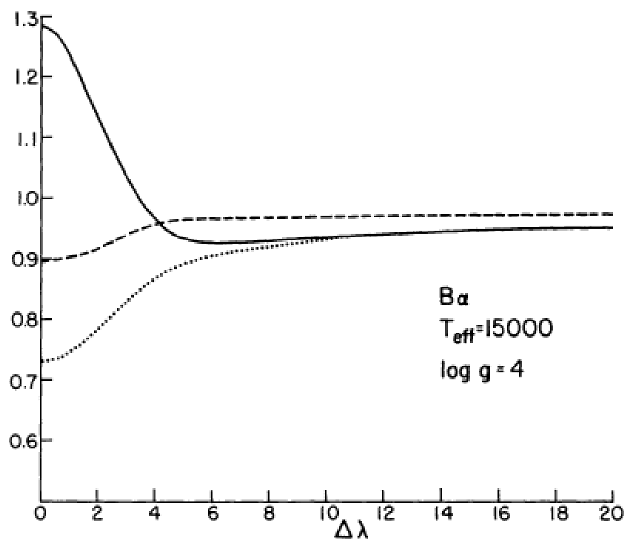

FIG. 1.—Bα line profiles. *Solid line:* non-LTE model, including six line transitions; *dotted line:* non LTE model with lines in detailed balance; *dashed line:* LTE model.

explanation – nebula-like situation in outer photosphere:
population of level 5 and 4 via recombination/electron cascades

level 4 becomes under-populated compared to level 5,
because of very efficient decay channel 4→3

→ emission in line core!

Weak winds – $\dot{M}$ from Brα

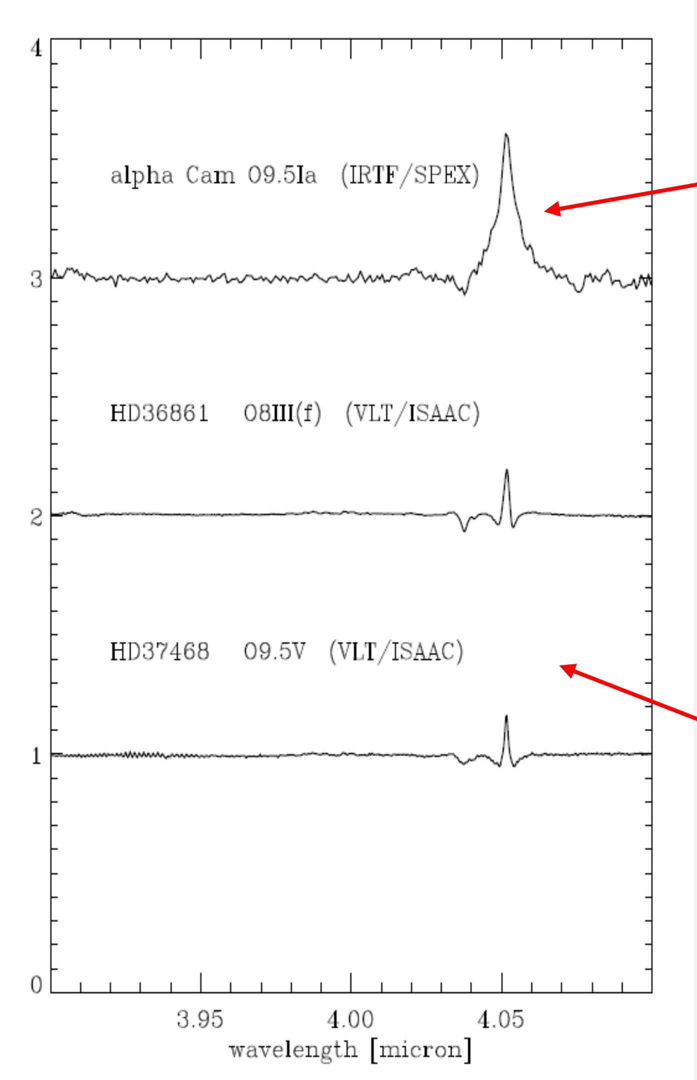

for comparison: Brα from α Cam (*“normal”* wind, wind emission)

Indeed, core emission observed in weak wind candidates (e.g., τ Sco)

Here: Brα from HD36861 O8III(f) and HD37468 (O9.5V)

From Najarro, Hanson & Puls, in prep.

Weak winds – $\dot{M}$ from Brα

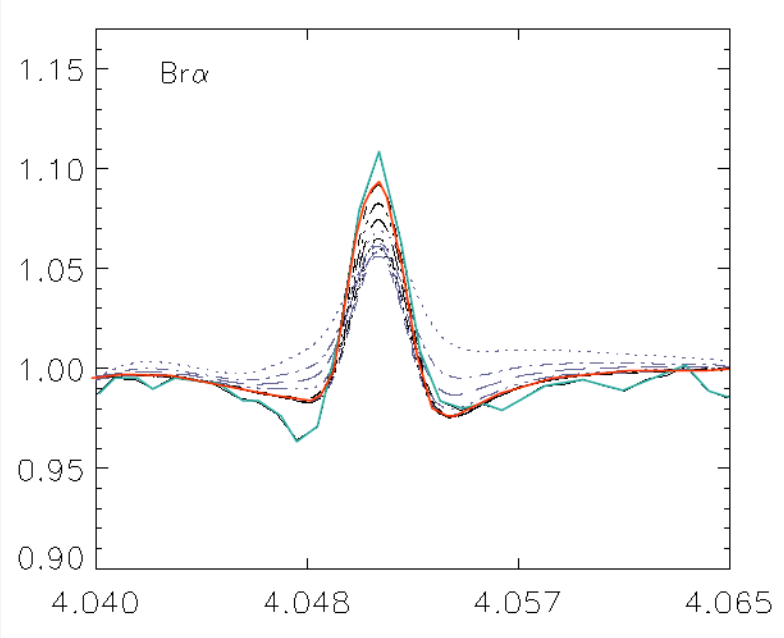

Fits to SpeX@IRTF Brα-profile HD37468 (O9.5V), varying the mass-loss rate

observed profile: turquoise

- $\dot{M}$ spans over three orders of magnitude (models with larger $\dot{M}$ are displayed in gray).
- the core of Br_α nicely traces changes in wind density even for the thinner wind
- peak increases with decreasing $\dot{M}$!
  (*onset of wind*, i.e. density/velocity structure and not RT-effects – suppresses relative under-population of level 4 due to efficient pumping from ground-state)
- only (very) weakly affected by X-rays
- $\dot{M} \approx 10^{-10}$ Msun/yr!
- if wind-base clumped, $\dot{M}$ even lower

From Najarro, Hanson & Puls, in prep.

Weak winds – origin?

Thus, weak winds seem to be a reality …

- Krticka & Kubat (2009): weak winded stars display enhanced X-ray emission, maybe related to extended cooling zones (due to low wind density)
- already Drew (1994) pointed out that strong X-ray emission can lead to reduced line acceleration (ionization equilibrium changed, higher ions have fewer lines)
- Speculation: stronger X-ray emission related to B-fields?
  - weak winds can be strongly affected by relatively weak B-fields → talk by S. Owocki (of order 40 Gauss, below present detection threshold)

  → colliding loops, generate strong and hard X-ray emission in the lower wind, might influence ionization and thus radiative driving from Maeder & Meynet, 2010 NewAR

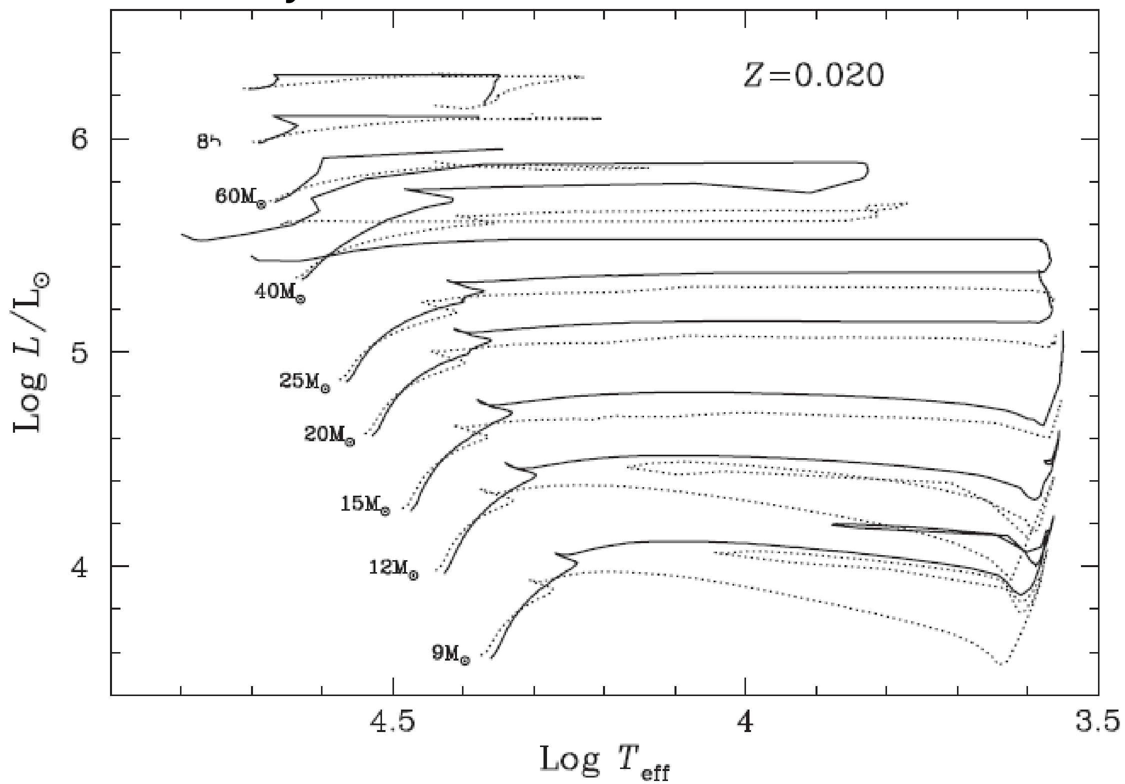

Fig. 5. Evolution in the HR diagram for massive stars with $Z = 0.02$, for rotating star with an initial velocity of 300 km s^{-1} (continuous line) and for non-rotating stars (dotted lines).

G. Meynet and A. Maeder: Stellar evolution with rotation. XI. Wolf-Rayet star populations at different metall.

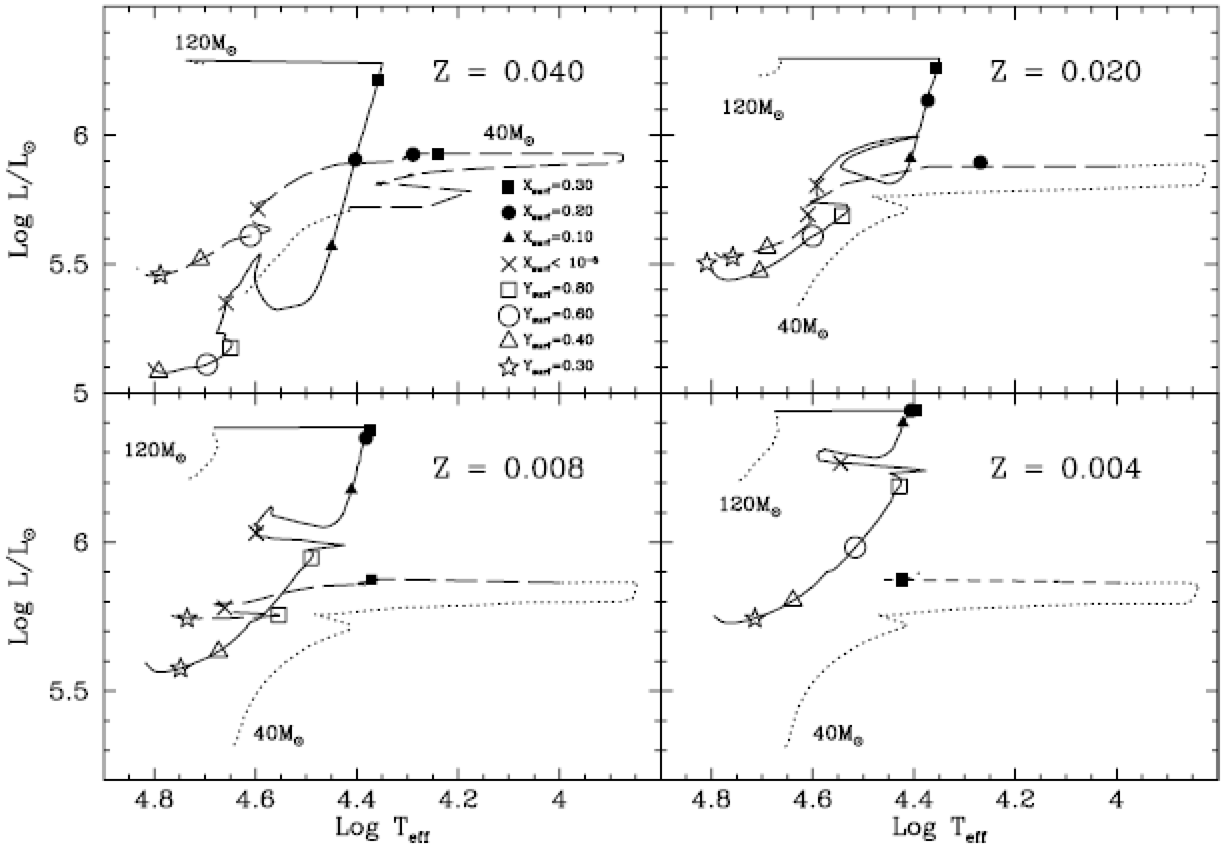

Fig. 3. Evolutionary tracks for 40 and 120 $M_\odot$ rotating models at different metallicities. The initial velocity is 300 km s^{-1}. The light dotted lines correspond to the non-WR part of the tracks. The tracks during the WR phase are shown by heavy lines (continuous for the 120 $M_\odot$ and dashed for the 40 $M_\odot$ model). Symbols along the tracks are placed where the indicated surface hydrogen (X_{surf}) and helium (Y_{surf}) abundances are reached.

- M > 90M: O – Of – WNL – (WNE) – WCL – WCE – SN (hypernova at low Z?)
- 60 – 90 M: O – Of/WNL ↔ LBV – WNL (H poor)- WCL-E – SN (SNIIn?)
- 40 – 60 M: O – BSG – LBV ↔ WNL -(WNE) – WCL-E – SN(SNIb) or – WCL-E – WO SN (SNIc)
- 30 – 40 M: O – BSG – RSG – WNE – WCE – SN (SNIb) or – RSG – OH/IR,LBV?
- 25 – 30 M: O -(BSG)- RSG – BSG (blue loop) – RSG – SN (SNIIb, SNIIL)
- 10 – 25 M: O – RSG – (Cepheid loop, M < 15M) RSG – SN (SNIIL, SNIIp)

from Maeder & Meynet, 2010 NewAR

Mass loss is pivotal…

… in the upper HRD!

- evolution/fate of massive stars

> "… a change of only a factor of two in the mass-loss rates of massive stars has a dramatic effect on their evolution"
> (Meynet et al. 1994)

- energy/momentum release
- stellar yields (→ chemical evolution of clusters and galaxies)

- "GRB range" critically depends on the loss of angular momentum due to mass loss

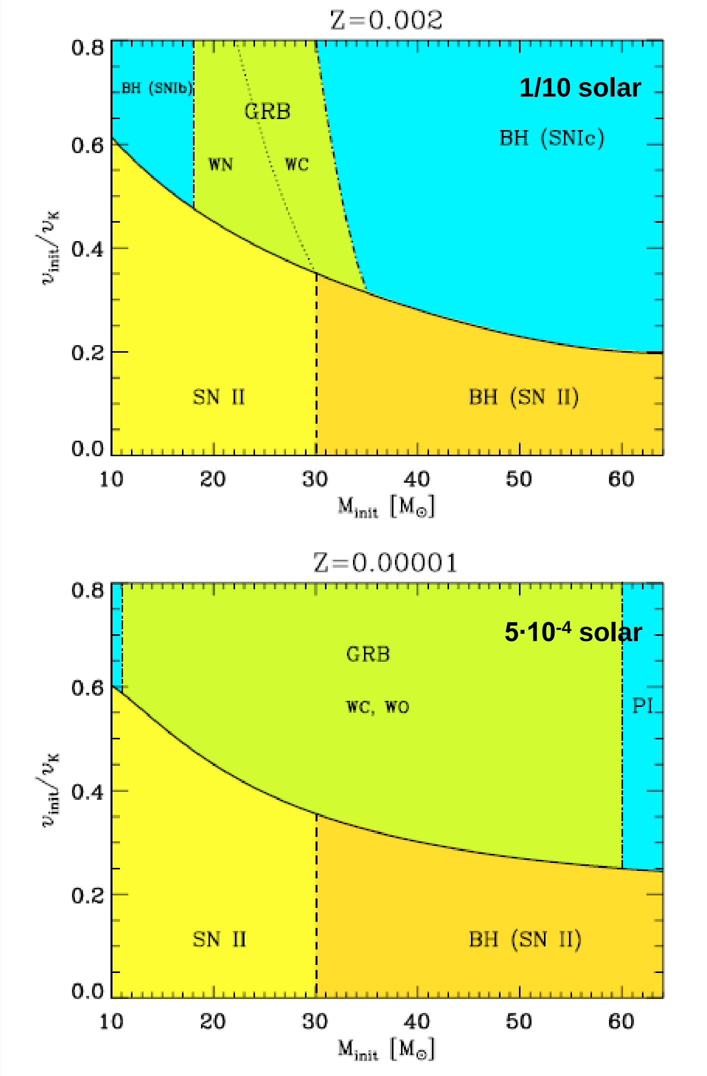

from Yoon, Langer & Norman 2005

Long Gamma Ray Bursts

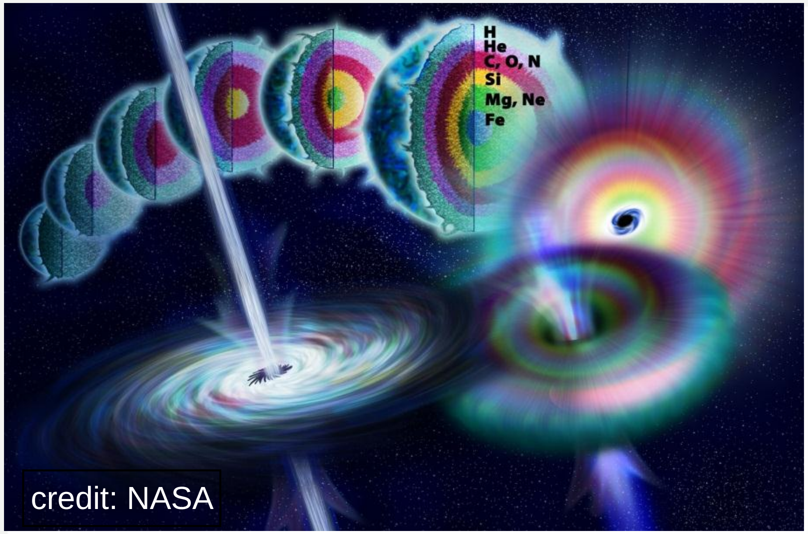

credit: NASA

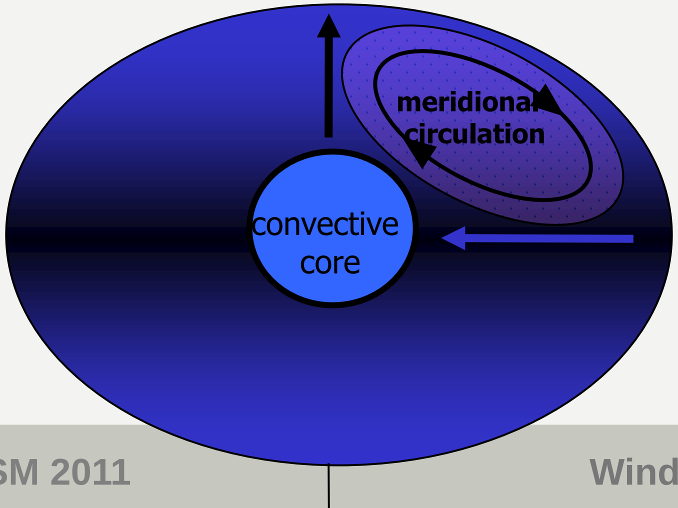

Collapsar Scenario for Long GRB (Woosley 1993)

- massive core (enough to produce a BH)
- removal of hydrogen envelope
- rapidly rotating core (enough to produce an accretion disk)

requires **chemically homogeneous evolution** of **rapidly rotating** massive star

- pole hotter than equator (von Zeipel)
- rotational mixing due to meridional circulation (Eddington-Sweet)

Chemically Homogeneous Evolution …

…if rotational mixing during main sequence *faster than* built-up of chemical gradients due to nuclear fusion (*Maeder 1987*)

bluewards evolution directly towards Wolf-Rayet phase (no RSG phase). Due to meridional circulation, envelope and core are mixed -> no hydrogen envelope

since no RSG phase, higher angular momentum in the core (*Yoon & Langer 2005*)

W/W_k: rotational frequency in units of critical one